Regulation of Apoptosis Following Mitochondrial Cytochrome *c* Release

by

Amanda Baumann Parrish

Department of Pharmacology and Molecular Cancer Biology
Duke University

Date:_____

Approved:

_____
Sally Kornbluth, Supervisor

_____
Donald McDonnell

_____
Ann Marie Pendergast

_____
Gerard Blobe

_____
Jeffrey Rathmell

Dissertation submitted in partial fulfillment of
the requirements for the degree of Doctor
of Philosophy in the Department of
Pharmacology and Molecular Cancer Biology in the Graduate School
of Duke University

2010

ABSTRACT

Regulation of Apoptosis Following Mitochondrial Cytochrome *c* Release

by

Amanda Baumann Parrish

Department of Pharmacology and Molecular Cancer Biology
Duke University

Date:_____

Approved:

_____
Sally Kornbluth, Supervisor

_____
Donald McDonnell

_____
Ann Marie Pendergast

_____
Gerard Blobe

_____
Jeffrey Rathmell

An abstract of a dissertation submitted in partial
fulfillment of the requirements for the degree
of Doctor of Philosophy in the Department of
Pharmacology and Molecular Cancer Biology in the Graduate School
of Duke University

2010

Abstract

Many pro-apoptotic signals trigger mitochondrial cytochrome *c* release, leading to caspase activation and ultimate cellular breakdown. Cell survival pathways, including the mitogen-activated protein kinase (MAPK) cascade, promote cell viability both by impeding mitochondrial cytochrome *c* release and by inhibiting subsequent activation of caspases. Cytosolic cytochrome *c* is directly responsible for initiating formation of the caspase-activating apoptosome, which, in many cell types, plays a crucial role in the apoptotic process. Given the important role of cytochrome *c* in dismantling the dying cell, we wanted to investigate the process of cytochrome *c*-induced apoptosis with the goal of understanding how this mechanism is altered in certain malignant conditions.

First, we examined cytochrome *c*-induced caspase activation in normal and tumorigenic mammary epithelial cells. Although most tumor types have developed mechanisms for evading apoptosis, we surprisingly discovered that breast cancer cells were hypersensitive to cytochrome *c* when compared with their normal counterpart. Specifically, breast cancer cells show increased binding of caspase-9 to the Apaf-1 caspase recruitment domain. This altered apoptosome formation is mediated by overexpression of the protein PHAPI in the malignant mammary epithelial cells. Immunoblot analysis demonstrated that protein levels of PHAPI are also elevated in human breast tumors. These results suggest a novel paradigm where breast cancer cells are refractory to cytochrome *c* release in response to certain stimuli, but they are quite sensitive to apoptosis downstream of the mitochondria.

Secondly, we describe a mechanism for the inhibition of cytochrome *c*-induced caspase activation by MAPK signaling, identifying a novel mode of apoptotic regulation exerted through Apaf-1 phosphorylation by the 90-kDa ribosomal S6 kinase (Rsk). This Apaf-1 phosphorylation results in impaired apoptosome formation, thereby inhibiting caspase activation. The Rsk effect on Apaf-1 is antagonized by protein phosphatase 1 (PP1), which promotes Apaf-1 dephosphorylation. High endogenous levels of Rsk in PC3 prostate cancer cells leads to Apaf-1 phosphorylation and renders them relatively insensitive to cytochrome *c*, suggesting a role for Rsk signaling in the apoptotic resistance of certain cancers. These results identify a novel locus of apoptosomal regulation wherein MAPK signaling promotes direct Rsk-catalyzed phosphorylation of Apaf-1, resulting in decreased cellular responsiveness to cytochrome *c*. Collectively, this work provides insight into novel mechanisms of regulation for cytochrome *c*-induced apoptosis.

Dedication

To my family-

My son, Tyler, who reminds me to enjoy the little things by continuously opening my eyes to the best things in life;

My late brother, Zachary, who I miss dearly everyday and whose life inspired me to never forget what's truly important;

My brother, Kevin, who keeps me laughing and reminds me not to take things too seriously;

My parents who are literally the best I could have asked for- endlessly supportive, constantly encouraging, and incredibly loving;

And, my husband, Judson, who has been instrumental in helping me learn to laugh at myself, is a wonderfully patient friend, and is there for me even during the most stressful of times.

Contents

List of Tables

List of Figures

List of Abbreviations

AChE	Acetylcholinesterase
AFP	α-fetoprotein
Akt/PKB	Protein kinase B
Apaf-1	Apoptotic protease activating factor-1
APIP	Apaf-1 interacting protein
BAC	Bacterial artificial chromosome
CAD	Caspase activated DNase
Caspase	Cysteine-dependant aspartate-directed protease
CARD	Caspase recruitment domain
CAS	Cellular apoptosis susceptibility protein
CDK	Cyclin dependent kinase
cIAP	Cellular inhibitor of apoptosis protein
CK2	Casein kinase 2
CML	Chronic myelogenous leukemia
DISC	Death induced signaling complex
DYRK1A	Dual-specificity tyrosine (Y)-phosphorylation-regulated kinase
ELB	Egg lysis buffer
ERK	Extracellular kinase
HBXIP	Hepatitis B X-interacting protein
HCA66	Hepatocellular carcinoma antigen 66
hCG	Human chorionic gonadotropin

HMEC	Human mammary epithelial cells
Hsp	Heat shock protein
IAP	Inhibitor of apoptosis protein
ICAD	Inhibitor of caspase activated DNase
$InsP_3R$	Inositol 1,4,5-triphosphate receptor
IPTG	Isopropyl-β-D-thiogalactopyranoside
JNK	c-Jun N-terminal kinase
MAPK	Mitogen activated protein kinase
MLC	Myosin light chain
NAC	NB domain and CARD
NBHE	Normal bronchial epithelial cells
NOD	Nucleotide-binding and oligomerization domain
NSCLC	Non-small cell lung carcinoma
OA	Okadaic acid
PARCS	Pro-apoptotic protein required for cell survival
PHAPI	Putative HLA-associated protein-I
PKA	Protein kinase A
PKC	Protein kinase C
PP1	Protein Phosphatase-1
PP2A	Protein Phosphatase-2A
PrEC	Prostate epithelial cells
ProT	Prothymosin-α

ROCK1	Rho associated kinase-1
Rsk	p90-kDa ribosomal S6-kinase
RT-PCR	Reverse-transcriptase polymerase chain reaction
tBid	Truncated Bid
tRNA	Transfer ribose nucleic acid
TUCAN	Tumor-up-regulated CARD-containing antagonist of caspase-9
XIAP	X-linked inhibitor of apoptosis protein

Acknowledgements

I have been quite lucky to be able to collaborate with so many wonderful people during my graduate career. These years at Duke have in no way been a solo journey, and for everyone's support, I am truly grateful. First of all, I need to thank my advisor, Sally Kornbluth. Although my road to this point has most certainly not been a straight one, Sally has been understanding, supportive, optimistic, and encouraging. I have benefited from her impressively constant stream of ideas and suggestions, and she has taught me much about how to be a good scientist, including how to think critically about a problem and design good questions/experiments. Finally, she is a wonderful female role model as she wears so many hats in both her personal and professional lives. As my career progresses, I hope that I develop the same passion for my work that I have seen in Sally; for everything Sally, thanks!

I also greatly appreciate the advice and support of my entire committee, Donald McDonnell, Gerry Blobe, Jeff Rathmell, and Ann Marie Pendergast. Furthermore, the work presented here would not be possible without many additional collaborators. We thank Christopher Counter (Duke University) for the HMEC hTERT and HEK-Ras12V cells; John Blenis (Harvard Medical School, Boston, MA) for the mammalian expression Rsk plasmids; Mohanish Deshmukh and Kevin Wright (UNC-Chapel Hill) for help with mammalian cell microinjection experiments; Xiaodong Wang (UT Southwestern, Dallas, TX) for the human Apaf-1 cDNA; the Duke Proteomics Facility (with special thanks to Erik Soderblom for his direct assistance); Gabriel Nunez (University of Michigan, Ann

Arbor, MI) for the pcDNA3 Apaf-1 mammalian expression plasmids; and Christopher Freel for help analyzing and preparing data.

To the Kornbluth Lab (both present and past members), thanks for these past few years. Thanks for talking science when I needed it and for distracting me when I didn't want to think about it ever again. Thanks for helping to make the lab fun, especially on days when my experiments would have had me beat. Mostly, thanks for keeping things interesting and for allowing me into your lives.

I must at least mention a few specific people without whom this work would not be possible. I am forever indebted to Zach Schafer for taking me under his wing during my first year and serving as a wonderful friend and mentor during my entire graduate career. Those students at Notre Dame are lucky to have you! Shortly after Zach left the lab, I inherited his desk and quickly become closer friends with Jen Perry. Despite working on vastly different topics, Jen was always willing to listen, helping me to troubleshoot and plan during some of my worst graduate school slumps. With Jen's graduation, Marisa moved into the Annex, and I cannot imagine having a better baymate to wrap up my graduate career. She has provided me with invaluable technical/experimental assistance, friendship, and laughter. As one can hopefully see, the Annex has been my home from the day I stepped into the Kornbluth lab, and I have been lucky to share time with such wonderful friends and scientists.

A more recent addition to the Annex, Jiyeon has been so much more than just a baymate. Immediately after joining the lab, Jiyeon has collaborated with me on a variety of experiments in the lab, and it has been such a pleasure. Her dedication and

independence propel her to the front of whatever she does. I am lucky to have had this opportunity to work with her, and I have no doubt that she will go on to do great things. Other members of the Kornbluth Lab "post-cytochrome *c* group" were also critical to my development as a graduate student. I must thank Manabu for advising me on a variety of issues, for helping me with gel filtration, and for talking me through many experiments/issues. I would also like to mention a previous lab member, Carrie Johnson, for teaching me to question constantly and for collaborating with me on a variety of projects.

I also thank my friends from the CMB Program. I must specifically mention Kristin, Sarah, and Bethany for your friendship, for your continued support even after we finished the CMB requirements, and for the celebratory birthday dates. Sarah, your friendship both in and out of the lab has helped make this time more enjoyable and manageable. I cannot imagine a better person to have shared these Kornbluthian experiences with; thanks for listening to me and for serving as a source of support on so many personal and professional issues.

I wouldn't be here today without the love and assistance of my family and friends. Even more than when I started her at Duke, these people are now intertwined with my life, shaping who I become. There is not possibly enough space to appropriately thank them for everything. Briefly, I thank Elizabeth, Maura, Katie, Meg, and Britt for listening to me talk about these crazy frogs/experiments even though they are in entirely unrelated fields. Your friendships since Marist have been a staple in my life. During my years at Duke, I was fortunate enough to marry into a wonderful family. I must thank Karen,

Tom, Kat, Liz, Charlie, Lisa, Lauren, Kyle, Kenleigh, Nigel, and Kaci for welcoming me with open arms and for making a visit with the “in laws” so much fun. My parents, Jim and Marlene, have been always been my biggest cheerleaders, and there was nothing different about my decision to return to school at Duke. They have supported me in ways I could not have expected, and they have always been there to help lift my spirits when I thought I couldn’t do it. My brothers, Zachary and Kevin, were paramount in helping me learn to not take myself too seriously and in developing a sense of humor about life, both of which have been necessary during my graduate career.

Finally, I need to thank my amazing husband, Judson, who moved up to Durham with me years ago without any questions. He has been listening to me and assisting me since day one. He challenges me and encourages me; his support through the good and the bad has, at times, kept my head above water. He brings laughter to my life, and more patience than I often offer myself. With the birth of our son Tyler almost one year ago, I have a greater appreciation for what it means to be a family, and I thank you both for giving my life new meaning. I love you!

1. Introduction

1.1 Apoptosis

Apoptosis is a form of programmed cell death that eliminates individual cells within an organism while preserving the overall structure of the surrounding tissue. The characteristics of apoptosis that distinguish it from other forms of cell death were first published in 1972 by Kerr, Wyllie, and Currie, who considered apoptosis to be a process "complementary but opposite to mitosis in the regulation of animal cell populations" (Kerr et al., 1972). Indeed, continued studies on apoptosis support their idea that apoptosis and mitosis involve intertwined but opposing signals within a cell, and a fine balance between these processes are necessary for healthy cellular homeostasis. Kerr and his colleagues described the morphological and structural changes of an apoptotic cell, and these are still characteristic of apoptotic cell death. However, it would be decades later when the molecular apoptotic signaling pathways, including caspases and cytochrome *c*, were more clearly delineated (Kluck et al., 1997; Liu et al., 1996; Nicholson et al., 1995; Zou et al., 1997).

Apoptosis is involved in many physiological processes, including the removal of cells during embryonic development and the maintenance of tissue homeostasis (Zimmermann et al., 2001). One specific developmental process dependent on apoptosis is proper digit formation as the interdigital webbing is removed through this regulated cell death (Figure 1.1) (Bandyopadhyay et al., 2006; Cecconi et al., 1998). Additionally, apoptosis facilitates proper brain development; homozygous knockout mice for critical apoptotic regulators, such as caspase-3, caspase-9, and Apaf-1, have enlarged brains and

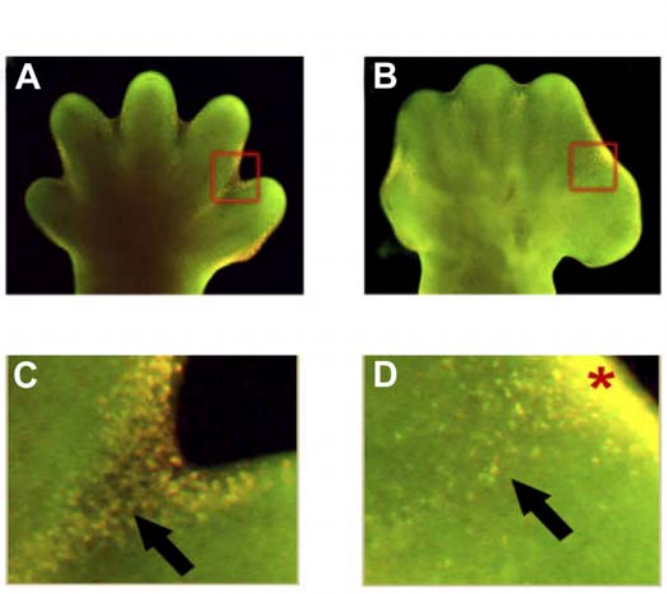

Figure 1.1: Developmental Apoptosis in the Interdigital Webbing.

Figure 1.1: A. Normal mouse hindlimb from an E15.5 embryo stained with acridine orange (in yellow) for apoptotic cells. Interdigital mesenchyme is disappearing due to apoptosis. **B.** Hindlimb from mutant mouse (*Bmp2*$^{C/C}$; *Bmp4*$^{C/C}$; *Prx1::cre*) stained as in A. Webbing still present due to reduced apoptosis. Although the genotype of this specific mouse is not discussed in the text, Apaf-1$^{-/-}$ mice have a similar phenotype **C and D.** Enlarged view of the boxed red areas from A and B, respectively, showing the acridine orange staining, indicative of apoptosis. Adapted from Bandyopadhyay *et al.* (2006), with permission from PLoS Genetics as an Open-Access Journal.

die early or before birth (Cecconi et al., 1998; Hakem et al., 1998; Kuida et al., 1998; Kuida et al., 1996; Yoshida et al., 1998). Beyond development, apoptosis functions as a homeostatic process, and thus, alterations in this process are involved in a variety of disease states. For example, degenerative disorders are characterized by excessive cell death whereas cancer and autoimmune diseases result from too little apoptosis (Danial and Korsmeyer, 2004; Katoch et al., 2002). While tumor cells often have mechanisms for evading apoptosis, many types of chemotherapeutic treatments attempt to activate the apoptotic pathway to promote tumor cell death (Hanahan and Weinberg, 2000). Thus, it is crucial that we understand normal apoptotic signaling in order to examine how these pathways have gone awry during tumor development, with the hope that we could design more direct treatments that would specifically kill the tumor cells.

At the cellular level, specific morphological features and characteristics indicate death by apoptosis. Initial cell shrinkage is followed by rounding, cell retraction, and membrane blebbing into "apoptotic bodies" (Figure 1.2). Other changes occurring include nuclear condensation, DNA fragmentation, and movement of phosphatidylserine to the extracellular surface of the plasma membrane (Danial and Korsmeyer, 2004; Fadok et al., 2000; Wyllie et al., 1980). While apoptosis was once synonymous with programmed cell death, recent work supports the idea that it is only one pathway playing a role during times of cellular stress. Necrosis and autophagy also appear to have important, defined molecular signaling events associated with them and are not just "default" death pathways, as once thought

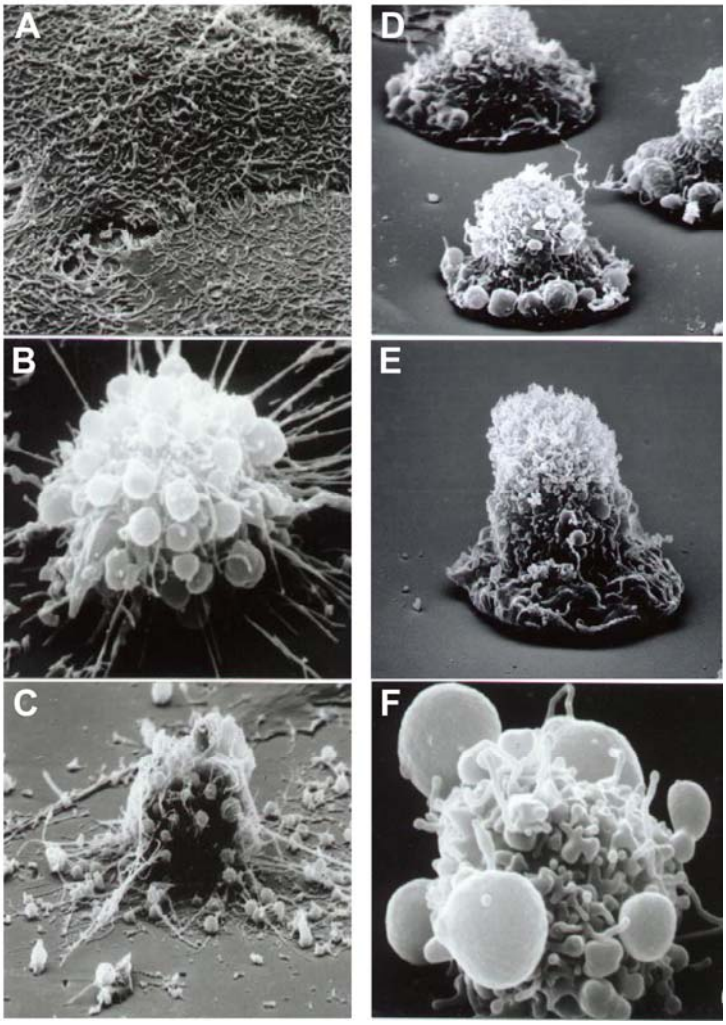

Figure 1.2: Morphological Features of Apoptosis.

Figure 1.2: A. Scanning electron microscopy (SEM) of normal epithelial cells with a mostly flat morphology. **B-E.** SEM capturing the apoptotic process; epithelial cells undergoing rounding, cell retraction, and surface blebbing. **F.** The typical SEM image of an apoptotic cell. Images from W. Malorni, published in: The Purdue Cytometry CD-ROM Volume 4, J. Watson, Guest Editor, J. Paul Robinson, Publisher. Purdue University Cytometry Laboratories, West Layfette, Indiana. 1997, ISBN: 1-890473-03-0

(Edinger and Thompson, 2004; Levine and Kroemer, 2009; Pattingre et al., 2005; Zong et al., 2004). However, the morphological features and activation of caspases still make apoptotic cell death unique. Although caspase-1 was cloned in 1992, it was in the mid-1990s that apoptosis was linked to the activation of these *c*ysteine dependent *a*spartate-driven prote*ases* (caspases) and cytochrome *c* was placed in this pathway upstream of caspase activation (Alnemri et al., 1996; Cerretti et al., 1992; Liu et al., 1996; Nicholson et al., 1995; Thornberry and Lazebnik, 1998). In a healthy cell, caspases exist as a zymogen or inactive monomer, unable to affect any downstream substrates. During apoptosis, caspases become activated, often through cleavage, and initiate the well-defined cellular changes resulting from cleavage of their substrates (Luthi and Martin, 2007; Nicholson, 1999).

1.1.1 Apoptosis Signaling

Apoptosis can be induced through one of two pathways, extrinsic or intrinsic; pro-death stimuli triggering the intrinsic pathway converge on the mitochondria, to induce release of cytochrome *c* to the cytosol (Danial and Korsmeyer, 2004). The cell tightly controls cytochrome *c* release through the balance of bcl-2 family member proteins, which can be either pro-apoptotic (Bax, Bak) or anti-apoptotic (Bcl-2, Bcl-X_L) (Danial and Korsmeyer, 2004; Youle and Strasser, 2008). After translocation to the cytosol, cytochrome *c* is incorporated into a cell-death complex known as the apoptosome, which serves as a platform for activation of the initiator caspase, caspase-9 (Kluck et al., 1997; Liu et al., 1996; Ow et al., 2008). To nucleate apoptosome formation, cytosolic cytochrome *c* binds the apoptotic protease activating factor (Apaf-1), inducing a

conformational change and dATP hydrolysis on Apaf-1. Subsequent nucleotide exchange allows Apaf-1 to oligomerize into a large heptameric structure, which can then recruit and bind the zymogenic form of caspase-9 (Kim et al., 2005; Kim et al., 2008). This interaction, mediated by binding between caspase recruitment domains (CARD) on caspase-9 and Apaf-1, promotes dimerization of caspase-9, leading to its activation by induced proximity (Pop et al., 2006; Riedl and Salvesen, 2007). The downstream effector caspases-3 and -7 are cleaved by active caspase-9, causing their activation and the subsequent cleavage of a large number of cellular substrates (Figure 1.3) (Inoue et al., 2009; Li et al., 1997).

The extrinsic pathway is initiated at the plasma membrane where an extracellular ligand (for example, FasL) binds to its receptor (Fas), inducing trimerization (Danial and Korsmeyer, 2004; Itoh and Nagata, 1993; Trauth et al., 1989). Interactions between the Fas receptor and the intracellular Fas-associated death domain (FADD) complete the DISC (death-induced signaling complex) and allow for recruitment and activation of the initiator caspase, caspase-8 (Kischkel et al., 1995). Similarly to capsase-9, caspase-8 is thought to become activated through induced proximity. Once active at the plasma membrane, caspase-8 can participate in two pathways. In type I cells, Fas-induced apoptosis is independent of the mitochondria (and, thus refractory to bcl-2) since caspase-8 can directly cleave the effector caspases, caspase-3 and -7, which leads to death. In type II cells, the mitochondrial amplification loop is required; caspase-8 signals through the intrinsic pathway, triggering cytochrome *c* release from the mitochondria by cleaving the BH3-only protein, Bid. As a member the bcl-2 family, truncated Bid (tBid), leads to

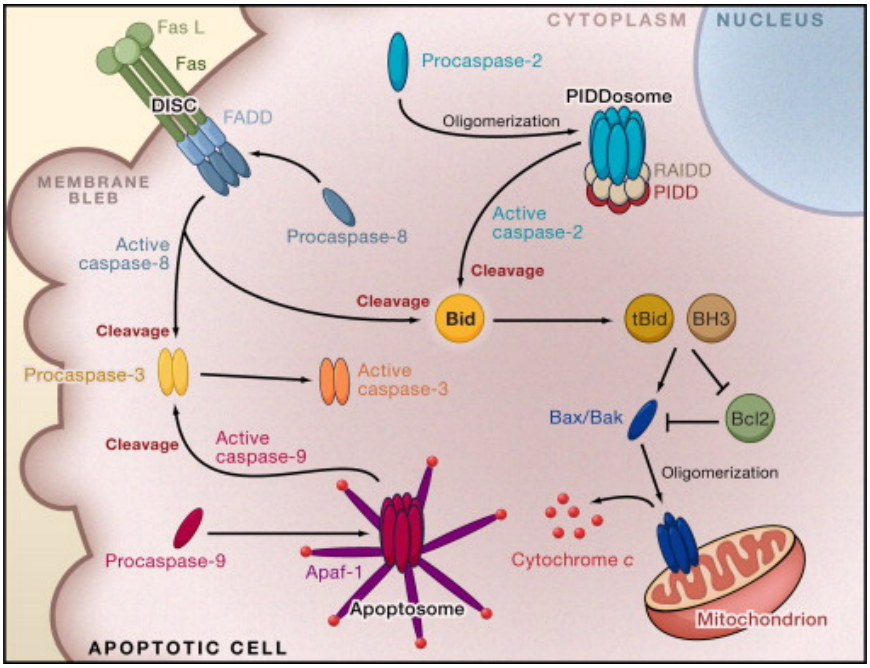

Figure 1.3: The Extrinsic and Intrinsic Apoptotic Pathways.

Figure 1.3: The three major initiator caspases pathways are shown relative to both extrinsic and intrinsic apoptosis. The extrinsic pathway activates caspase-8/-10 and is initiated at the plasma membrane by the binding of a ligand (such as FasL) to its receptor (Fas), forming the death-induced signaling complex (DISC). Along with the receptor, the DISC involves a death domain containing adaptor (FADD), which allows for recruitment of caspase-8. Following activation, caspase-8 can directly cleave effector caspases, such as caspase-3, and/or the BH3-only protein Bid, which is known as truncated Bid or tBid. tBid can activate the intrinsic apoptotic pathway through modulation of bcl-2 family members at the mitochondria, including the pro-apoptotic proteins, Bax and Bak. The anti-apoptotic bcl-2 family members regulate Bax/Bak oligomerization and activation, which ultimately modulate mitochondrial cytochrome *c* release. Cytochrome *c* translocation into the cytosol facilitates the intrinsic apoptotic pathway, which induces oligomerization of Apaf-1. This heptameric complex, known as the apoptosome, recruits and activates the initiator caspase, caspase-9, which can directly cleave caspase-3. Caspase-2 is activated by the PIDDosome, consisting of the adaptor proteins PIDD (p53-induced protein with a death domain) and RAIDD (RIP-associated ICH-1/CED-3 homologous protein with a death domain). Caspase-2-mediated death is believed to progress through cleavage of Bid; there are not many direct caspase-2 substrates that have been identified. From Kurokawa and Kornbluth (2009), with permission from Elsevier.

activation of the protein Bax, which causes mitochondrial cytochrome *c* release (Figure 1.3).

1.2 Post-mitochondrial Apoptosis and its Regulation

1.2.1 Structure of the Apoptosome

The apoptosome complex has 7-fold symmetry with Apaf-1 forming the backbone of the structure. It looks somewhat like a wheel with seven spokes where the N-terminal CARDs on Apaf-1 are located in the central region of the apoptosome and form the platform for activating caspase-9. Radiating outward, the nucleotide and oligomerization domain (NOD) on Apaf-1 forms the central part of the structure and is responsible for the interaction with other Apaf-1 proteins during apoptosome formation (Acehan et al., 2002; Yu et al., 2005). The 13 WD40 repeats in the COOH-terminus of Apaf-1 form the regulatory region, which is thought to be critical for binding cytochrome *c*. Indeed, the three dimensional crystal structure generated by electron cyromicroscopy indicates that one cytochrome *c* molecule fits between the two β propellers formed by the WD40 regions of Apaf-1 (Acehan et al., 2002; Yu et al., 2005). The stoichiometry of Apaf-1 to cytochrome *c* in this context appears to be 1:1, instead of the previously reported 1:2 (Purring-Koch and McLendon, 2000). Additionally, the apoptosome contains dATP bound to Apaf-1, supporting the nucleotide requirement for proper formation of the apoptosome. While it appears that there is room for seven caspase-9 monomers to interact with the seven CARDs in the middle of the apoptosome, more recent studies suggest that perhaps only two caspase-9 monomers (allowing for the formation of one dimer) are activated on an apoptosome at one time (Malladi et al., 2009).

1.2.1.1 Cytochrome *c* and Apaf-1 Oligomerization

The binding of cytosolic cytochrome *c* to Apaf-1 is the most apical step in apoptosome formation, and their interaction is regulated through the physical separation of these two proteins within the cell. Located in the intermembrane space of the mitochondria, cytochrome *c* functions in the electron transport chain, moving electrons between complex III (cytochrome cb1) and complex IV (cytochrome *c* oxidase) (Skulachev, 1998). Due to its primary location in the mitochondria, cytochrome *c* is only able to interact with the predominantly cytosolic Apaf-1 after its regulated release. Apaf-1 exists in the cytosol as an auto-inhibited monomer with three main domain structures (Figure 1.4A). The N-terminal CARD is both necessary and sufficient for its interaction with caspase-9. However, in this monomeric conformation, the CARD is not exposed and thus fails to interact with caspase-9. The NOD is the central region of the protein, which can be further subdivided into areas necessary for nucleotide binding and self-association (Yu et al., 2005). The COOH-terminus of the protein is comprised of 13 WD40 repeats that can interact with the N-terminus of the protein, and although there is no crystal structure for monomeric, full length Apaf-1, it is thought that this region folds over on the N-terminus of the protein, inhibiting caspase-9 recruitment and Apaf-1 oligomerization (Hu et al., 1998; Yu et al., 2005). A crystal structure for a truncated mutant of Apaf-1 (1-559), lacking this regulatory region, has been isolated, and it demonstrates the nucleotide binding pocket and the locations of relative domains in 3-dimensional space (Riedl et al., 2005; Yu et al., 2005) (Figure 1.4B). It has been suggested that cytochrome *c* binds to the COOH-terminal, WD40-containing region of Apaf-1, relieving autoinhibition, allowing

for oligomerization and subsequent caspase-9 recruitment. However, this hypothesis regarding the cytochrome *c* binding site on Apaf-1 is mostly based on biochemical studies demonstrating that recombinant Apaf-1 protein lacking the WD40 region can interact with caspase-9 independent of cytochrome *c* (Hu et al., 1998; Srinivasula et al., 1998). Structural studies on the apoptosome and recent work with the recombinant WD40 domains of Apaf-1 both provide further support for hypothesis that the WD40 regions serve as the docking site for cytochrome *c*, although the specific amino acids necessary for this interaction have yet to be identified (Figure 1.4C) (Rao et al., 2009; Yu et al., 2005).

Although the regions of Apaf-1 responsible for its interaction with cytochrome *c* are still unclear, the structure of cytochrome *c* provides more information regarding its binding to Apaf-1. In the mitochondria, cytochrome *c* exists in its holo-form, bound to a heme group that is required for its apoptotic function (Kluck et al., 1997). Apocytochrome *c* (lacking the heme) is synthesized in the cytosol, where it is unable to trigger apoptosis until its transportation into the mitochondria where the heme group is added by heme lyase (Diekert et al., 2001). Studies substituting copper or zinc for the iron in the attached heme group indicated that the redox state of cytochrome *c* is not critical for its pro-apoptotic functions (Kluck et al., 1997). However, more recent studies suggest that having cytochrome *c* in a reduced or oxidized state can affect its caspase-activating ability, and this mode of regulation will be discussed in greater detail below (Brown and Borutaite, 2008; Vaughn and Deshmukh, 2008).

Interestingly, much of our initial knowledge regarding the interaction between cytochrome *c* and Apaf-1 came from an examination of cytochrome *c* in the yeast, *Saccharomyces cerevisiae*. The sequences between human and *Saccharomyces cerevisiae* cytochrome *c* are very similar except that yeast cytochrome *c* is tri-methylated at lysine 72 (Kluck et al., 1997; Yu et al., 2001). Modification of this lysine residue is sufficient to inhibit its binding to Apaf-1. Thus, yeast cytochrome *c* is incapable of driving apoptosome formation and caspase activation. Additional mutants of cytochrome *c* have been made to further investigate its ability to facilitate apoptosome formation. Interestingly, mutating many of the surface-exposed lysines, including 7, 25, 39, and 62-65, leads to reduced activity toward Apaf-1 (Yu et al., 2001). There is also a naturally occurring variant of cytochrome *c*, discovered in a New Zealand family with dominant thrombocytopenia (Morison et al., 2008). A glycine substitution for a serine at amino acid 41 in cytochrome *c* appears to enhance its activity in activating the apoptosome.

Although the exact residues or regions responsible for the Apaf-1/cytochrome *c* interaction are unknown, it is clear that cytochrome *c* facilitates an important conformational change necessary for apoptosome formation. When these apoptosome components were first discovered over a decade ago, Xiaodong Wang and colleagues performed a myriad of elegant experiments to characterize apoptosome formation using an *in vitro* reconstitution system (Liu et al., 1996; Zou et al., 1997). They noticed a dATP requirement for caspase activation, but it was not until recently that a precise role for dATP was understood. This work has demonstrated that monomeric Apaf-1 exists in the cytosol bound to dATP (Kim et al., 2005). Similar studies using truncated Apaf-1 protein

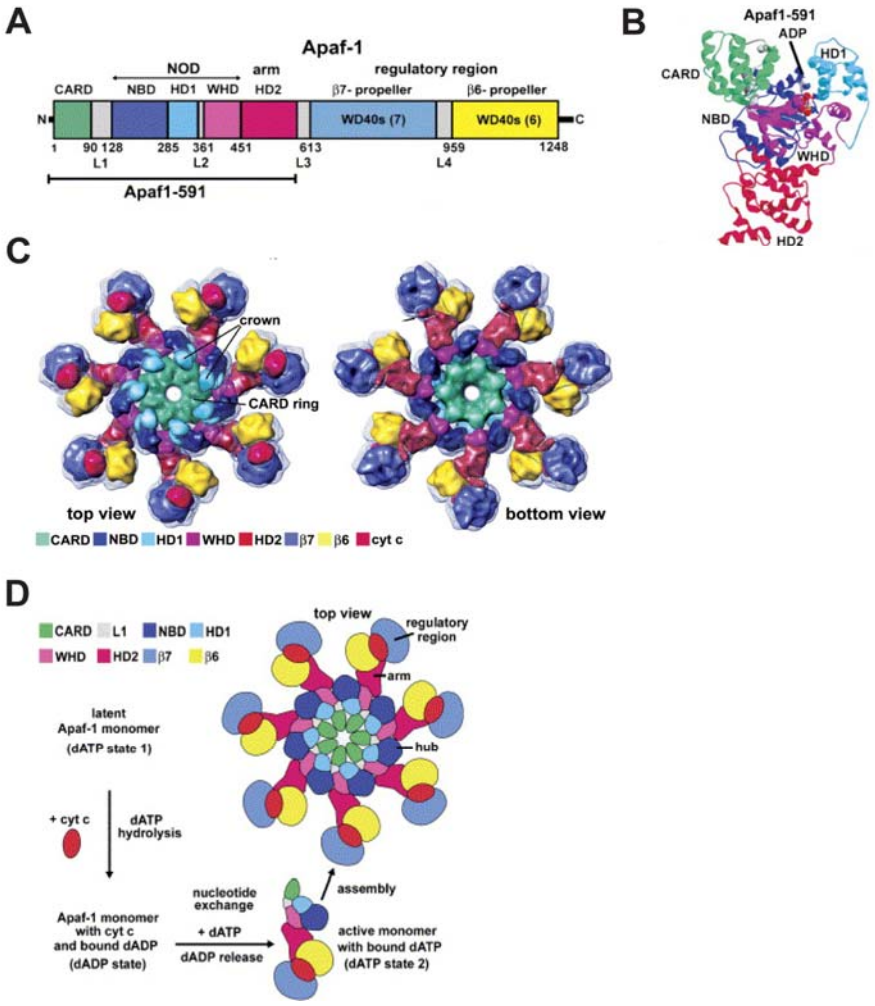

Figure 1.4: Apaf-1 Structure and Apoptosome Formation.

Figure 1.4: A. Linear diagram depicting seven major Apaf-1 domains, shown color-coded with the four linker regions in grey. **B.** Crystal structure of Apaf-1 1-591 (lacking WD40 regulatory domain) with color-coded ribbons. **C.** Top and bottom views of the apoptosome (at 12 A resolution) with color-coded domains demonstrate its seven-fold symmetry. The top view easily displays cytochrome *c* in its binding pocket and the CARD ring, where caspase-9 binding and activation occurs. From the bottom view, the interactions between each Apaf-1 monomer are more apparent. **D.** Model for apoptosome assembly (described in detail in the text). Adapted from Yu *et al.*, with permission from Elsevier.

lacking the WD40 repeats confirm that Apaf-1 is bound to nucleotide, although in this case, it was ADP instead of dADP (Riedl et al., 2005). Following cytochrome *c* binding, dATP is hydrolyzed to dADP, and it is the subsequent exchange of dADP for a fresh dATP that is necessary to drive proper Apaf-1 oligomerization (Kim et al., 2008). If the concentration of dATP is insufficient for nucleotide exchange, Apaf-1 appears to oligomerize into an inactive complex of higher molecular weight than the apoptosome. This exchange between dADP and dATP is facilitated by an exchange factor complex composed of the cellular apoptosis susceptibility protein (CAS), pp32/putative human HLA class II-associated protein (PHAPI), and heat shock protein 70 (hsp70) (Kim et al., 2008). Following these conformational changes, one Apaf-1 monomer is brought together with six others to form the heptameric foundation of the apoptosome. The exposed CARDs in the center of the structure are then able to recruit caspase-9, initiating the caspase cascade. A model for this process is shown in Figure 1.4D, which was proposed by Akey *et al.* in their structural analysis of the apoptosome.

1.2.1.2 Apaf-1 and Caspase-9 Activation

As previously indicated, the recruitment of caspase-9 to its caspase-activating platform, the apoptosome, is mediated through N-terminal CARD/CARD interactions between itself and its adaptor protein (Apaf-1). Once complexed, activation of caspase-9 is similar to that of other initiator caspases, which are thought to be activated through induced proximity dimerization (Boatright et al., 2003; Pop et al., 2006; Renatus et al., 2001). Another school of thought asserts that monomeric caspase-9 undergoes an allosteric conformational change inducing its activation, and although it is still unclear

exactly how caspase-9 and other initiator caspases are activated, these two hypotheses don't have to be mutually exclusive (Chao et al., 2005).

Caspase-9 monomers artificially driven to dimerize are active and can cleave caspase-3. However, these caspase-9 dimers are not nearly as active as caspase-9 that is activated on the apoptosome (Yin et al., 2006). Interestingly, it has also been suggested that only one of the two active sites on a caspase-9 dimer is actually active (Renatus et al., 2001). Additional studies in cell lysates and *in vitro* demonstrate that much of the cleaved (and, therefore presumably active) caspase-9 is dissociated from the apoptosome and is not nearly as active as that which is still apoptosome-bound (Malladi et al., 2009; Yin et al., 2006). One possibility is that the apoptosome provides some very slight, yet important, conformational changes in caspase-9, which make it more active than cytosolic, cleaved caspase-9. Another hypothesis is that apoptosome-bound caspase-9 has an enhanced affinity for its direct target, caspase-3 (Yin et al., 2006).

While caspase-9 can be cleaved, its cleavage is not required for activation. Non-cleavable mutants of caspase-9 are still recruited to the apoptosome and demonstrate activity toward caspase-3 (Boatright et al., 2003; Renatus et al., 2001). Therefore, unlike the effector caspases activated by the apoptosome, caspase-9 is able to be cleaved, but this step is not necessary for its activation. In fact, recent work from Shawn Bratton suggests that cleavage of caspase-9 actually facilitates its dissociation from the apoptosome (thus reducing its activity) (Malladi et al., 2009). Bratton and colleagues propose a "CARD-displacement model" for caspase-9 in which an active caspase-9 dimer dissociates from the apoptosome, leaving behind accessible Apaf-1 CARDs for

subsequent caspase-9 binding and activation. By demonstrating that caspase-9 lacking a functional CARD cannot be cleaved by the apoptosome, this displacement model was better supported than a "CARD-static model" where active caspase-9 remains attached to the apoptosome and activates cytosolic caspase-9. This new model implicates the apoptosome as a molecular timer based on the rate at which auto-processed capsase-9 dissociates from the apoptosome complex. Furthermore, it asserts that the rate of exchange involved in apoptosomal recruitment of fresh procaspase-9 is the molecular timer for how quickly caspases will be activated. Additional studies on this model are important; survival signals that affect caspase-9 recruitment to Apaf-1 effectively delay the timer, and perhaps there are other signals regulating the dissociation of active caspase-9 from the apoptosome, accelerating effector caspase activation.

Initial studies on the apoptosome have suggested that one caspase-9 monomer is recruited to each Apaf-1 CARD (leading to seven caspase-9 monomers per apoptosome) (Qin et al., 1999; Zou et al., 1999). However, more recent data suggest that perhaps each apoptosome backbone only recruits and activates two caspase-9 molecules at a time (Malladi et al., 2009). Interestingly, SEM studies from 2002 identified a dome-like structure on the central hub of Apaf-1 where the CARDs are located. While it appeared that caspase-9 would interact with Apaf-1 at this location, the dome appeared too small to contain seven caspase-9 molecules (Acehan et al., 2002). Additionally, work in our lab and others has shown that the active apoptosome fractionates around 700 kDa using gel filtration (instead of ~1 MDa), which would correlate with two caspase-9 monomers, not

seven (Chandra et al., 2006). However, further studies are needed to determine the exact ratio of caspase-9 to Apaf-1 on the active apoptosome.

1.2.1.3 Effector Caspase Activation and Cellular Dismantling

Effector caspases exist in the cell as dimers, but they require cleavage by an initiator caspase to be fully activated (Fuentes-Prior and Salvesen, 2004; Riedl and Shi, 2004; Rotonda et al., 1996). Through the apoptosome pathway, caspase-9 directly activates effector caspases-3 and -7; caspase-6 also functions as an effector caspase downstream of caspase-9, but it appears that caspase-6 is cleaved by active caspase-3 and is thus not a direct caspase-9 substrate (Slee et al., 1999). More recent studies in cells have also demonstrated that active caspase-7 can directly cleave caspase-6 downstream of caspase-9 (Inoue et al., 2009). These effector caspases can also act on other initiator caspases (such as -2, -8, and -10), although the significance of their cleavage away from their activation platforms is not entirely clear.

Effector caspases have many substrates within the cell; cleavage of these substrates can halt pro-survival signals (to indirectly advance apoptosis) and/or facilitate the apoptotic process (to directly alter caspase activity/cellular morphology). In the former case, caspase cleavage of a pro-survival protein likely results in a truncated protein, which reduces or inhibits its function, terminating its anti-death signaling capacity. The kinase Akt can be cleaved at three possible sites, resulting in a loss of kinase activity (Luthi and Martin, 2007). In other signaling pathways, MEK and EGFR are cleaved by caspases, and in both cases, cleavage decreases survival signals through

reduced phosphorylation of direct targets ERK and PLCγ-1, respectively (Luthi and Martin, 2007).

In contrast to the above examples, caspase cleavage can also directly enhance apoptotic progression by altering substrate preferences, by removing a regulatory domain on a protein, or by altering the subcellular localization of a protein. Cleavage of the protein ICAD (inhibitor of CAD) falls into the first category above, as it usually functions to inhibit the caspase activated DNase (CAD). After removing the inhibitory ICAD protein, CAD becomes fully active, cleaving DNA between nucleosomes and creating the DNA fragmentation pattern characteristic of apoptotic cells (Nicholson, 1999). Caspase-3 cleavage of Rho associated kinase-1 (ROCK1) removes a C-terminal inhibitory domain and results in a constitutively active N-terminal kinase region. ROCK1 is thought to play an important role in many of the morphological changes during apoptosis through phosphorylation of myosin light chain (MLC). MLC facilitates both plasma membrane blebbing and nuclear fragmentation through reorganization of the actin-myosin cytoskeleton and proteolysis of nuclear lamins, respectively (Coleman et al., 2001; Dix et al., 2008). Finally, some proteins undergo a change in cellular localization following caspase cleavage. Kinases PKCδ and Abl are both localized to the nucleus following caspase cleavage (Barila et al., 2003; DeVries et al., 2002). Even these truncated kinases still retain intact, functional kinase domains, leading to phosphorylation of nuclear substrates that facilitate apoptosis.

Interestingly, recent approaches involving proteomics have helped identify additional proteolytic peptides corresponding with apoptosis and caspase activity (Dix et

al., 2008; Mahrus et al., 2008). Although these methods appeared to validate the many caspase substrates already identified, they also generated many new (and, only partially overlapping) lists of caspase substrates. While these putative substrates need to be validated, and perhaps placed in the apoptotic process, the results are important to suggest that effector caspases specifically target important cellular pathways, such as transcription and DNA repair, to ensure that the cell is fully committed to apoptosis (Mahrus et al., 2008).

1.2.2 Post-translational Modification of Core Apoptosome Components

Cytochrome *c*-induced caspase activation and apoptosome formation are regulated by a variety of post-translational modifications, most of which function to inhibit or reduce caspase activation (Table 1.1) (Allan and Clarke, 2009; Kurokawa and Kornbluth, 2009). Phosphorylation of cytochrome *c* has been reported to occur at tyrosines 48 and 97, though the apoptotic consequences of these modifications remain unclear (Lee et al., 2006; Yu et al., 2008). Interestingly, cytochrome *c* also appears to be nitrosylated on its heme iron during apoptosis (Schonhoff et al., 2003). Although *in vitro* experiments suggest that this modification enhances cytochrome *c*-induced caspase activation, further experiments are needed to determine its mechanistic effect on the apoptosome specifically.

The most intensively-studied post-translational modifications occur on caspase-9 where phosphorylation (at a variety of sites) is known to reduce its activation and/or cleavage. Phosphorylation of threonine 125 (T125) on caspase-9, which was first identified as an Erk modification, decreases caspase-9 activation and processing (Allan et

al., 2003). More recently, the cyclin dependent kinase cdk1, DYRK1A, and p38α have been shown to phosphorylate caspase-9 at this site, reducing its activity and the downstream activation of caspase-3 (Allan and Clarke, 2007; Laguna et al., 2008; Seifert et al., 2008; Seifert and Clarke, 2009). Phosphorylation at threonine 125 can be reversed by protein phosphatase 1α (PP1α)-mediated caspase-9 dephosphorylation, to relieve this inhibition (Dessauge et al., 2006). In addition to phosphorylation at threonine 125, PKCζ phosphorylates caspase-9 at threonine 144 in response to hyperosmotic stress. This modification also suppresses caspase activity (Brady et al., 2005). Three different PKA phosphorylation sites, serines 99, 183, and 195, were characterized on caspase-9, but the importance of these sites in PKA suppression of caspase activity is unclear since mutating these sites failed to render the apoptosome resistant to PKA (Martin et al., 2005). Akt and CK2 have also been reported to phosphorylate caspase-9 at serine 196 and serine 348, respectively (Cardone et al., 1998; McDonnell et al., 2008). The overall relevance of these sites is unclear since they are only present in the initially chosen model organism (human and mouse, respectively) and don't appear to be otherwise conserved. Most commonly, these modifications of caspase-9 serve to at least partially protect the cell from caspase activation. However, one kinase, c-Abl phosphorylates caspase-9 at tyrosine 153 following DNA damage, which enhances caspase activity (Raina et al., 2005). These modifications, along with those affecting the caspase-3, are summarized in Table 1.1.

In terms of the third core apoptosome component, no specific and functional post-translational modifications for Apaf-1 have been reported. Previously, while looking at

Table 1.1: Post-Translational Modifications and the Apoptosome.

Substrate	Kinase/Phosphatase	Sites	+/-	Reference
Cytochrome *c*	ND	Y48	ND	(Yu et al., 2008)
Cytochrome *c*	ND	Y97	ND	(Lee et al., 2006)
Cytochrome *c*	n/a; nitrosylation	ND	+	(Schonhoff et al., 2003)
Full length Apaf-1	Rsk	S357/S760	-	(Parrish et al., in submission)
Full length Apaf-1	PP1	ND- Rsk sites	-	(Parrish et al., in submission)
Caspase-9	Erk1/2	T125	-	(Allan et al., 2003)
Caspase-9	CDK1	T125	-	(Allan and Clarke, 2007)
Caspase-9	DYRK1A	T125	-	(Seifert et al., 2008)
Caspase-9	p38α	T125	-	(Seifert and Clarke, 2009)
Caspase-9	PP1α	T125	-	(Dessauge et al., 2006)
Caspase-9	PKCζ	S144	-	(Brady et al., 2005)
Caspase-9	c-Abl	Y153	+	(Raina et al., 2005)
Caspase-9	PKA	S99, S183, S195	Unclear	(Martin et al., 2005)
Caspase-9	Akt	S196 (human)	-	(Cardone et al., 1998)
Caspase-9	CK2	S348 (mouse)	-	(McDonnell et al., 2008)
Caspase-3	PKCδ	ND	+	(Voss et al., 2005)
Caspase-3	p38	S150	-	(Alvarado-Kristensson et al., 2004)
Caspase-3	PP2A	S150	-	(Alvarado-Kristensson and Andersson, 2005)

The effect of phosphorylation at specific residues is listed as activating (+) or inactivating (-). ND= not determined.

PKA regulation of the apoptosome, Paul Clarke and colleagues reported that PKA can phosphorylate the truncated GST-tagged Apaf-1 1-543 *in vitro*. However, there were no functional consequences reported for this modification (Martin et al., 2005). Another report demonstrated JNK binding to Apaf-1, which appeared to delay apoptosome formation and caspase-9 activation, but there was no evidence of JNK phosphorylating an apoptosome component. Although Apaf-1 appeared serine-phosphorylated in their model system (cardiac myocyte), this phosphorylation did not correlate with JNK activity (Tran et al., 2007). Work in this dissertation demonstrates Rsk phosphorylation of Apaf-1, which we believe to be one of the first reported post-translational modifications for Apaf-1.

1.2.3 Apoptosomal-associated Factors and Other Mechanisms of Regulations

In addition to post-translational modifications, apoptosome formation is also regulated, in both inhibitory and activating manners, through many other mechanisms, including changes in cellular localization and the association of cellular factors and/or proteins. Even the most apical step in apoptosome formation, the binding of cytochrome *c* to Apaf-1, is affected, and cytosolic cytochrome *c* itself serves as a target for some of these regulatory mechanisms. Physiological levels of nucleotides, such as ATP and dATP, can directly bind to cytochrome *c*, inhibiting its interaction with Apaf-1 (Chandra et al., 2006). Proteins, such as the chaperone hsp27, can also interact with cytochrome *c*, inhibiting its ability to activate the apoptosome (Bruey et al., 2000). As mentioned above, the redox state of cytochrome *c* can alter its caspase activating ability, and recent work demonstrates that cellular metabolism and nutrient levels within the cell can regulate this

state (Vaughn and Deshmukh, 2008). Using both neurons and cancer cells, Vaughn and Deshmukh demonstrated that the redox state of cytochrome *c* affects its caspase-activating capacity. In healthy cells where nutrients are plentiful, cytochrome *c* is reduced and thus less potent in activating caspases. Under certain apoptotic conditions, increases in reactive oxygen species (ROS) lead to the oxidation of cytochrome *c*, which enhances its caspase-activating ability (Vaughn and Deshmukh, 2008). Recent work also characterized an interesting role for RNA in apoptosome regulation; an interaction between transfer RNA (tRNA) and cytochrome *c* reduces binding of the latter with Apaf-1, which decreases subsequent apoptosome formation (Mei et al., 2010).

The direct binding partner of cytochrome *c*, Apaf-1, is susceptible to various forms of regulation as well. The nucleotide exchange complex consisting of hsp70, CAS, and PHAPI was characterized by Xiaodong Wang and colleagues (Kim et al., 2008). The role of these proteins in apoptosome regulation is one of activation, as they facilitate proper Apaf-1 oligomerization and caspase-9 recruitment through nucleotide exchange on Apaf-1. While a direct interaction between these proteins and Apaf-1 is undetectable, it is likely that they form at least a transient complex. At physiological concentrations of protein and in the absence of these factors, cytochrome *c* forces Apaf-1 into a high molecular weight complex (even larger than the apoptosome) that is inactive. Other studies have shown that physiological concentrations of ions, such as potassium and calcium, can regulate Apaf-1 by preventing proper oligomerization (Bao et al., 2007; Cain et al., 2001; Karki et al., 2007). Another chaperone, hsp90, can bind to Apaf-1 and prevent apoptosome formation through inhibition of Apaf-1 self-association (Pandey et

al., 2000). The interaction between hsp90 and Apaf-1 is itself regulated by the phosphorylation status of hsp90, and this mechanism is very important in the reduced caspase activation detected in tyrosine kinase leukemias (Kurokawa et al., 2008). Interestingly, in a somewhat unique mechanism for apoptosome regulation, post-mitotic neurons and cardiomyocytes actually downregulate Apaf-1 protein (and likely RNA levels), making the cells very resistant to cytochrome *c*-induced apoptosis due to lack of core apoptosome components (Potts et al., 2005; Wright et al., 2004).

As discussed above, caspase-9 activation is heavily regulated by post-translational modifications. However, other mechanisms have also developed for modulating caspase-9 activity or activation. Proteins such as APIP (apaf-1-interacting protein) and TUCAN (tumor-up-regulated CARD-containing antagonist of caspase-9) inhibit apoptosome-mediated caspase activation by preventing caspase-9 recruitment to the complex (Cho et al., 2004; Pathan et al., 2001). The inhibitor of apoptosis proteins (IAPs) like XIAP and cIAP diminish caspase-9 activity through direct binding to active caspase-9. XIAP not only binds caspase-9 but also has an affinity for active caspase-3 (Deveraux et al., 1997). This inhibitor has even been detected on the apoptosome (Hill et al., 2004).

These proteins, along with the post-translational modifications discussed above, have been studied as factors regulating apoptosome formation and/or subsequent caspase activation (Table 1.2). While the summary here mostly includes cellular proteins capable of altering cytochrome *c* responsiveness, many small molecules and/or natural compounds have also been shown to modulate apoptosome formation and/or activity (Jiang et al., 2003; Nguyen and Wells, 2003; Perez-Paya et al., 2010).

Table 1.2: Apoptosomal Regulators.

Factor	Apoptosome Effect	+/-	Reference
IAP (XIAP)	Bind and inhibit active caspase-9	-	(Deveraux et al., 1997)
Aven	Inhibit Apaf-1 oligomerization	-	(Chau et al., 2000)
hsp70	Facilitate nucleotide exchange on Apaf-1; Inhibit apoptosome formation	+/-	(Beere et al., 2000; Kim et al., 2008; Saleh et al., 2000)
hsp90	Inhibit Apaf-1 oligomerization	-	(Kurokawa et al., 2008; Pandey et al., 2000)
CAS	Facilitate nucleotide exchange on Apaf-1	+	(Kim et al., 2008)
hsp27	Interact with cytochrome *c*	-	(Bruey et al., 2000)
PHAPI	Facilitate nucleotide exchange on Apaf-1	+	(Kim et al., 2008)
p21	Interact with caspase-3	-	(Suzuki et al., 1998) (Sohn et al., 2006)
Ca^{++}	Inhibit Apaf-1 nucleotide exchange	-	(Bao et al., 2007)
K^{+}	Inhibit Apaf-1 oligomerization	-	(Cain et al., 2001; Karki et al., 2007)
Glucose Metabolism	Redox inactivation of cytochrome *c*	-	(Vaughn and Deshmukh, 2008)
APIP	Inhibit caspase-9 binding to Apaf-1	-	(Cho et al., 2004)
TUCAN	Bind and inhibit caspase-9 recruitment	-	(Pathan et al., 2001)
HCA66	Interact with Apaf-1; enhances caspase-9 activation	+	(Piddubnyak et al., 2007)
HBXIP	Bind and inhibit caspase-9 recruitment	-	(Marusawa et al., 2003)
Nucling	Interact with Apaf-1 and caspase-9	+	(Sakai et al., 2004)
NAC	Interact with Apaf-1	+	(Chu et al., 2001)
ProT	Inhibit apoptosome formation	-	(Jiang et al., 2003)
AFP	Enhance caspase-9 binding to Apaf-1	+	(Semenkova et al., 2003)
AChE	Enhance cytochrome *c*/Apaf-1 interaction	+	(Park et al., 2004)
Nitric Oxide Donors	Inhibit Apaf-1 oligomerization	-	(Zech et al., 2003)
Nucleotides	Interact with cytochrome *c*	-	(Chandra et al., 2006)
Diarylurea Compounds	Inhibit Apaf-1 oligomerization	-	(Lademann et al., 2003)
Histone H1.2	Interact with apoptosome complex	+	(Ruiz-Vela and Korsmeyer, 2007)
JNK	Interact with Apaf-1	-	(Tran et al., 2007)
tRNA	Inhibit Apaf-1 oligomerization	-	(Mei et al.)
PARCS	Interact with Apaf-1	+	(Sanchez-Olea et al., 2008)

The overall effect on the apoptosome is listed as activating (+) or inactivating (-).

1.3 Apoptosis and Cancer

One of the first suggestions that apoptosis functions as a barrier to tumor cell survival was proposed in 1972, by the same researchers who characterized the morphological features of the process, Kerr, Wyllie, and Currie (Kerr et al., 1972). In this report, they discussed the idea that "the spontaneous occurrence of apoptosis in growing malignant neoplasms suggests that it might be implicated in some types of therapeutically induced tumour regression" (Kerr et al., 1972). If controlled cell death can be utilized as a mechanism for clearing "dangerous" cells, resistance to apoptosis could be considered a necessary acquisition for tumor cell survival. In 2000, Hanahan and Weinberg published a review on this topic, addressing six capabilities that most tumor cells acquire during tumorigenesis. These hallmarks of cancer include evasion of apoptosis, self-sufficiency in growth signals, insensitivity to anti-growth signals, sustained angiogenesis, limitless replicative potential, and tissue invasion/metastasis (Hanahan and Weinberg, 2000). While there is almost an infinite combination of steps that can be taken during tumorigenesis to obtain these characteristics, they do seem to be shared across most human tumors.

Evasion of apoptosis usually develops through one of two main pathways: reduced expression/activity of a pro-apoptotic protein or enhanced expression/activity of an anti-apoptotic protein. In the case of the former, losing a pro-apoptotic protein renders a tumor cell less sensitive to cell death stimuli. The most commonly occurring alteration in this category is probably loss of the p53 tumor suppressor gene, most often through mutation (Harris, 1996). The p53 protein normally senses cellular abnormalities,

including DNA damage, hypoxia, and oncogene overexpression (Levine, 1997). As a cellular transcription factor, p53 impacts many different cell signaling pathways, including the expression of pro-apoptotic bcl-2 family member proteins like PUMA (p53 upregulated modulator of apoptosis) and Noxa (Yu and Zhang, 2005).

In contrast to the loss of an apoptotic-inducing protein, tumor cells can also avoid apoptotic stimuli through overexpression of anti-apoptotic proteins. The bcl-2 protein normally functions in this capacity by inhibiting cytochrome *c* release from the mitochondria, and it is upregulated through chromosomal translocation in follicular lymphoma (Vaux et al., 1988). Increased activity of prosurvival pathways through mutation (Ras) or overexpression (ErbB2), also serves to render the cell more resistant to pro-death stimuli (Dhillon et al., 2007). Interestingly, in other cases, increased expression levels of oncogenic proteins, such as myc, can actually facilitate apoptosis (Evan and Littlewood, 1998; Pelengaris et al., 2002). Since myc is one of the most commonly overexpressed oncogenes in human tumors, it seems counterintuitive that it would actually enhance apoptosis. Perhaps this relationship demonstrates a naturally-occurring mechanism in place to clear mutant cells from the body, by enhancing their sensitivity to pro-death signals. To overcome this selection, the tumor cells likely evolve other dominant mechanisms for reducing their sensitivity to death.

Even the apoptotic pathway downstream of bcl-2 appears to be inhibited in a variety of tumor types. For example, in chronic myleogenous leukemia, it has been demonstrated that the oncogenic tyrosine kinase Bcr-Abl inhibits cytochrome *c*-induced caspase activation (Deming et al., 2004). Specifically, hypophosphorylation of hsp90β in

the Bcr-Abl-expressing cells leads to defective Apaf-1 oligomerization. Hsp90β binds to Apaf-1 more strongly in the leukemic cells, inhibiting Apaf-1 oligomerization and subsequent caspase-9 recruitment and activation. This paradigm also occurs in leukemias driven by other oncogenic tyrosine kinases, such as Tel-PDGFRβ and Flt3/D835Y (Kurokawa et al., 2008).

One of the earliest reports linking the apoptosome to apoptotic sensitivity in cancer came from studying melanoma, where Apaf-1 expression was shown to be down-regulated (Baldi et al., 2004; Fujimoto et al., 2004; Soengas et al., 2001; Soengas et al., 2005). While there is some debate regarding this particular mechanism in melanoma, many other types of cancers have now been characterized with regard to their cytochrome *c* sensitivity (Allen et al., 2005; Peltenburg et al., 2005). One of the most unique mechanisms for apoptotic resistance might occur in Burkitt lymphoma where Apaf-1 is sequestered at the plasma membrane, associated with lipid rafts (Sun et al., 2005). Non-small cell lung carcinomas (NSCLC) contain high levels of XIAP, which diminishes caspase activity downstream of the mitochondria (Yang et al., 2003). Apoptosome inhibition in cancer has also been demonstrated in ovarian cancer, bladder cancer, cervical cancer, and fibrosarcoma, just to name a few (Table 1.3) (Haga et al., 2003; Jia et al., 2001; Leo et al., 2005; Wolf et al., 2001). Despite the growing understanding of apoptosome regulation in various cancers, it seemed that little was known about apoptotic control downstream of cytochrome *c* release in some of the most common tumors, including breast cancer. Thus, we wanted to investigate cytochrome *c*-induced caspase activation in malignant mammary epithelial cells. In contrast to previously reported

Table 1.3: Cancer and the Apoptosome.

Cancer	Mechanism/Alteration	+/-	Reference
Melanoma	Reduced Apaf-1 expression (promoter methylation)	-	(Dai et al., 2004; Soengas et al., 2001; Soengas et al., 2005)
Non-small cell lung carcinoma (NSCLC)	Increased XIAP expression; Decreased PHAPI stability	-	(Hoffarth et al., 2008; Yang et al., 2003)
Chronic Myleogenous Leukemia (CML)	Reduced Apaf-1 expression	-	(Jia et al., 2003; Jia et al., 2001)
Tyrosine Kinase Leukemias	Decreased Apaf-1 oligomerization	-	(Kurokawa et al., 2008)
Bladder	Reduced Apaf-1 expression	-	(Jia et al., 2001)
Cervical	Reduced Apaf-1 expression	-	(Leo et al., 2005)
Glioblastoma	Reduced Apaf-1 expression (LOH)	-	(Watanabe et al., 2003)
Glioblastoma/Medulloblastoma/Astrocytoma	Increased Apaf-1 expression	+	(Johnson et al., 2007)
Fibrosarcoma	Reduced Apaf-1 and caspase-9 expression	-	(Haga et al., 2003)
Ovarian	Reduced recruitment of caspase-9 to Apaf-1	-	(Liu et al., 2002; Wolf et al., 2001)
Breast	Increased PHAPI expression	+	(Schafer et al., 2006b)
Pancreatic	Decreased Apaf-1/caspase-9 expression	-	(Corvaro et al., 2007)
Colon	Reduced Apaf-1 expression	-	(Zlobec et al., 2007)
Stomach, Colon, Lung, Breast, Brain	ND; cell lines appear more sensitive to cytochrome *c*	+	(Mashima et al., 2005)
Burkitt lymphoma	Apaf-1 sequestration at plasma membrane	-	(Sun et al., 2005)
Non-clear cell renal carcinoma	ND	-	(Gerhard et al., 2003)

The effect on the apoptosome and/or the sensitivity of the cancer to cytochrome *c* is listed as activating/hypersensitive (+) or inactivating/resistant (-); comparison is to appropriate normal counterpart if possible. ND= not determined.

cases, work from this dissertation demonstrates that breast cancer cells are actually hypersensitive to cytochrome *c* compared with normal mammary epithelial cells. More recent work from our laboratory has shown that brain tumors abide by this same paradigm, although this differential sensitivity occurs through a unique mechanism (Johnson et al., 2007). Normal neurons are remarkably refractory to cytochrome *c* due to downregulation of Apaf-1 and enhanced protein expression of IAPs (Wright et al., 2004). However, brain tumor cells reacquire Apaf-1 expression at the mRNA level, increasing protein levels, and enhancing their sensitivity to cytochrome *c*. Meanwhile, the surrounding normal neurons are still resistant to cytochrome *c*.

Thus, it is clear that there are many different ways that apoptotic evasion can manifest on the road to tumor formation. While mechanisms of resistance often directly affect the apoptotic machinery, changes can occur in more peripheral proteins, often in upstream signaling pathways involved in maintaining/monitoring cell survival.

1.4 The MAPK Pathway and Cell Survival

The mitogen-activated protein kinase (MAPK) pathway is activated in response to a variety of stimuli, including growth factors, serum, and phorbol esters (Anjum and Blenis, 2008). Most commonly, it directs extracellular signals to transcription factors in the nucleus, influencing a wide range of cell processes including proliferation, growth, migration, and survival. This pathway is comprised of a three-tiered kinase model where a mitogen-activated protein kinase (MAPK) is activated through phosphorylation by a mitogen-activated protein kinase kinase (MAPKK). These MAPKKs are activated by a mitogen-activated protein kinase kinase kinase (MAPKKK), which serves as the most

apical MAPK sensor. The MAPKKKs are usually activated by a stimulus, as opposed to directly initiating the signal themselves (Figure1.5). The most well-known arm of this signaling family is probably the Erk (MAPK) pathway, which has a potent role in cell survival. In contrast, the c-Jun N-terminal kinase (JNK) and p38 kinase often antagonize survival by enhancing apoptosis, but these effects can vary considerable based on the model system (Raman et al., 2007).

1.4.1 The c-Jun N-terminal Kinase (JNK) and p38 Kinase

Of the three major MAPK pathways, the two involving the kinases p38 and JNK are usually involved in orchestrating responses to various types of cellular stress, which can have effects on cell survival (Wagner and Nebreda, 2009). Otherwise known as the stress-activated protein kinase (SAPK), the JNK family of kinases can phosphorylate and regulate the expression of 14-3-3 proteins and various bcl-2 family members, including Bax and Bad (Kim et al., 2006). In the case of 14-3-3, JNK phosphorylation releases 14-3-3 from binding pro-apoptotic proteins, like Bax and FOXO, in an inactive state, which then allows them to function in their pro-apoptotic roles (Sunayama et al., 2005; Tsuruta et al., 2004; Weston and Davis, 2007). In contrast, JNK can also function as an oncogene, negatively regulating the p53 tumor suppressor pathway (Das et al., 2007). Many of these oncogenic, pro-survival functions of JNK are mediated through transcription factors, such as c-Jun. Thus, JNK can promote or inhibit apoptosis, and the outcome is often cell type (and, stimulus) specific. Additionally, it appears as though the role of JNK in cell survival is rooted in the strength and/or duration of the signal.

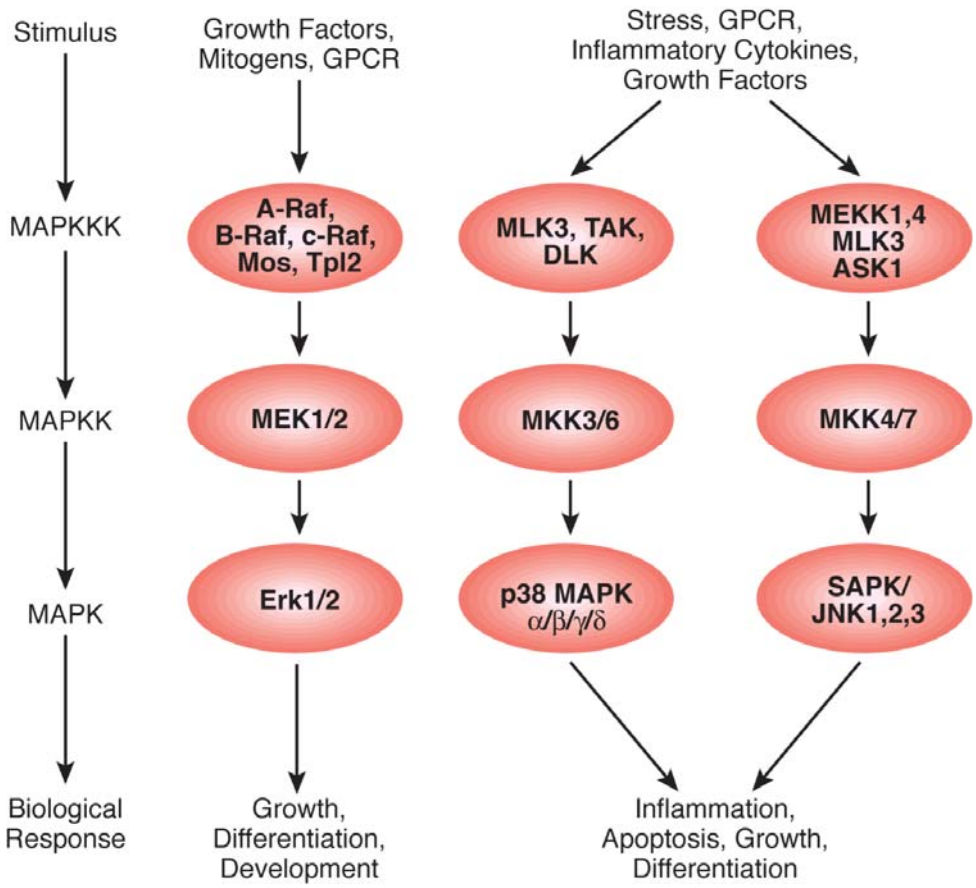

Figure 1.5: The Mitogen-Activated Protein Kinase (MAPK) Pathway.

Figure 1.5: Basic illustration of the major MAPK pathways emphasizing the three-tiered activation. The Erk1/2 pathway functions predominantly in a pro-survival manner, following direct activation by MEK1/2 and indirect activation by a variety of signals/MAPKKKs. JNK and p38 signaling pathways are known to play a more antagonistic role in a cell, depending on the cell type and stimulus. Adapted from pathway diagram courtesy of Cell Signaling Technology, Inc. (www.cellsignal.com).

The other commonly pro-apoptotic MAPK, p38, is also stimulated under conditions of cell stress. Specifically, the p38 family members, of which there are four, can respond to a range of cues, including osmotic shock, hypoxia, UV radiation, and pro-inflammatory cytokines (Raman et al., 2007). Characterization of the mice lacking expression of both MEK3 and 6 (the upstream MAPKKs for p38) suggests that p38 functions as a tumor suppressor, which would support its role in facilitating apoptosis (Dhillon et al., 2007). However, increased levels of active (phosphorylated) p38 have also been correlated with malignancies, including follicular lymphoma and lung, breast, and thyroid carcinomas (Elenitoba-Johnson et al., 2003; Esteva et al., 2004; Greenberg et al., 2002; Pomerance et al., 2006; Wagner and Nebreda, 2009). Although complicated, these data suggest that (similarly to JNK) p38 may be able to play both pro-survival and pro-death roles in a cell, depending on the stimulus, cell type, and/or tumor stage (Wagner and Nebreda, 2009).

1.4.2 The Extracellular Signal-Related Kinase (ERK)

The third major arm of the MAPK pathway, the extracellular signal-related kinases (Erk), is the best understood of the mammalian MAPK pathways. It most often functions to inhibit cell death, contrasting with the more complicated roles of p38 and JNK in cell survival. The specific effectors involved in the ERK pathway include the MAPKKs, MEK1/2, which lead to activation of the MAP kinases Erk1/2. This pathway, through the MAPKKK Raf and its upstream activator Ras, is deregulated in about one-third of all human cancers, most frequently due to mutations in these upstream signaling effectors (Dhillon et al., 2007). Constitutively activated Ras is probably the most

common mechanism for hyperactivating Erk in cancer as it is mutated in over 30% of tumors (Bos, 1989). Ras mutations occur in a myriad of tumor types, including pancreatic, liver, and thyroid (Downward, 2003). Raf is also commonly altered in tumors, including mutations in melanoma and colon cancer, among others (Davies et al., 2002). Apical of Ras and Raf, various receptor tyrosine kinases, including EGFR and ErbB2, are overexpressed in tumors as well.

The Erk pathway promotes cell survival both directly and indirectly. In terms of the former mode of regulation, Erk can negatively impinge on the apoptotic pathway. It has been shown to phosphorylate the BH3-only protein Bim at three sites (serines 55, 65, and 100), reducing its interaction with Bax (Harada et al., 2004). Farther downstream the apoptotic pathway, Erk inhibits caspase activation through phosphorylation of caspase-9 as was previous discussed in this introduction (Allan et al., 2003).

Erk can also promote cell survival indirectly through other effectors/kinases. Under a variety of circumstances, Erk activates the p90 kDa ribosomal S6 kinase (Rsk) through phosphorylation. Rsk was first identified as a kinase that phosphorylated rpS6 in unfertilized *Xenopus laevis* eggs, and the MAPK/Rsk pathway is highly active during *Xenopus* oocyte maturation and mitosis (Erikson and Maller, 1985, 1989). Two Rsk isoforms have been characterized in *Xenopus* eggs, while there are four known human isoforms. Both Erk and Rsk have direct substrates that are involved in the regulation of cell survival; Rsk1 can phosphorylate the BH3-only protein, Bad at serine 112, inhibiting Bad-mediated apoptosis upstream of mitochondria, while Rsk1 and Rsk2 have both been

shown to suppress the pro-apoptotic activity of DAPK through phosphorylation at serine 289 (Anjum et al., 2005; Shimamura et al., 2000).

In sum, MAPK signaling plays critical roles in regulating cell survival. In response to a variety of stimuli, the three main effector pathways (JNK, p38, and ERK) interact with apoptotic regulators and machinery, ultimately weighing in on the decision regarding a cell's fate.

1.5 Studying Apoptosis Using *Xenopus laevis*

Eggs from the amphibian *Xenopus laevis* are poised to undergo the rapid and synchronized divisions that occur after fertilization. They can perform these initial events in the absence of any novel transcription and are thus densely packed with cellular components. Arrested in metaphase II of meiosis, these eggs experience a dramatic rise in the concentration of cytosolic Ca^{++} upon fertilization, which initiates cellular division. This process can be mimicked in making egg extract through centrifugation, which crushes the eggs and releases internal stores of Ca^{++}. Similarly to fertilization, this cell-free extract can re-synthesize cyclin B after its initial degradation, allowing it to cycle in and out of mitosis (Murray, 1991). This ability makes the *Xenopus* extract a unique model system for the field of cell division.

Permanent interphase extracts can be made by adding cyclohexamide prior to centrifugation, which inhibits the novel translation of cyclin B (Smythe and Newport, 1991). However, even this extract can be driven into a mitotic state through the addition of a recombinant, non-degradable cyclin B. In addition to using this interphase egg extract to study the cell cycle, the cell-free system can recapitulate cellular events such as

protein movement through the nuclear pore complex, DNA replication, entry into mitosis, and apoptosis (Blow and Laskey, 1986; Kluck et al., 1997; Murray and Kirschner, 1989; Newmeyer et al., 1994; Newport and Forbes, 1987). Apoptosis in the extract was initially characterized in 1994 by Newmeyer and colleagues (Newmeyer et al., 1994). They noted that after incubating the extract at room temperature (25^{o}C) for two to four hours, the extract spontaneously entered apoptosis, condensing chromatin and shrinking/fragmenting the nuclei (Newmeyer et al., 1994). Subsequent studies would demonstrate that caspases are also activated in this process (Kluck et al., 1997). However, it was more than ten years later when studies from our lab demonstrated that this spontaneous apoptosis was a result of nutrient depletion in the extract (Nutt et al., 2005). Interestingly, these initial observations by Newmeyer *et al.* suggested the requirement for an organelle fraction enriched with mitochondria, which we can now explain by the need for mitochondrial cytochrome *c* release under apoptotic conditions.

In addition to mitochondria and cytosol, the crude extract discussed above also contains nuclear components. This crude cell-free extract (interphase and/or mitotic) can be fractionated into these components using high speed centrifugation. Specifically, ultracentrifugation yields cytosol, light membrane (endoplasmic reticulum), heavy membrane (mitochondria and rough endoplasmic reticulum), and an insoluble fraction (ribosomes, glycogen, assembled cytoskeletal proteins, and large protein complexes). This cytosolic extract is ideal for analyzing apoptosis downstream of cytochrome *c* release from the mitochondria because it is completely devoid of mitochondrial contamination and can be produced in large quantities. Exogenous cytochrome *c* can be

added back to this extract with energy regenerating mix, leading to apoptosome formation and subsequent effector caspase activity. In addition, this extract can be easily manipulated to examine the importance of certain proteins and pathways. For example, immunodepletion assays can be used to eliminate the presence or activity of certain proteins. Additionally, certain pharmacological inhibitors can be used in a similar manner without any regard for cell permeability. Recombinant proteins can be easily added to the extract in an eluted form or on beads. These types of experiments, in crude or cytosolic extract, can be utilized characterize or identify components involved in general apoptosis and apoptosome formation.

2. Materials and Methods

2.1 Cell Culture

Primary HMECs were obtained from Clonetics, and hTERT immortalized HMECs were a kind gift from Stephen Kendall and Christopher Counter (Duke University). All other cell lines were obtained from ATCC. Cells were maintained according to the specifications of the American Type Culture Collection (ATCC) except during the serum starve when the cells were incubated with media containing only .5% FBS. Specifically, HMEC, HMEC hTERT, and MCF-10a cells were maintained in MEGM (Clonetics). T47D, BT-474, LNCaP, and NCI-H460 cells were maintained in RPMI media supplemented with 10% FBS, 4.5 g/L glucose, 10 mM HEPES, 1 mM sodium pyruvate, and 0.2 units/mL insulin. 293T, MDA-MB-231, MDA-MB-361, and MDA-MB-453 cells were maintained in DMEM supplemented with 10% FBS. PC-3 and A549 cells were maintained in Hams F12K media supplemented with 10% FBS. DU-145 cells were maintained in EMEM supplemented with 10% FBS, 1 mM sodium pyruvate, and 0.1 mM non-essential amino acids. HT-29, HCT-116, and SK-Ov-3 cells were maintained in McCoys 5A media plus 10% FBS. NHBE cells were maintained in BEGM (Clonetics) and PrEC cells were maintained in PrEGM (Clonetics).

For transfection, Fugene-6 (Roche) was used in a ratio of 3:2 with DNA. Prior to phorbol 12-myristate 13-acetate (PMA) treatment, 293T cells were serum-starved for 24 hours. PMA was added for 30 minutes at a final concentration of 25 ng/mL. Cells were then harvested and lysed.

2.2 *Xenopus* Egg Extract

To induce egg laying, mature female frogs were injected as described previous (Smythe and Newport, 1991). Jelly coats were removed from the eggs by incubating with 2% cysteine, pH 8.0. Eggs were then washed three times with modified Ringer's solution (MMR: 1 M NaCl, 20 mM KCl, 10 mM $MgSO_4$, 25 mM $CaCl_2$, 5 mM Hepes, pH 7.8, 0.8 mM EDTA) and three times in egg lysis buffer (ELB: 250 mM sucrose, 2.5 mM $MgCl_2$, 1.0 mM dithiothreitol, 50 mM KCl, 10 mM Hepes, pH 7.7). Eggs were centrifuged at 400 *g*, and cytochalasin B (5 μg/mL), aprotinin/leupeptin (5 μg/mL), and cyclohexamide (50 μg/mL) were added. Lysis was performed by centrifugation for 12 minutes at 10,000 *g*. Crude egg extracts were supplemented with 2 mM ATP, 50 μg/mL creatine kinase, and 20 mM phosphocreatine. Mitotic extracts were prepared by adding non-degradable cyclin B1 to interphase extracts. Cytosolic interphase and mitotic extracts were made by centrifuging crude extract at 55,000 rpm (250,000 *g*) for 70 minutes in a Beckman TLS-55 rotor for the TL-100 ultracentrifuge (Beckman Instruments). The cytosolic fraction was removed and recentrifuged at 55,000 rpm for an additional 30 minutes. The pure cytosol was then removed, aliquoted, frozen in liquid nitrogen, and stored at -80^{o}C for future use.

2.3 Mammalian Extract Preparation

2.3.1 Breast Cancer Cell Lysates

Cell-free extracts were prepared from the cell lines described above. Cells were collected, washed in PBS, pelleted, and resuspended in an equal volume of cell lysis buffer (50 mM Pipes, pH 6.7, 50 mM KCl, 5 mM EGTA, 2 mM $MgCl_2$, 1 mM DTT, 1

mM PMSF, 5 µg/mL leupeptin, 5 µg/mL aprotinin). Cells were lysed by freeze-thawing three times and centrifuged for 30 minutes at 14,000 rpm at 4°C (Eppendorf 5415C) (Cain et al., 1999). The supernatants were collected, assayed for protein concentration using the Bradford Assay (BioRad), and stored in aliquots at -80°C. For measuring cytochrome *c* release in response to adriamycin or cisplatin treatment, cells were harvested, washed once with phosphate buffered saline (PBS), and pelleted. Cell pellets were then resuspended in two times the pellet volume of hypotonic lysis buffer (20 mM HEPES, pH 7.4, 10 mM KCL, 1.5 mM $MgCl_2$, 1 mM EDTA, 1 mM EGTA, 1 mM DTT, 1 mM PMSF, 5 µg/mL leupeptin, 5 µg/mL aprotinin) and rocked at 4°C for 20 minutes. The cells were then lysed by passage through a 27.5 gauge needle 10 times and subsequently centrifuged at 1500 rpm for 10 minutes. The supernatant was then spun at 10000 rpm for 10 minutes in order to remove the mitochondria.

2.3.2 Breast Tumor Tissue Lysate

The integrity of frozen specimens was examined with H/E staining. Specimens were then added to a bead beater tube and 300 µl of lysis buffer (50 mM Tris, pH 8.0, 5 mM EDTA, 150 mM NaCl, 0.5% NP-40, 1 mM PMSF, 5 µg/mL leupeptin, 5 µg/mL aprotinin, 50 mM NaF) was added. Tissue was homogenized for 40 seconds on a bead beater. Lysate was then collected and spun at 14,000 rpm (Eppendorf 5415C) for 30 minutes at 4°C. Lysate concentration was then tested via Bradford assay.

2.3.3 Rsk-related Mammalian Lysates

Cytosolic extracts were made as previously described (Johnson et al., 2007; Kurokawa et al., 2008). Briefly, cells were harvested and washed once with PBS.

Following centrifugation to pellet the cells, they were resuspended in buffer X (20 mM Hepes, pH 7.5, 10 mM KCl, 1.5 mM $MgCl_2$, 1 mM EDTA, 1 mM EGTA, 250 mM sucrose, 1 mM DTT, 1 mM PMSF, 5 μg/mL aprotinin/leupeptin) at a volume approximately equal to that of the cell pellet. They were incubated on ice for 30 minutes and then lysed by passage through a 25 gauge needle 40 times. They were subsequently centrifuged at 14,000 rpm (Eppendorf 5415C) for 30 minutes at 4°C.

Whole cell lysates were prepared by incubating cells in RIPA buffer (50 mM Tris, pH 7.5, 1% NP-40, .25% sodium deoxycholate, 1 mM EDTA, .1% SDS, 10 mM β-glyercophosphate, 5 μg/mL leupeptin, 5 μg/mL aprotinin, 1mM sodium vanadate, 1 mM PMSF) or extraction buffer T (20 mM Hepes, pH 7.5, 150 mM NaCl, 12.5 mM β-glycerophosphate, 1.5 mM $MgCl_2$, 2 mM EGTA, 10 mM NaF, 2 mM DTT, 1 mM sodium vanadate, 1 mM PMSF, 20 μM aprotinin, 0.5% Triton-X 100) for 20-30 minutes on ice. The cells were then centrifuged at 14000 rpm (Eppendorf 5415C) for 30 minutes, and the supernatant was harvested. All lysates were quantitated by Bradford Assay using the (Bio-Rad).

2.4 Kinase Assays

2.4.1 Kinase Assays in Extract

For the Apaf-1 kinase assays in extract, approximately 10 μg of nickel-agarose bound His-Apaf-1 was incubated in 100 μL of interphase or mitotic extract with 2 μCi γ-^{32}P ATP. After 1 hour at 30^{o}C, the beads were removed and washed three times in washing buffer M (1 mM Hepes-KOH, pH 7.5, 1 mM β-glycerophosphate, 15 mM KCl,

.1% NP-40, 1 mg/mL imidazole, 500 mM NaCl, 1 mM sodium vanadate, 5 μg/mL leupeptin, 5 μg/mL aprotinin). The entire sample was then subjected to SDS-PAGE and analyzed with autoradiography. The kinase assays with an antibody proceeded similarly except that less total protein was incubated in extract for 30 minutes at 25^{o}C. Samples were subjected to SDS-PAGE, followed by immunoblot analysis.

2.4.2 *In Vitro* Kinase Assays

For the *in vitro* kinase assay, nickel-agarose bound His-Apaf-1 protein was incubated in kinase buffer (10 mM Tris-HCl, pH 7.5, 0.1 mM ATP, 10 mM $MgCl_2$, 1 mM DTT, pH 7.2) with 2 μCi γ-^{32}P ATP and the appropriate kinase. The reaction proceeded for 30 minutes at 30°C, at which point, the beads were washed with buffer M (same as in extract kinase assay). Samples were then run on SDS-PAGE, and incorporation of ^{32}P was evaluated by autoradiography.

2.5 Dephosphorylation Assays

2.5.1 Dephosphorylation Assays in Extract

For the dephosphorylation assay in extract, nickel-agarose bound His-Apaf-1 was pre-phosphorylated *in vitro* by Rsk2 as described above. The pretreated protein was then washed in buffer X (20 mM Hepes, pH 7.5, 10 mM KCl, 1.5 mM $MgCl_2$, 1 mM EDTA, 1 mM EGTA, 1 mM DTT, 1 mM PMSF, 5 μg/mL leupeptin, 5 μg/mL aprotinin) and dipped into interphase or mitotic extracts for the indicated times. Upon retrieval, beads were washed in buffer X and then subjected to SDS-PAGE. Phosphorylation of Apaf-1 was examined via autoradiography.

2.5.2 Dephosphorylation Assay with dipped PP1

The dephosphorylation assay using recombinant PP1 proceeded as above except that the pre-phosphorylated Apaf-1 was incubated with nickel-agarose bound His-PP1, which had been pre-incubated in interphase extract for 1 hour.

2.6 Caspase Assays

2.6.1 Mammalian Caspase Assays

Mammalian caspase assays were performed similarly to those previously described by our lab (Deming et al., 2004). Briefly, mammalian lysates at 10 mg/mL were incubated at 37^{o}C with various concentrations of cytochrome *c* and 1mM dATP. Fifty micrograms of protein was utilized to assess caspase activation in a 96-well plate assay with the caspase assay buffer (50 mM Hepes, pH 7.4, 100 mM NaCl, 0.1% CHAPS, 10 mM DTT, 1 mM EDTA, 10% glycerol) and the colorimetric substrate, Ac-DEVD-pNA (BioMol). All samples were read at 405 nm on a Bio-Rad Plate Reader (Bio-Rad Microplate Reader, Model 680).

2.6.2 *Xenopus* Egg Extract Caspase Assay

Xenopus caspase assays were performed similarly to those previously described by our lab (Deming et al., 2004). Following the addition of an energy regenerating mix (2 mM ATP, 20 mM phosphocreatine, 50 μg/mL creatine kinase), cytosolic extract was incubated at 25^{o}C with purified cytochrome *c*. Three microliters of cytosolic extract was added to the caspase assay buffer (50 mM Hepes, pH 7.4, 100 mM NaCl, 0.1% CHAPS, 10 mM DTT, 1 mM EDTA, 10% glycerol) with the colorimetric substrate. All samples

were read at 405 nm on a Bio-Rad Plate Reader (Bio-Rad Microplate Reader, Model 680).

2.7 *In vitro* Reconstitution of the Apoptosome

Recombinant Apaf-1 protein (200 nM) was pre-phosphorylated by Rsk2 at 30°C for 30 minutes in kinase buffer (same as for *in vitro* kinase assay). Apaf-1 was then incubated with 10 μM dATP, 250 nM cytochrome *c*, 25 nM caspase-9, and ^{35}S-labeled, i*n vitro* translated caspase-3 at 30^{o}C for an additional 30 minutes. The reaction was stopped with 2x SDS sample buffer, and caspase-3 processing was assessed by SDS-PAGE and autoradiography.

2.8 Cloning and Recombinant Protein Expression

2.8.1 GST-tagged Caspase-9 Prodomain

The GST-tagged caspase-9 prodomain (along with all subsequently listed GST proteins) was produced using the Kornbluth standard GST protocol previously described (Evans et al., 1997). In sum, the GST-caspase-9 prodomain was produced in BL21 DE3 bacteria induced at 18^{o}C overnight with .5 mM IPTG (Deming et al., 2004). Bacteria were lysed in 2.5 mL of Buffer A (2.3 M sucrose, 5 mM Tris, pH 7.5, 1 mM EDTA) with 1 mM PMSF. Then, 10 mL buffer B (50 mM Tris, pH 7.5, 10 mM KCl, 1 mM EDTA, 1 mM DTT), 4 mg lysozyme, and 100 μL of 100 mM PMSF were added to the pellet. The bacteria were incubated on ice for 1 hour, at which point 175 μL of 10% sodium deoxycholate, 263 μL of 1 M $MgCl_2$, 25 μL of DNase I (5 mg/mL) were added. The mixture was centrifuged at 12,000 rpm for 30 minutes. The supernatant was then pooled and incubated with glutathione-sepharose beads for ~2 hours at 4°C. Beads were washed

three times with buffer C (10 mM Hepes, pH 8.0, 1 mM DTT) and 300 mM NaCl, followed by three times of additional washing with buffer C alone.

To make the T125A mutant prodomain, the wildtype DNA was subjected to site-directed mutagenesis using the QuickChange Mutagenesis Kit, per the manufacturer's instructions (Strategene), and the following primers:

Forward: 5'-GGTTCTCAGACCGGAAGCACCCAGACCAG-3'

Reverse: 5'-CTGGTCTGGGTGCTTCCGGTCTGAGAACC-3'

2.8.2 GST-tagged Apaf-1 CARD

The GST-tagged Apaf-1 CARD was produced as above following induction in BL21 bacteria with .5 mM IPTG at 18^{o}C overnight.

2.8.3 GST-tagged Apaf-1 1-543

The GST-tagged Apaf-1 1-543 was produced as above following induction in BL21 DE3 bacteria with .5 mM IPTG for 4 hours at 30^{o}C.

2.8.4 GST-tagged XIAP

The GST-tagged XIAP was produced as above following induction in BL21 bacteria with 50 μM IPTG at 23 ^{o}C overnight.

2.8.5 His-tagged full length Apaf-1

Full-length human Apaf-1 baculovirus was provided by Xiaodong Wang (UT Southwestern). For protein production, 2x10^{6} sf9 cells were infected with 20 mL of Apaf-1 baculoviruses and pre-incubated for 2 hours. HyQ SFX-Insect Media (Hyclone) was then added, and the cells were incubated at 25^{o}C for an additional 28 hours. The cells

were harvested, and washing buffer X (same as in dephosphorylation assays) was added to the cell pellets. Cells were homogenized by douncing 100 times on ice, and lysates were centrifuged at 10,000 *g* for 1 hour. The clear supernatant was incubated with 1 mL of packed nickel-agarose beads (Qiagen) for 90 minutes, followed by washing with buffer X including 1 M NaCl and 14.8 mM imidazole. The beads were then washed twice in buffer X alone, and Apaf-1 protein was eluted with 250 mM imidazole in buffer X (8 fractions of 500 µL). The eluants were dialyzed into buffer X, aliquoted, and snap-frozen in liquid nitrogen. The proteins were stored in -80°C.

2.8.6 GST-tagged Inhibitor-2

Recombinant GST-inhibitor-2 (GST-I2) was made from bacteria induced with .5 mM IPTG while incubating at 37^{o}C for 4-6 hours. Protein purification proceeded as above in 2.8.1 except that GST-I2 proteins were eluted with 5 mM Glutathione in buffer C, pH 8 and dialyzed into buffer X.

2.8.7 His-tagged Protein Phosphatase-1

Recombinant rabbit PP1 (wildtype and T320A) were produced as previously described (Wu et al., 2009). Briefly, bacteria were induced with .5 mM IPTG and 1 mM $MnCl_2$ overnight at 25^{o}C. Cells were harvested and lysed as indicated above for the GST proteins. After addition of the DNase, the pellet was also sonicated. The cleared supernatant was incubated with 1 mL nickel-agarose beads for 2 hours at 4^{o}C. The column was washed with buffer C, including 30 mM imidazole and 300 mM NaCl. PP1 was eluted with buffer C and 200 mM imidazole. Eluted fractions were dialyzed into ELB with 1 mM $MnCl_2$.

2.8.8 Radiolabled, *In Vitro* Translated Proteins

To produce radiolabeled *in vitro* translated protein, 5 μg of pcDNA3 caspase-3 or 5 μg of pcDNA3 caspase-9 cDNA was added to rabbit TNT reticulocyte lysate (Promega) with 0.4 μCi/μL ^{35}S-Translabel and additional components in accordance with the manufacturer's protocol.

2.9 Affinity Binding Assays

2.9.1 Cytochrome *c* and Apaf-1

To examine the recruitment of Apaf-1 to cytochrome *c*, 50 μL of *Xenopus* extract or 500 μg of mammalian lysate was added to 20 μL of packed agarose-bound cytochrome *c* (Sigma). Beads were incubated at 25^{o}C for 20 minutes or 37^{o}C for 10 minutes, respectively. They were then washed three times in lysis buffer containing 500 mM NaCl.

2.9.2 Apaf-1 and the Caspase-9 Prodomain

To characterize recruitment of Apaf-1 to the caspase-9 prodomain, glutathione-sepharose bound GST-capsase-9 (WT or T125A) was incubated in *Xenopus* egg extract for 30 minutes at 25^{o}C. Beads were then retrieved and washed three times with ELB supplemented with 500 mM NaCl.

2.9.3 Caspase-9 and the Apaf-1 1-543

To assay caspase-9 binding to the GST-Apaf-1 1-543, glutathione-sepharose bound GST-Apaf-1 1-543 was incubated in *Xenopus* egg extract with ^{35}S-labeled caspase-9 at 25^{o}C for the indicated times. Beads were then washed three times in ELB.

2.9.4 Rsk and Apaf-1

To assess binding of Rsk to Apaf-1, nickel-agarose bound His-Apaf-1 (or empty nickel-agarose, Qiagen) was blocked at 4^{o}C for 1 hour with 1% casamino acids. The empty beads had been pre-blocked with .125 M histidine. These blocked beads were then incubated in interphase or mitotic extract for 1 hour at 25^{o}C. Beads were washed with ELB with 500 mM NaCl.

2.9.5 PP1 and Apaf-1

In order to assess binding of endogenous *Xenopus* PP1 to Apaf-1, nickel-agarose bound His-Apaf-1 (or empty nickel-agarose, Qiagen) was blocked at 4^{o}C for 1 hour with 1% casamino acids. The empty beads had been pre-blocked with .125 M histidine. These blocked beads were then incubated in interphase or mitotic extract for 1 hour at 25^{o}C. Beads were then washed with buffer M (same as in kinase assays above).

2.10 Gel Filtration Chromatography

Xenopus cytosolic lysates were incubated in the presence of 2 ng/μL cytochrome *c* at 25^{o}C for 45 minutes. Buffer X was then added to a final volume of 300 μL. After incubation, the reaction mixture was loaded onto a Superdex 200 column at a flow rate of 0.3 mL/min. Fractions were collected and analyzed by immunoblotting.

2.10.1 Cleavage of *In Vitro* Translated Caspase-9 in Gel Filtration Fractions

To analyze the cleavage of ^{35}S-labeled *in vitro* translated caspase-9, 2 μL of caspase-9 was added to 40 μL of each fraction. The reaction proceeded at 30^{o}C for 1

hour, at which point it was stopped by adding SDS sample buffer. Samples were subjected to SDS-PAGE and autoradiography to assess caspase-9 cleavage.

2.11 Immunoprecipitation Assays

2.11.1 Caspase-9 Immunoprecipitation

To immunoprecipitate the apoptosome on caspase-9, 10 μg caspase-9 antibody (Upstate) was pre-coupled to 25 μL of Protein G-sepharose beads. Fifty microliters of lysate (at 10 μg/μL) was then activated with 1 mM dATP and 1 ng/μL cytochrome *c* for 10 minutes at 37°C. Activated lysate was precleared on 25 μL of Protein G-sepharose and then incubated with precoupled antibody/beads overnight at 4°C. Beads were washed 3 times with RIPA buffer and resolved via SDS-PAGE and subsequent western blotting.

2.11.2 Apaf-1 Immunoprecipitation

Approximately, 1 μg of Apaf-1 (or IgG control) antibody was used per 500 μ*g* of whole cell lysate, and they were incubated together for 1 hour at 4^{o}C. The antibody (along with bound proteins) was retrieved at 4^{o}C for 1 hour using Protein G-sepharose resin that had been pre-blocked in 10% BSA. The beads were washed in RIPA lysis buffer. Samples were then subjected to SDS-PAGE and immunoblotting.

2.12 b-VAD-fmk Caspase-9 Activity Assay

Biotin-VAD-fmk (Alexis) was used to isolate active caspase-9. To 500 μg of cell-free lysate (at 10 mg/mL), 20 μM b-VAD-fmk, 3 ng/μL cytochrome *c*, and 1 mM dATP were added and incubated at 37^{o}C for 30 minutes. Reaction volume was then brought up to 300 μL with cell lysis buffer, and 30 μL of packed streptavadin sepharose beads

(Pierce) were added for overnight incubation at 4°C. Beads were then washed three times in cell lysis buffer and resolved via SDS-PAGE.

2.13 Rsk2 Immunodepletion

For the Rsk immunodepletion, 5 μg of IgG control or Rsk2 antibody were used per 150 μL of crude extract. After three rounds of depletion for 30 minutes each, the depleted crude extract was removed from the beads and utilized in subsequent assays, as usual. For the add back experiment, 50 μM active Rsk2 was added back to mitotic extract before incubation with agarose-bound cytochrome *c*.

2.14 PHAPI Assays

2.14.1 PHAPI Addition

Recombinant PHAPI (Calbiochem, packaged as $I1^{PP2A}$) was added at 75 ng to 500 μg of cell-free extract (at 10 mg/mL) and incubated at 37°C for 30 minutes. Cytochrome *c* was then added at 3 ng/μL, and caspase-3 activation was assessed as described above.

2.14.2 PHAPI Antibody Block

For antibody blocking experiments, 15 μg of PHAPI antibody (Abcam) was added to 500 μg of cell-free extract (at 10 mg/mL), and incubated at 4°C for 1 hour. Cytochrome *c* was then added at 3 ng/μL, and caspase-3 activation was assessed as described above. For the add back experiments, 10 μL of PHAPI protein was incubated with 15 μg of antibody prior to antibody addition to the extract.

2.14.3 PHAPI siRNA

PHAPI knockdown was achieved using siRNA duplexes generated by Eurogentec. T47D cells were transfected using the Transit-TKO reagent (Mirus) with either the siRNA negative control duplex or the following duplex targeting PHAPI (100 nM) (Yu et al., 2004): (5'-GGACGCCCUCUGAUGUGAATT-3', 5'-UUCACAUCAGAGGGCGUCCTT-3').

2.14.4 PHAPI and Phosphatase Assay

Phosphatase activity in the various lysates was measured as described previously (Margolis et al., 2003).

2.15 RT-PCR

RNA was isolated using the Trizol Reagent (Invitrogen) per the manufacturer's instructions; it was then treated with DNase I (Ambion). For RT-PCR, first-strand cDNA was synthesized with an oligo(dT) primer by adding ≈300 μg of RNA with SuperScript III Reverse Transciptase (Invitrogen). Real-time PCR was performed using iQ SYBR Green Supermix (BioRad), 5 ng of cDNA, and 10 μM of the primers listed below. Real-time quantitation was performed using a BioRad iCycler iQ System. Data were normalized to GAPDH, and fold change was determined with the $2^{-\Delta\Delta CT}$ method (Livak and Schmittgen, 2001).

PHAPI Forward: 5'-ACCAACCTGAACGACTACCGA-3'

PHAPI Reverse: 5'-CGTCTTCCACTACCTGAGCAT-3'

GAPDH Forward: 5'-TGCACCACCAACTGCTTAGCACCC-3'

GAPDH Reverse: 5'-CCACCACTGACACGTTGGCAG-3'

2.16 Microinjection

Cells were microinjected with soluble cytochrome *c* as previously described (Potts et al., 2003; Wright et al., 2004). The concentration of bovine heart cytochrome *c* (Sigma) injected was 10 μg/μL. In order to mark the microinjected cells, the microinjection solution (100 mM KCl and 10 mM KPi, pH 7.4) contained 4 mg/mL of rhodamine dextran. Cell viability was determined by counting the number of rhodamine-positive cells that had intact, phase-bright cell bodies, immediately after injection and at varying times post-injection. Cell survival is expressed as a percentage of the original number of cells microinjected.

2.17 Mass Spectrometry (performed in collaboration with the Duke Proteomics Facility)

2.17.1 Sample Preparation: In-Solution Digestion and Phosphopeptide Enrichment

Approximately 50 μg of eluted Apaf-1 protein was used for an *in vitro* kinase assay with active Rsk2. They were incubated in kinase assay buffer (from the *in vitro* kinase assay detailed above) for 30 minutes at 30^{o}C. Since both proteins were in solution, the reaction was stopped by flash freezing and placing at -80^{o}C for submission to the Proteomics Facility. Prior to in-solution digestion, samples were buffer exchanged into 50 mM ammonium bicarbonate, pH 8.0 using a 7 KDa MWCO Zeba Spin gel filtration spin column according to the manufacturer's protocol (Thermo Scientific). Rapigest acid labile surfactant (Waters Corp.) was added to samples at a final concentration of 0.1%. Samples were reduced with 10 mM dithiothreitol for 15 minutes at 70°C and alkylated with 20 mM iodoacetamide for 45 minutes at room temperature followed by proteolytic

digestion with sequencing grade modified trypsin (Promega) at a ratio of 50:1 (protein:enzyme, w/w) for 18 hours at 37°C . Digested samples were acidified to pH 2.0 by adding neat TFA, incubated at 60°C for 2 hours to hydrolyze Rapigest surfactant, and then spun at 15,000 rpm for 10 minutes to remove insoluble material.

The digested peptide mixture was enriched for phosphopeptides using a 4 μg binding capacity TiO_2 ProteaTip pipette tip (Protea Biosciences). Prior to enrichment, samples were brought to dryness using vacuum centrifugation and resuspended in 100 μL 80% acetonitrile, 1% TFA, and 100 mg/mL dihydroxybenzoic acid. Each sample was loaded by aspirating the sample twenty times and by then washing twice with 100 μL of 80% acetonitrile, 1% TFA, 50 mg/mL dihydroxybenzoic acid and twice with 100 μL of 80% acetonitrile, 1% TFA. Enriched phosphopeptides were eluted from the TiO_2 column by aspirating ten times in 100 μL of 20% acetonitrile, 5% aqueous ammonia, pH 10.0. Samples were brought to dryness using vacuum centrifugation, and they were resuspended in 10 μL of 2% acetonitrile, 0.1% TFA, 50 mM citric acid prior to LC-MS analysis.

2.17.2 LC MS/MS

A 5 μL injection of the phosphopeptide enriched peptide mixture was loaded onto a Waters NanoAcquity HPLC equipped with a 180 μm x 2 cm Symmetry guard column (Waters Corp.) coupled in-line with a 75 μm x 15 cm BEH130 UPLC analytical column (Waters Corp.) packed with 1.7 μm C18 reversed-phase particles. Peptides were eluted using a linear gradient from 5% acetonitrile/0.1% formic acid to 40% acetonitrile/0.1%

formic acid over 60 minutes at a flow rate of 300 nL/min. Analytical column temperature was maintained at 55°C throughout analysis. The NanoAcquity system was coupled to a Thermo LTQ-Orbitrap XL mass spectrometer through an electrospray ionization interface. Ionization was accomplished by applying 1.9 kV to a PicoTip Emitter (New Objective) with a 10 μm spray tip.

The mass spectrometer was operated in full FT-FT mode with precursor scans from m/z 400-2000 in the orbitrap at a resolution of 60,000 and 3 MS/MS scans in the orbitrap at a resolution of 7500 for precursor ions which were 2+ charged and above ions above a threshold of 10000 counts. MS/MS fragmentation was accomplished using collision-induced dissociation (CID) with Argon gas with a CID setting of 35%. Each product ion selected for MS/MS fragmentation was subsequently placed on an exclusion list for 60 seconds to increase dynamic range.

2.17.3 Data Analysis

MS/MS data were searched against a SwissProt (*Homo sapiens* taxonomy) protein database using Mascot database searching algorithm (Matrix Science). Data was searched using trypsin specificity, and mass tolerances were set to 20 ppm for precursor MS scans and 0.02 Da for product ion scans. Static modifications of +57.0 Da on Cys residues corresponded to alkylation, and dynamic modifications of +16.0 Da on Met and +80.0 Da on serine, threonine, and tyrosine residues corresponded to oxidation and phosphorylation modifications, respectively. Data was visualized in Scaffold (Proteome Software) with peptide confidence thresholds set to achieve an approximate 1% false positive rate.

2.18 Western Blot Analysis

Cytosolic egg extract (~80 μg) or cell-free extracts lysates (100 μg) were subjected to SDS-PAGE analysis, and proteins were transferred to PVDF membranes (Immobilon/Millipore). Membranes were subsequently immunoblotted with antibodies listed below. Alexa-fluor secondary antibodies to rabbit, mouse, or rat were then used to visualize primary antibodies (Molecular Probes). Blots were then developed using the Li-Cor Odyssey Infrared Imaging System. Protein array of human normal/malignant breast tissue was from the BioChain Institute (A1235713-1).

2.18.1 Antibodies

The following antibodies were used for immunoblotting: anti-Apaf-1 (polyclonal, 1:1000) from Stressgen; anti-Apaf-1 (monoclonal, 1:1000) and anti-PHAPI (monoclonal, 1:1000) from Alexis; anti-cytochrome *c* (monoclonal, 1:500) from PharMingen; anti-RXRXXS*/T* (monoclonal, 1:1000), phospho-Erk (polyclonal, 1:1000), cleaved caspase-3 (polyclonal, 1:1000), and anti-pS6 (Ser235/236) (polyclonal, 1:1000) from Cell Signaling; anti-Rsk2 (rabbit polyclonal, 1:1000) and anti-β-actin (polyclonal, 1:2000) from Santa Cruz; human caspase-9 (polyclonal, 1:1000) from Neomarkers; anti-caspase-3 (polyclonal, 1:1000) from Upstate; anti-PHAPI (polyclonal, 1:1000) from Prosci; and anti-β-actin (monoclonal, 1:4000) from Sigma-Aldrich. The *Xenopus* PP1 antibody was made previously as described (Wu et al., 2009).

2.19 Reagents

Active Rsk was obtained from Upstate/Millipore. Roscovitine, cytochalasin B, and active ERK were from Calbiochem. Cytochrome *c*-agarose beads, ATP, horse cytochrome *c*, yeast cytochrome *c*, phosphocreatine, okadaic acid, and PMA were purchased from Sigma-Aldrich. The MEK1/2 inhibitor U0126 was from Biosource. Aprotinin, leupeptin, FuGENE 6, and creatine kinase were acquired from Roche. The Rsk inhibitor, SL0101, was purchased from Toronto Research Chemicals, Inc. Recombinant PHAPI was obtained from Calbiochem (packaged as I1PP2A). The Rsk inhibitor BI-D1870 was acquired from B-Bridge International.

2.20 Statistics

Unless otherwise indicated, standard error of the mean (SEM) was calculated and graphed from at least three independent experiments using the equation $SEM=SD/\sqrt{N}$ where SD equals the standard deviation, and N is the number of experiments. To calculate the p values, a two-tailed t-test was performed.

3. Enhanced Sensitivity to Cytochrome *c*-Induced Apoptosis Mediated by PHAPI in Breast Cancer Cells

(This Chapter appears in modified form in: Cancer Res. 2006 Feb 15; 66(4): 2210-2218.)

3.1 Introduction

As discussed in Chapter 1, apoptosis is cellular process that has a paramount role in development and tissue homeostasis (Danial and Korsmeyer, 2004). Altered apoptotic signaling also often contributes to disease progression; indeed, in cancer, evasion of apoptosis has been characterized as a fundamental property of tumorigenesis (Hanahan and Weinberg, 2000). These mutations or modifications of the apoptotic pathway allow malignant cells to survive and proliferate under cellular conditions that would normally trigger cell death.

Paradoxically, many cancer treatments, including chemotherapies, attempt to stimulate tumor regression through activation of apoptosis, which facilitates tumor cell death and removal. Unfortunately, these approaches are often unsuccessful due to defects in the apoptotic pathway discussed above. Additionally, these chemotherapeutic regimens are not specifically designed to target the malignant cells for death; for example, many of them target rapidly dividing cells, encompassing tumor cells in addition to other normal tissues. Thus, patients often experience unwanted side effects, such a hair loss, reducing their overall morale in addition to the chemotherapeutic efficacy. This chemoresistance commonly leads to treatment failure and, possibly, cancer recurrence and/or metastasis (Johnstone et al., 2002).

To help solve this problem, researchers have been working to design more targeted therapies, which take advantage of unique molecular differences between normal and malignant cells. Some of the recent chemotherapeutics with clinical effectiveness include Gleevec (imatinib mesylate), Herceptin (trastuzumab), and Iressa (gefitinib) (Chang et al., 2004; Dan et al., 1998; Mohsin et al., 2005). While there is still much progress to be made in these areas (relative to designing targeted cancer therapies for more cancer types), understanding differences in apoptotic regulation between normal and malignant cells may provide the necessary foundation for developing more specific and effective chemotherapeutic strategies.

To continue proliferating even in the presence of these chemotherapeutic treatments, malignant cells could have altered apoptotic signaling upstream and/or downstream of mitochondrial cytochrome *c* release. As discussed in Chapter 1, many reports have characterized tumor-related mechanisms for regulating caspases after mitochondrial cytochrome *c* release (Table 1.3). However, we were interested to find that little is known about cytochrome *c*-induced apoptosis in one of the most common and frequently studied cancers types, breast cancer. While a few reports have demonstrated reduced expression of the effector capsase-3 in breast cancer cells, the relevance and frequency of these changes are unclear (Devarajan et al., 2002; Janicke et al., 1998). Additionally, the IAP survivin is upregulated in many types of cancer, including breast (Kennedy et al., 2003b; Tanaka et al., 2000). It has been characterized as a negative regulator of apoptosis and as a player in the cell cycle; studies in breast cancer have suggested it is a predictor of early recurrence (Andersen et al., 2007; Yamashita et al.,

2007). Treating hormone responsive breast cancer with the anti-estrogen tamoxifen has facilitated growth arrest and apoptosis in malignant mammary epithelial cells (Mandlekar and Kong, 2001). However, chemoresistance remains an enormous issue due to the acquired hormone independence of some breast cancers and their subsequent increase in metastases (Campbell et al., 2001). Treatment of breast cancers with another small molecule inhibitor for ErbB2, lapatinib (GW572016/Tykerb), yields a similar problem, with many patients showing initial promise only to later have recurrence of lapatinib-resistant tumors (Chen et al., 2008; Xia et al., 2006). A detailed analysis of the apoptotic difference between normal and malignant mammary epithelial cells (specifically downstream of cytochrome *c* release) could possibly facilitate the development of novel and more effective treatments for breast cancer.

We have found that breast cancer cells display an unusual sensitivity to cytochrome *c*-induced apoptosis, which is quite different from the apoptosome inhibition described in most other cancers. Specifically, in comparison with their normal counterparts, malignant mammary epithelial cells show increased caspase activation in response to cytochrome *c*. This sensitivity, not observed in other tumors, appears to stem from increased recruitment of caspase-9 to the Apaf-1 CARD. We have identified PHAPI, a putative tumor suppressor protein, as the mediator of this enhanced apoptosome formation. PHAPI is overexpressed in breast cancer cells and in breast tumors. Furthermore, we demonstrate that direct cytochrome *c* microinjection into the cytosol of mammary epithelial cells preferentially killed malignant mammary epithelial

cells, suggesting that direct activation of the apoptosome might serve to a chemotherapeutic strategy for specifically targeting breast cancer cells to die.

3.2 Results

3.2.1 Cytosolic Extracts from Breast Cancer Cells are Hypersensitive to Cytochrome *c*

The addition of exogenous cytochrome *c* to cytosolic cell lysates has been previously shown to serve as a functional model for the reconstitution of apoptotic events downstream of the mitochondria (Liu et al., 1996). For this study, we utilized this approach to compare the cytochrome *c*-induced caspase activation of various normal and malignant mammary epithelial cell lines. In response to the addition of cytochrome *c*, lysates prepared from the breast cancer cell lines T47D, MDA-MB-231, MDA-MB-361, BT-474, and MDA-MB-453 demonstrated enhanced cleavage of the synthetic caspase-3 substrate Ac-DEVD-pNA compared to lysates from immortalized normal mammary epithelial cell lines (MCF-10a, HMEC hTERT) or from primary human mammary epithelial cells (HMEC) (Figure 3.1A). This result suggests that breast cancer cells are hypersensitive to cytochrome *c* compared to their normal counterparts. Additionally, although the breast cancer cells uniformly showed higher levels of cytochrome *c*-induced caspase activation, they were variable with respect to other characteristics, including estrogen-receptor and HER2 status, aggressiveness, and tumorigenicity in mice (Lacroix and Leclercq, 2004). In addition to the dose-responsive sensitivity to cytochrome *c*, the breast cancer cells were also able to activate caspases more robustly to a fixed dose of cytochrome *c* (Figure 3.1B).

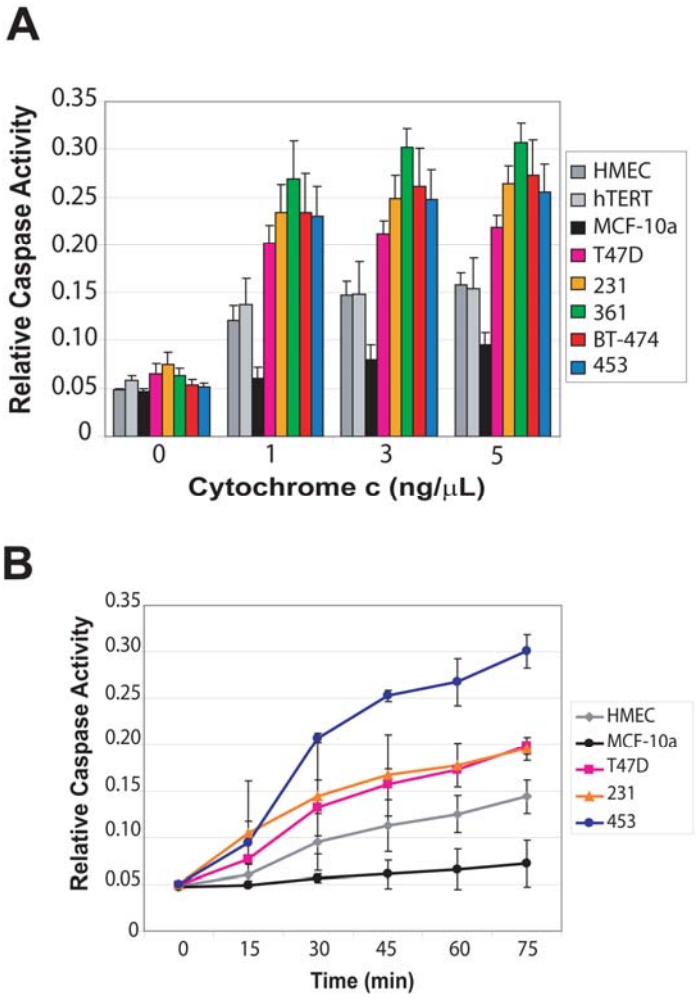

Figure 3.1: Malignant Mammary Epithelial Cells are Sensitive to Cytochrome *c*-Induced Apoptosis.

Figure 3.1: A. Cytosolic lysates from the indicated cell lines were supplemented with varying amounts of cytochrome *c*, and caspase activation was monitored via cleavage of the colorimetric caspase-3 substrate, Ac-DEVD-pNA. **B.** Cytochrome *c* was added to the indicated cell lines at 3 ng/μL, and the cleavage of Ac-DEVD-pNA was monitored over time. Data shown are mean +/-SEM for at least three independent experiments.

3.2.2 Breast Cancer Cells are Resistant to Chemotherapy-Induced Mitochondrial Cytochrome *c* Release

Given our counterintuitive finding, we sought a mechanistic explanation for the hypersensitivity of breast cancer cells to cytochrome *c*. Our initial hypothesis was that malignant mammary epithelial cells might be refractory to apoptotic stimuli due to inhibition of mitochondrial cytochrome *c* release and thus would be unlikely to have high levels of cytosolic cytochrome *c*. To test this hypothesis, we treated cells with adriamycin and cisplatin, two apoptotic-inducing chemotherapeutic agents. While both drugs caused only a small amount of cell death in the cytochrome *c*-hypersensitive breast cancer cell line MDA-MB-231, the normal HMEC cells were almost completely killed in response to these treatments (Figure 3.2A). To ensure that adriamycin and cisplatin were inducing a cytochrome *c*-mediated cell death, we immunoblotted cytosolic cell lysates from the drug-treated normal and malignant mammary epithelial cells. Consistent with the above observations, we found that both adriamycin and cisplatin induced mitochondrial cytochrome *c* release in normal HMEC cells whereas the breast cancer cells released considerably less cytochrome *c* (Figure 3.2B).

3.2.3 Breast Cancer Cells are Unique in Their Hypersensitivity

We also wanted to compare the cytochrome *c* sensitivity of breast cancer cells to that of other cancers. Therefore, we prepared cytosolic lysates from tumors of epithelial origin, including malignant prostate, ovarian, lung, and colon cells. Surprisingly, upon testing their response to cytochrome *c* using the caspase-3 substrate Ac-DEVD-pNA, we realized that the breast cancer cells were unique in their hypersensitivity to cytochrome *c*

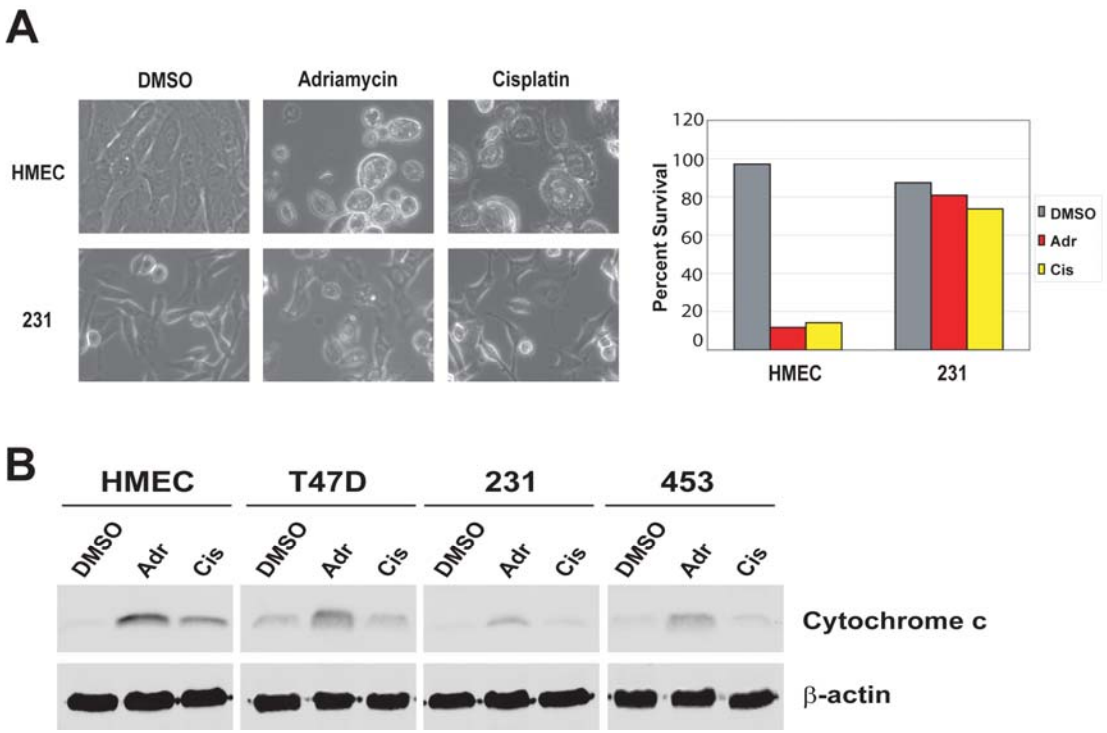

Figure 3.2: Resistance of Breast Cancer Cells to Chemotherapy-Induced Cytochrome *c* Release.

Figure 3.2: A. HMEC and MDA-MB-231 cells were treated with 100 μM adriamycin or cisplatin for 24 hours. Representative pictures are shown. **B.** Cytosolic lysates were prepared from the treated cells, and immunoblotting was performed using cytochrome *c* and β-actin antibodies.

(Figure 3.3). As previously reported, malignant ovarian (Sk-Ov-3) and lung (A549, NCI-H460) cells were refractory to cytochrome *c*-induced caspase activation (Krepela et al., 2004; Liu et al., 2002; Wolf et al., 2001; Yang et al., 2003). Both prostate (DU145, PC3, LNCaP) and colon (HT-29, HCT-116) cancer cells also demonstrated resistance to cytochrome *c*-induced apoptosis (Figure 3.3). These data separate breast cancer cells from other epithelial malignancies regarding their apoptotic sensitivity following release of mitochondrial cytochrome *c*.

3.2.4 Hypersensitivity of Breast Cancer Cells is Independent of Changes in Expression of Core Apoptosome Components

Several previous reports on the regulation of post-mitochondrial apoptosis in cancer demonstrate that altered expression levels of core apoptosomal components serve as the mechanistic locus of control (Janicke et al., 1998; Soengas et al., 2001). Therefore, we immunoblotted normal and malignant mammary epithelial cell lysates for caspase-9, Apaf-1, and caspase-3. All of the hypersensitive breast cancer cell lines, in addition to the non-malignant controls (HMEC and MCF-10a), expressed equivalent levels of caspase-9, Apaf-1, and caspase-3 protein (Figure 3.4A-C). Furthermore, the majority of the cell lines expressed similar levels of the caspase inhibitors XIAP and cIAP-1 (Figure 3.4D). Even though MCF-10a and MDA-MB-361 cell lines both contain less XIAP, they display differential responses to cytochrome *c*, which demonstrates that changes in levels of XIAP are not responsible for the cytochrome *c* hypersensitivity of breast cancer cells (Figure 3.4D).

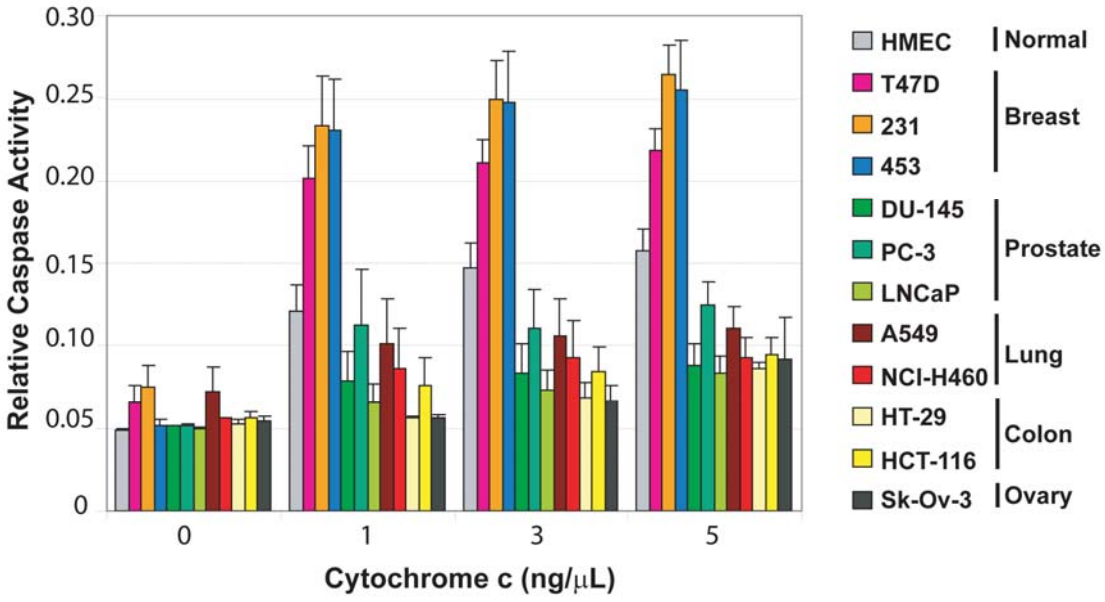

Figure 3.3: Breast Cancer Cells Are Unique in Their Cytochrome *c* Sensitivity.

Figure 3.3: Cytosolic lysates were prepared from the indicated cell lines and supplemented with varying doses of cytochrome *c*. Caspase activation was monitored through cleavage of the colorimetric caspase-3 substrate, Ac-DEVD-pNA. Data shown are mean +/-SEM for at least three independent experiments.

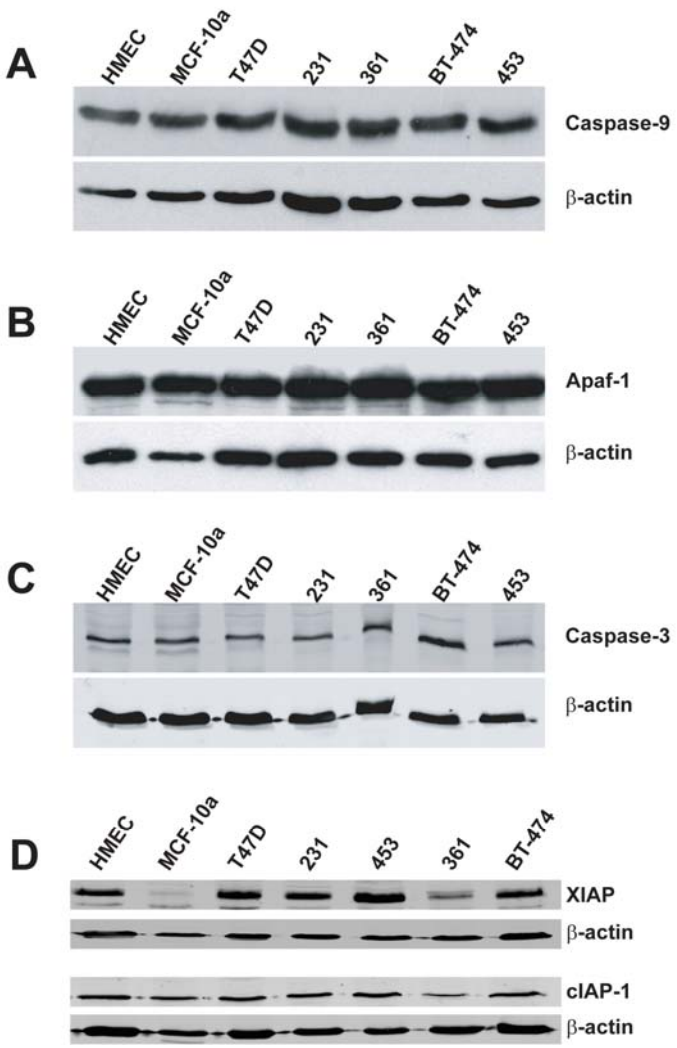

Figure 3.4: Expression of Core Apoptosome Components.

Figure 3.4: A-D. Cytosolic lysates from the indicated cell lines were immunoblotted for caspase-9 **(A)**, Apaf-1 **(B)**, caspase-3 **(C)**, and XIAP/cIAP-1 **(D).** Immunoblotting with the β-actin antibody was used as a loading control.

3.2.5 Malignant Mammary Epithelial Cells Have Increased Caspase-9 Activation in Response to Cytochrome *c*

Although the cytochrome *c* sensitivity of malignant mammary epithelial cells did not appear to be due to changes in the levels of various apoptosomal proteins, the differences in hypersensitivity correlated well with the degree of caspase-3 and caspase-9 cleavage in cytochrome *c*-supplemented lysates (Figure 3.5A,B). Even though cleavage of caspase-9 is not necessary for its enzymatic activity, processing does reflect the activity of caspase-3 and caspase-9 as both contribute to the cleaved caspase-9 doublet seen via immunoblot (Boatright et al., 2003). To more closely examine the amount of cleaved caspase-9 in these lysates, we produced recombinant XIAP fused to an N-terminal glutathione S-transferase (GST) tag. The XIAP binding site on caspase-9 is only accessible following dimerization-induced cleavage at amino acid 315 (aspartic acid) (Srinivasula et al., 2001). Thus, glutathione sepharose-bound GST-XIAP served as an affinity reagent for cleaved caspase-9. We could determine the amount of cleaved caspase-9 present in each lysate by examining the amount bound to GST-XIAP. Caspase-9 binding to GST-XIAP was less abundant in lysates from the normal HMECs, compared to the T47D, MDA-MB-231, and MDA-MB-453 cells (Figure 3.5C). Taken together, these results further suggest that increased apoptosome activation mediates the sensitivity of breast cancer cells to cytochrome *c*. It has also been shown that caspase activation can be monitored by assaying caspase recruitment to a biotinylated caspase substrate (b-VAD-fmk) that only interacts with the active site of the caspase while it is active

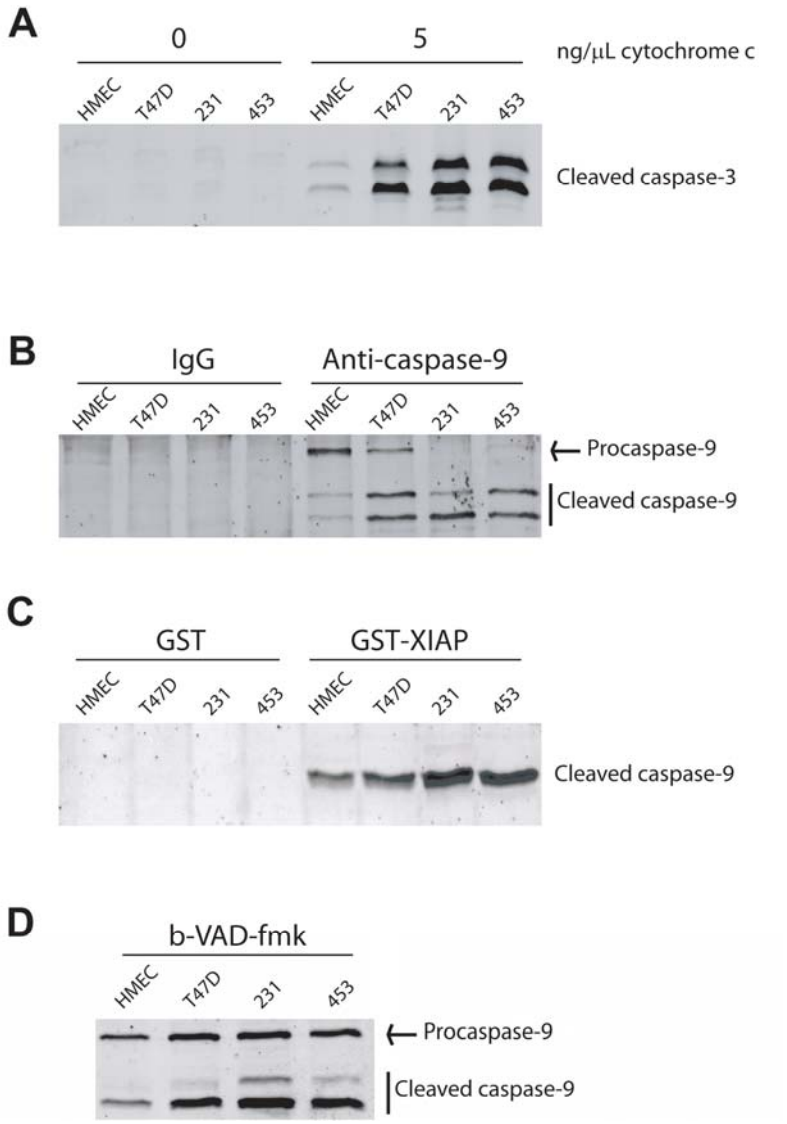

Figure 3.5: Increased Activation of Caspase-3 and Caspase-9 in Breast Cancer Cells.

Figure 3.5: A. Lysates from the indicated cell lines were supplemented with either 0 or 5 ng/μL of cytochrome *c*, and immunoblotting was preformed with a cleaved caspase-3 antibody. **B.** Immunoprecipitation with IgG or caspase-9 antibody was performed in equal concentrations of cell lysates following the addition of 1 ng/μL cytochrome *c*. Proteins were then isolated on protein G sepharose and immunoblotted for caspase-9. **C.** GST or GST-XIAP was added to lysates from the indicated cell lines. Lysates were then activated with 1 ng/μL of cytochrome *c*, and sepharose-bound glutathione was used to isolate proteins. Beads were immunoblotted for caspase-9. **D.** Cytochrome *c* at 3 ng/μL and b-VAD-fmk (20 μM) were added to lysates from the indicated cell lines. Streptavadin beads were then used to isolate the b-VAD-fmk and associated proteins. Beads were immunoblotted for caspase-9.

(Read et al., 2002). In the breast cancer lysates, the b-VAD-fmk binds to more caspase-9 compared to the normal HMECs (Figure 3.5D). This result is consistent with the idea of breast cancer cells having a hyperactivated apoptosome in response to cytochrome *c*.

3.2.6 Increased Binding Between Caspase-9 and Apaf-1 CARD in Malignant Mammary Epithelial Cells

The results presented thus far suggest that the apoptosome is hyperactive in malignant mammary epithelial cells, and to further examine the mechanism for this increased activity, we tested the hypothesis that altered apoptosome assembly was causing this change. We started with the most apical step in apoptosome formation, the binding between cytochrome *c* and Apaf-1. To characterize this interaction, we use a cytochrome *c*-agarose resin to recruit endogenous Apaf-1 from lysates. Specifically, we incubated cytosolic lysates from normal and malignant mammary epithelial cells with mammalian cytochrome *c* resin or yeast cytochrome *c* resin. The yeast cytochrome *c* resin serves as a negative control since it lacks the capacity to bind Apaf-1 (Kluck et al., 2000). Using immunoblotting, we then examined the amount of associated Apaf-1 on the cytochrome *c* resin. As seen in Figure 3.6A, the cell lysates had equivalent levels of Apaf-1 recruited to the mammalian cytochrome *c* resin, which suggests that a change in the interaction between cytochrome *c* and Apaf-1 was unlikely to underlie the increased responsiveness of breast cancer cells to cytochrome *c*.

As discussed in Chapter 1, once cytochrome *c* interacts with Apaf-1, the Apaf-1 monomer undergoes a conformational change, allowing for oligomerization and subsequent binding of caspase-9 to the newly exposed Apaf-1 CARD. Therefore, we next

examined the recruitment of caspase-9 to the Apaf-1 CARD. There are many different tools for evaluating this step in the process; we utilized one of the most simple since it does not require cytochrome *c*. The isolated Apaf-1 CARD was used to retrieve caspase-9 from cytosolic lysates by adding the GST-Apaf-1 CARD to cytosolic lysates from normal and malignant mammary epithelial cells. The Apaf-1 CARD (and associated proteins) could then be isolated on glutathione-sepharose beads. Sepharose-bound proteins were examined by immunoblotting to detect any associated caspase-9. As seen in Figure 3.6B, we detected an increased caspase-9 association with the Apaf-1 CARD in the breast cancer (T47D, MDA-MB-231, and MDA-MB-453) lysates compared to lysates from normal HMECs (Figure 3.6B). To examine this finding in a more endogenous setting, we immunoprecipitated the apoptosome on caspase-9 (Hill et al., 2004). Supporting our results using the Apaf-1 CARD, we observed an enhanced association between endogenous Apaf-1 and caspase-9 in the lysates from malignant mammary epithelial cells when compared to normal mammary epithelial cells (Figure 3.6C). Taken together, these data strongly support the hypothesis that an enhanced association between caspase-9 and Apaf-1 in malignant mammary epithelial cells renders them more susceptible to cytochrome *c*-induced apoptosis than the normal mammary cells.

3.2.7 Overexpression of PHAPI in Breast Cancer Cells Drives Their Increased Responsiveness to Cytochrome *c*

The increased recruitment of caspase-9 to Apaf-1 in malignant mammary epithelial cells appeared to be driving the hypersensitivity of these cells to cytochrome *c*.

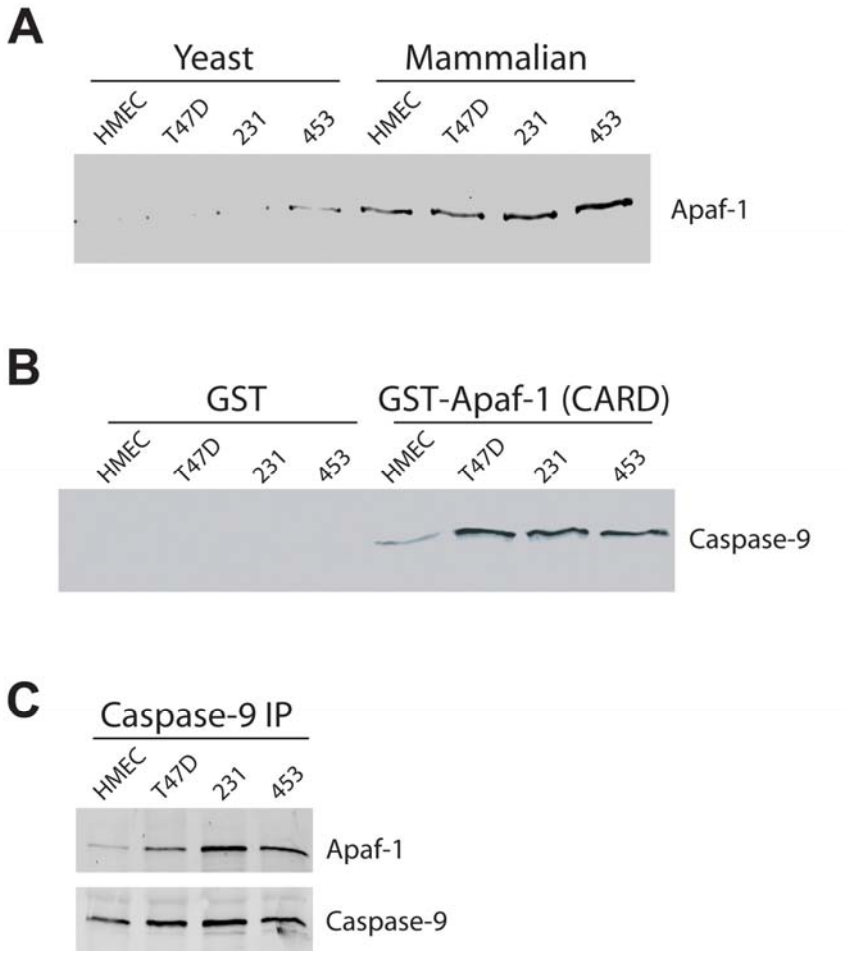

Figure 3.6: Enhanced Caspase-9 Recruitment to the Apaf-1 CARD in Breast Cancer Cells.

Figure 3.6: A. Sepharose-bound yeast or mammalian cytochrome *c* was added to the indicated cell lysates. Beads were then immunoblotted for Apaf-1. **B.** GST or GST-Apaf-1 (CARD) was added to the indicated cell lysates, and beads were subsequently immunoblotted for associated caspase-9. **C.** Caspase-9 was immunoprecipitated from the indicated extracts in the presence of 1 ng/μL cytochrome *c*, and precipitates were blotted for both caspase-9 and Apaf-1.

However, we were also interested in the molecular mechanism governing this change. A report published just a few years prior to this work demonstrated that PHAPI could stimulate and enhance the association between caspase-9 and Apaf-1 (Jiang et al., 2003). PHAPI, which is also known as pp32, mapmodulin, and $I1^{PP2A}$, can function as a putative tumor suppressor, opposing Ras and Myc-induced oncogenic transformation; its highly acidic carboxyl terminus appears to be required for this function (Bai et al., 2001; Brody et al., 1999). PHAPI has also been implicated as an inhibitor of protein phosphatase 2A (PP2A), a binding partner/regulator of microtubule-associated proteins, and as a modulator of histone acetylation and transcription as a member of the INHAT complex (Li et al., 1996; Seo et al., 2002; Ulitzur et al., 1997). Importantly, the role of PHAPI in regulating the apoptosome does not appear to necessitate a direct physical interaction with the complex (Hill et al., 2004). Recent studies published after our work define a more clear role for PHAPI in regulating the apoptosome, suggesting that it serves as part of the nucleotide exchange complex for Apaf-1 (Kim et al., 2008). Given that PHAPI was reported to mediate an apoptosome-related phenotype mimicking that which we observe in breast cancer cells (increased recruitment of caspase-9 to the Apaf-1 CARD), we immunoblotted the mammary epithelial cell lysates for PHAPI. Interestingly, we discovered that PHAPI was overexpressed in the cytochrome *c* responsive breast cancer cells, compared to the normal HMECs (Figure 3.7A).

To elucidate the role of PHAPI overexpression in the cytochrome *c* sensitivity of breast cancer cells, we performed a caspase assay in cytosolic lysates from the non-tumorigenic HMECs supplemented with recombinant PHAPI at levels roughly equivalent

to those found the cancer cells. Adding PHAPI to the HMEC lysates was sufficient to restore caspase activity to levels similar to those observed in malignant cells, which suggests that the levels of PHAPI in breast cancer cells are elevated enough to increase their sensitivity to cytochrome *c* (Figure 3.7B). Much like the *Xenopus* egg extract described in Chapter 1, these lysates do not support transcription or translation. Thus, these results suggest that PHAPI increases caspase-9 activation post-translationally.

We also performed loss-of-function experiments to demonstrate the effects of inhibiting PHAPI in breast cancer cells. One method for interfering with PHAP's function was to utilize the PHAPI antibody as a potential blocking agent in cytosolic lysates. We pre-incubated cytosolic lysates from cells expressing high levels of PHAPI (breast cancer cells) with an IgG or PHAPI antibody. We then activated these lysates with cytochrome *c* to assess caspase activity. Interestingly, the PHAPI antibody did act as a neutralizing agent in the cytochrome *c* hypersensitive breast cancer cell lines by diminishing caspase-3 activity (Figure 3.7C), which argues that the high levels of PHAPI in the tumor lines significantly influence the altered apoptosome activity seen in these cells. To further validate this result, we attempted to neutralize the PHAPI blocking antibody with recombinant PHAPI by pre-incubating them together. We then added this antibody to lysate from the MDA-MB-231 cell line and assessed caspase activity after cytochrome *c* addition. Incubating recombinant PHAPI with the antibody was sufficient to reduce the effect of the antibody, maintaining cytochrome *c* sensitivity in the lysate and confirming the specificity of the PHAPI antibody to the target, endogenous PHAPI (Figure 3.7D).

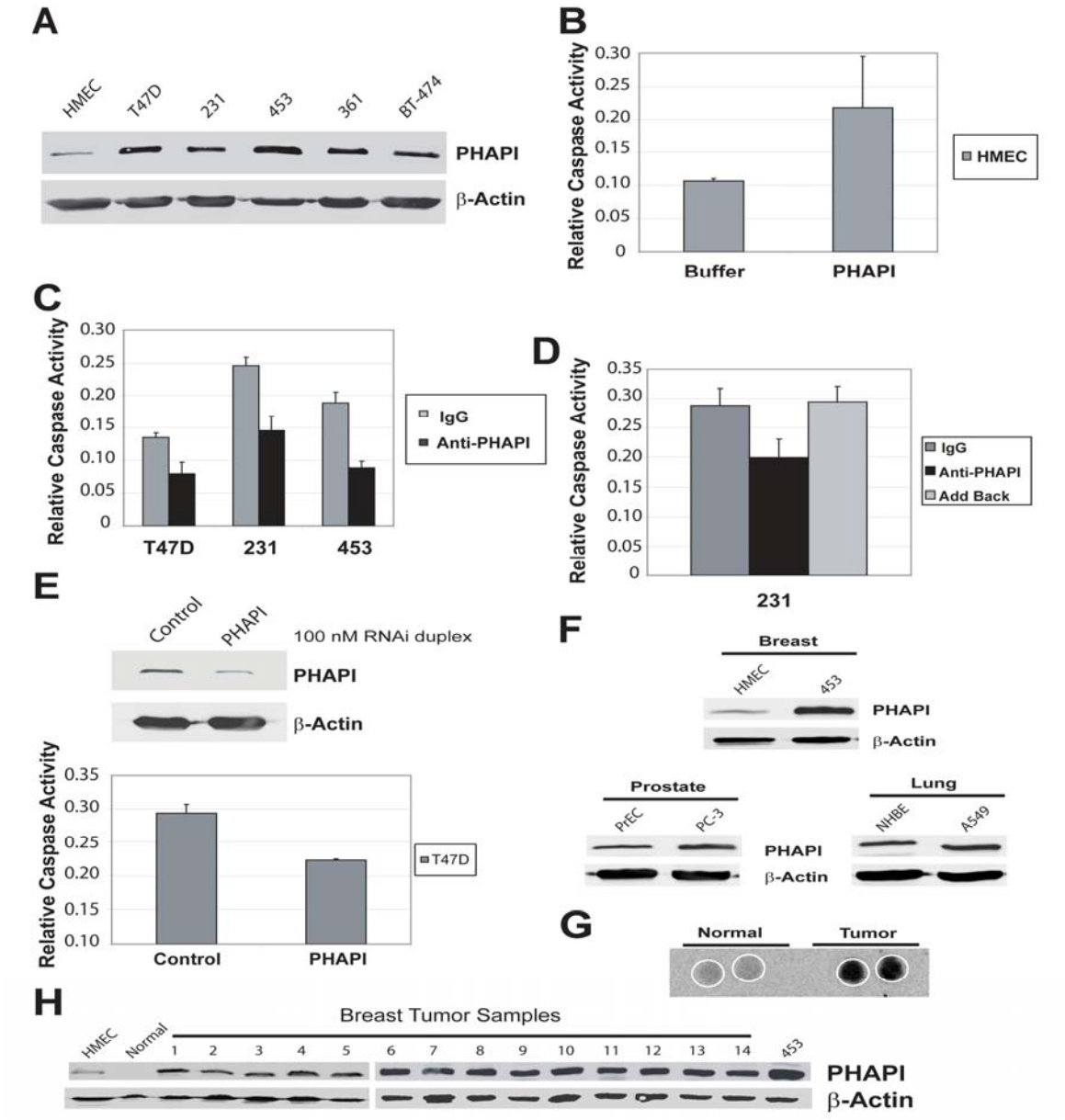

Figure 3.7: PHAPI Mediates the Sensitivity of Breast Cancer Cells to Cytochrome *c*.

Figure 3.7: A. Cell lysates from the indicated cell lines were immunoblotted for PHAPI while β-actin was used as a loading control **B.** Recombinant PHAPI (or buffer) was added to HMEC lysates, and cytochrome *c* was subsequently added at 3 ng/μL. Caspase activation was then measured via cleavage of Ac-DEVD pNA. Data shown are mean +/- SEM for at least three independent experiments. **C.** PHAPI antibody (or IgG) was pre-incubated with the indicated cell lysates, which were then activated with 3 ng/μL cytochrome *c*. Cleavage of Ac-DEVD-pNA was used to monitor caspase activation. Data shown are mean +/- SEM for at least three independent experiments. **D.** Recombinant PHAPI protein was added to PHAPI antibody prior to its addition into MDA-MB-231 cytosolic lysate. Lysate was then activated with 3 ng/μL cytochrome *c*, and caspase activation was measured via Ac-DEVD-pNA cleavage. Data shown are mean +/- SEM for at least three independent experiments. **E.** T47D cells were transfected with either a control or PHAPI siRNA duplex, and knockdown was confirmed via western blotting for PHAPI. Lysates were then supplemented with 3 ng/μL cytochrome *c*, and caspase activation was monitored via the cleavage of the colorimetric caspase-3 substrate, Ac-DEVD-pNA. Data shown are mean +/- SEM for at least three independent experiments. **F.** Cytosolic extracts from the indicated cell lines were immunoblotted for PHAPI and β-actin. **G.** Human tissue dot blot with duplicated samples demonstrates PHAPI levels in normal breast tissue and in breast tumor tissue from a poorly differentiated invasive ductal carcinoma. Areas within in white circles represent sample location. **H.** Lysates were prepared from normal breast tissue or breast tumor samples and then immunoblotted (along with HMEC and 453 lysate) for PHAPI and β-actin for a loading control.

We also wanted to examine the consequences of reducing PHAPI expression in the cytochrome *c* hypersensitive beast cancer cells; previous data would suggest that decreasing PHAPI could restore their normal apoptotic response to cytochrome *c*. Accordingly, we used RNA interference (RNAi) to reduce PHAPI expression in T47D cells, and we subsequently examined caspase activity in response to cytochrome *c*. Decreasing the expression of PHAPI led to a correlative reduction in the cytochrome *c*-induced caspase activation of the T47D cells (Figure 3.7E). Taken together, these data demonstrate that overexpression of PHAPI is necessary for the augmented sensitivity of breast cancer cells to cytochrome *c*.

Given our previous results in Figure 3.3 where we compared the sensitivity of breast cancer cells with that of other tumor types, we were interested in characterizing the PHAPI expression in other cell types that were more refractory to cytochrome *c*-induced apoptosis. Therefore, we prepared cytosolic lysates from normal (non-malignant) prostate epithelial cells (PrEC) and normal bronchial epithelial cells (NHBE) to compare the levels of PHAPI in these cells with their tumorigenic counterparts. In contrast to mammary epithelial cells, immunoblotting normal and malignant epithelial cells of prostate or lung origin revealed no significant changes in PHAPI expression (Figure 3.7F). This result further supports the unique nature of the hypersensitivity of the breast cancer cells and suggests that high levels of PHAPI are critical to their cytochrome *c* sensitivity.

Given our surprising finding that the breast cancer cell lines were so remarkably sensitive to cytochrome *c*, we wanted to examine PHAPI expression in human patient

samples of breast tumor tissue. First, a human tissue dot blot revealed a dramatic increase in PHAPI expression between the normal tissue and a poorly differentiated, invasive ductal carcinoma (Figure 3.7G). Additionally, immunoblotting equal amounts of total protein from breast tumor tissue demonstrated PHAPI overexpression in all of the breast tumor samples when compared to both normal breast tissue (which demonstrated no detectable expression) and primary mammary epithelial cells (Figure 3.7H). The degree of PHAPI overexpression in these patient samples was quite similar to that observed in the malignant tissue culture cell line MDA-MB-453.

3.2.8 Protein Stability and mRNA Levels May Contribute to Overexpression of PHAPI in Breast Cancer Cells

In order to examine possible mechanisms for the elevated levels of PHAPI in the breast cancer cells, we first wanted to compare PHAPI protein stability in the normal and malignant mammary epithelial cell lines. After treating the HMECs or MDA-MB-231 cells with cyclohexamide at various times over a six-hour period, we immunoblotted whole cell lysate for PHAPI expression. While there was significantly diminished PHAPI expression in the HMECs (half-life of approximately three hours) throughout this timecourse, the MDA-MB-231 cells appeared to maintain consistent levels of the protein (Figure3.8A). These data suggest that PHAPI protein may be increasingly stable in the breast cancer cells, resulting in more total protein and an enhanced responsiveness to cytochrome *c*. Since PHAPI has been shown localized to both the cytosol and the nucleus, subsequent experiments may be necessary to separately evaluate the turnover of the nuclear and cytosolic pools of PHAPI.

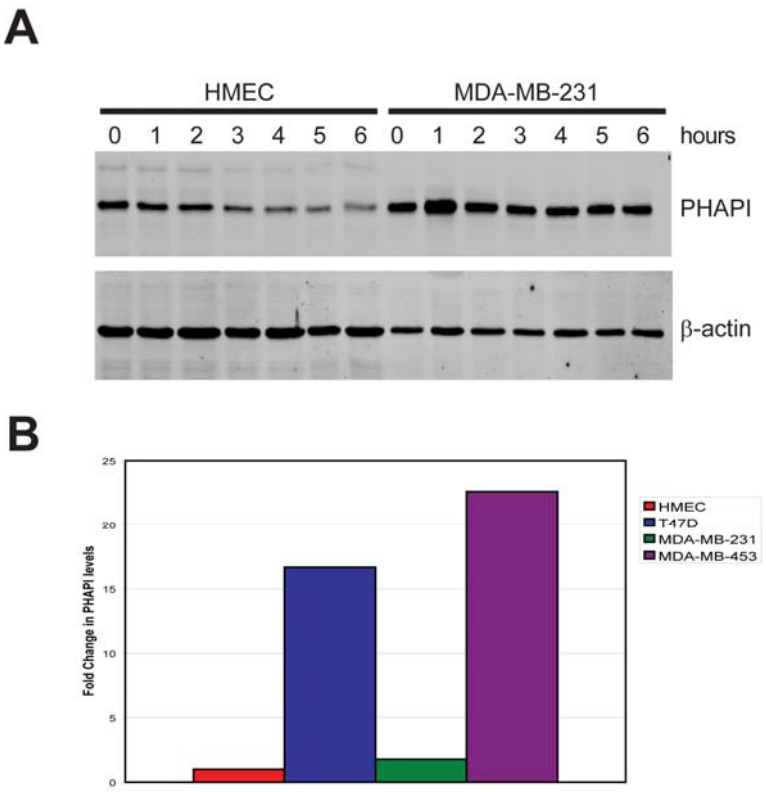

Figure 3.8: Increased PHAPI Protein Stability and mRNA Levels in Breast Cancer Cells.

Figure 3.8: A. HMEC and MDA-MB-231 cells were treated with cyclohexamide for the indicated times. Whole cell lysates were then immunoblotted for PHAPI expression and β-actin as a loading control. **B.** Quantitative analysis from RT-PCR shows the fold change in PHAPI mRNA levels, relative to HMECs, which was arbitrarily set as one.

Even though we detected changes in PHAPI protein stability, we also wanted to determine if there was regulation at the transcriptional level by examining the levels of PHAPI mRNA in the normal and tumor cells. Quantitative RT-PCR revealed that PHAPI mRNA was more abundant in the breast cancer cell lines (T47D, MDA-MB-231, MDA-MB-453) compared to the normal HMECs (Figure 3.8B). Although the absolute fold change was quite variable between the cancer cell lines, all of them were elevated relative to the normal mammary epithelial cells. These data suggest that perhaps there is more than one mechanism regulating PHAPI overexpression in the breast cancer cells; many further experiments are needed to probe the mechanism(s) for these changes.

3.2.9 Role of PHAPI as a PP2A Inhibitor Appears Unrelated to its Apoptosomal Effects

Kinase regulation of the apoptosome is not uncommon (as described in Chapters 1 and 4), and given the fact that PHAPI has been characterized as a protein phosphatase 2A (PP2A) inhibitor, we speculated that this function may contribute to its ability to regulate caspase activation downstream of mitochondrial cytochrome *c* release. Therefore, we performed a dephosphorylation assay using a common PP2A substrate, phosphorylase A, to assess PP2A activity in the mammary epithelial cell lysates. As shown in Figure 3.9A, dephosphorylation of phosphorylase A was relatively equivalent in lysates prepared from normal and malignant mammary epithelial cells, suggesting that the overall activity of PP2A is not dramatically different in these extracts. Furthermore, reducing the PHAPI levels in the T47D cells using RNAi did not significantly alter PP2A-directed activity

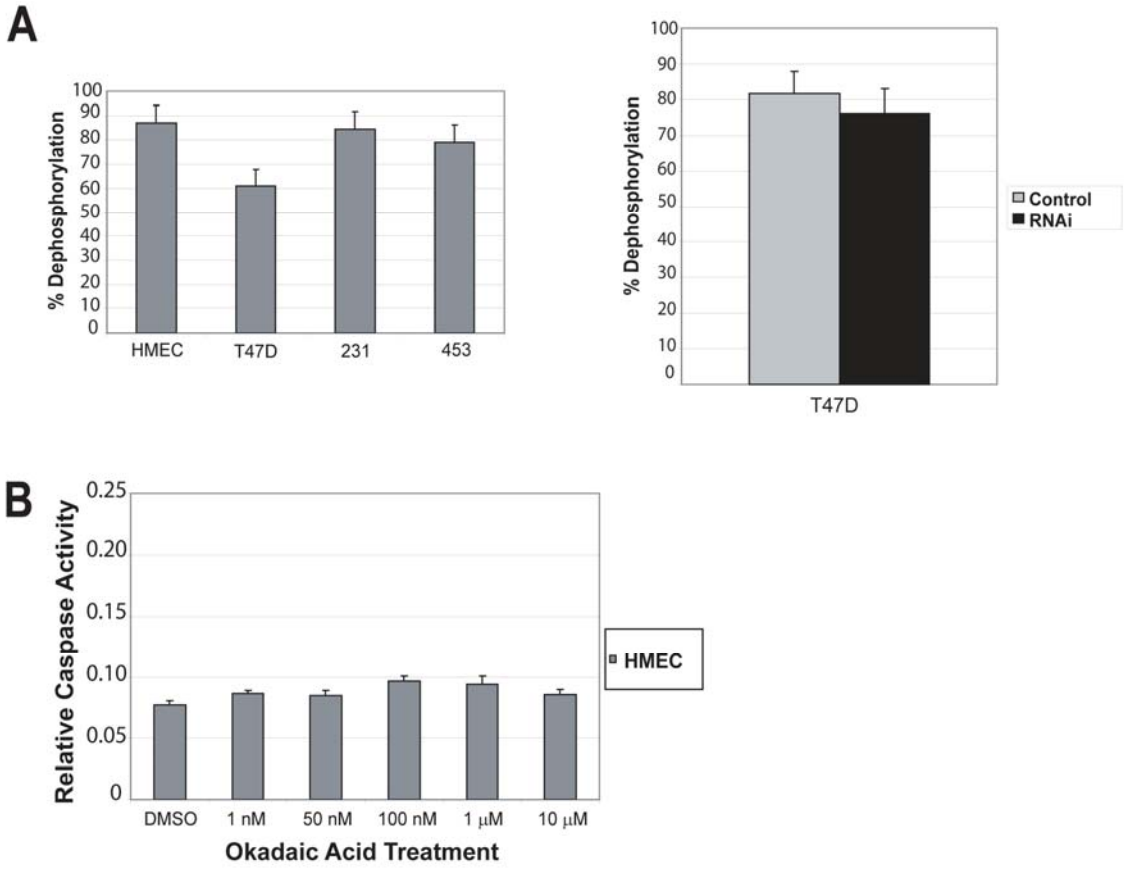

Figure 3.9: Changes in PP2A Activity Do Not Impact the Hypersensitivity of Breast Cancer Cells to Cytochrome *c*.

Figure 3.9: A. Radiolabeled phosphorylase A was incubated in the indicated lysates, and dephosphorylation was monitored on a scintillation counter. Data shown is mean +/- SEM for at least three independent experiments. **B.** Cytosolic lysates from the HMECs were treated with the indicated concentrations of okadaic acid. After supplementing the lysates with cytochrome *c*, caspase activation was monitored via the cleavage of the colorimetric caspase-3 substrate Ac-DEVD-pNA. Data shown are mean +/- SEM for at least three independent experiments.

towards phosphorylase A (Figure 3.9A, right panel). If the role of PHAPI as a PP2A inhibitor was responsible for the hypersensitivity of breast cancer cells, presumably the use of another PP2A inhibitor in the normal HMECs would enhance sensitivity to cytochrome *c* (as PHAPI addition did in Figure 3.7B). Treating HMEC lysates with okadaic acid, a potent inhibitor of PP2A and other phosphatases, did not increase caspase activity in response to cytochrome *c* (Figure 3.9B). Taken together, these data suggest that the ability of PHAPI to inhibit PP2A does not significantly contribute to the enhanced cytochrome *c*-induced caspase activation in breast cancer cells.

3.2.10 Microinjection of Cytochrome *c* into Breast Cancer Cells Induces Apoptosis More Quickly than in Normal Mammary Epithelial Cells

Thus far, our data suggests that malignant mammary epithelial cells have elevated caspase activity following cytochrome *c* addition to lysates. However, we also wished to validate these findings by demonstrating that microinjection introducing cytochrome *c* directly into the cytosol of breast cancer cells would activate caspases and kill these cells more quickly than normal mammary epithelial cells. In addition, thinking therapeutically, these results imply that cytochrome *c*, or an agent that could also activate Apaf-1 (a cytochrome *c* mimetic), might potentially be used as a chemotherapeutic to selectively eliminate tumorigenic mammary epithelial cells. Upon microinjection of cytochrome *c* into the cytosol of normal and malignant mammary epithelial cells, we found that a significantly higher percentage of tumor cells underwent apoptosis following cytochrome *c* microinjection (Figure 3.10A). Representative pictures also depict the preferential apoptosis in the breast cancer cells (Figure 3.10B). These data confirm our *in vitro*

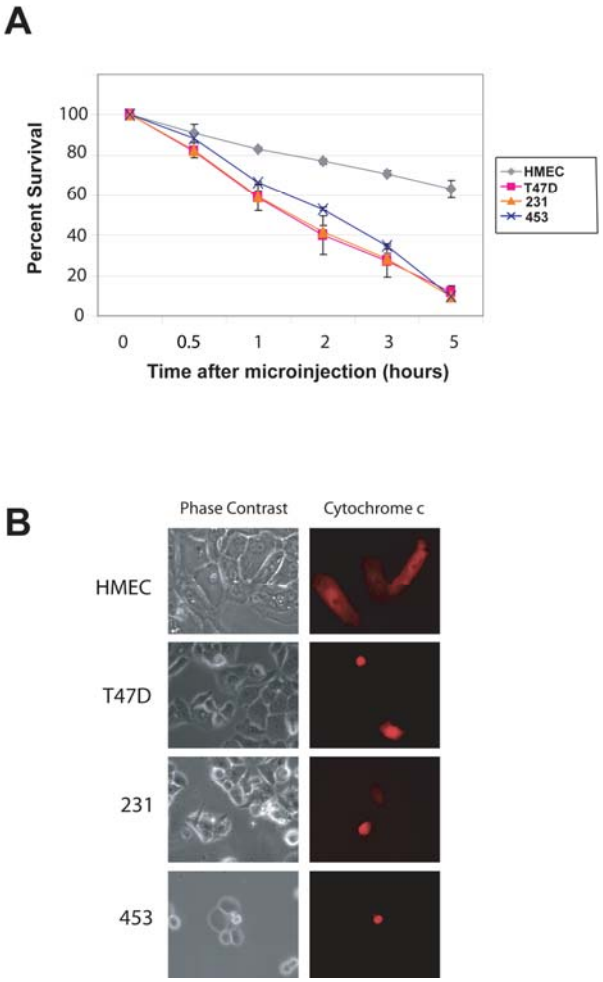

Figure 3.10: Microinjection of Cytochrome *c* Preferentially Kills Mammary Epithelial Cells.

Figure 3.10: A. Cytochrome *c* at 10 mg/mL was microinjected into the cytosol of the indicated cell lines. To visualize the injected cells, rhodamine dextran was coinjected. Percent survival was measured by counting red cells that had lifted off the plate. Data shown are mean +/- SEM for at least three independent experiments. Representative pictures are shown in **B.**

findings and indicate the potential for chemotherapeutically exploiting the cytochrome *c* hypersensitivity in breast cancer cells to specifically terminate cancerous (but not non-cancerous) mammary epithelial cells.

3.3 Discussion

It is well-known now that cancer cells have a wide variety of alterations in the apoptotic pathway, most of which make them refractory to apoptotic stimuli. Interestingly, by examining the cytochrome *c* responsiveness of mammary epithelial cells, we have made the discovery that breast cancer cells are actually hypersensitive to cytochrome *c*-induced apoptosis. While this finding initially contradicts the idea that tumorigenesis grants most cells the ability to evade cell death signals, the malignant mammary epithelial cells do maintain apoptotic inhibition; treatment with cisplatin and adriamycin failed to induce release of mitochondrial cytochrome *c* (Figure 3.2). Enhanced cytochrome *c* responsiveness is unique to breast cancer cells, when compared with a panel of other epithelial based tumors (Figure 3.3). Although many previous reports examining the apoptosome in cancer observed inhibited caspase activity due to changes in core apoptosomal proteins, we have shown that breast cancer cells express these proteins at levels similar to normal mammary epithelial cells (Figure 3.4) (Janicke et al., 1998; Soengas et al., 2001). Instead, these malignant cells have increased caspase-9 and caspase-3 activation, which correlates with enhanced recruitment of caspase-9 to the Apaf-1 CARD (Figure 3.5). The protein PHAPI is overexpressed in malignant mammary epithelial cells, mediating apoptosomal changes and the augmented caspase activation. The specific function of PHAPI was initially unclear, although our studies demonstrated

that the role of PHAPI as a PP2A inhibitor appears inconsequential for its apoptosomal effects in breast cancer (Figure 3.9). Validating our *in vitro* results, microinjection studies showed that cytosolic cytochrome *c* was able to more easily kill malignant mammary epithelial cells compared to their normal counterparts (Figure 3.10). These findings leave us with this model and have the potential to impact breast cancer treatments through the development of direct apoptosome activators or cytochrome *c* mimetics (Figure 3.11).

3.3.1 Enhanced Caspase Activation Mediated by PHAPI in Breast Cancer

There have been very few reports demonstrating apoptosome regulation that enhances caspase activation. In addition to these data provided here for breast cancer, brain tumors are also hypersensitive to cytochrome *c* compared to surrounding normal neural tissue, although this mechanism is based on the elevation of Apaf-1 expression in the tumor cells (Johnson et al., 2007). These data from cancer cells provide evidence that apoptosome assembly can actually be regulated to promote caspase activation. In the case of breast cancer, the increased association of caspase-9 with Apaf-1 enhances caspase-9 activation, which subsequently augments caspase-3 activation. Our data indicate that PHAPI is regulating a post-translational mechanism responsible for the increased association between Apaf-1 and caspase-9. Supporting this hypothesis, we demonstrated that supplementing normal mammary epithelial cells with recombinant PHAPI increased caspase activation following cytochrome *c* addition to lysate (Figure3.7B). Additionally, loss of function studies in the malignant mammary epithelial cells, using both anti-PHAPI antibody addition and an RNAi-based PHAPI knockdown, reduced their sensitivity to cytochrome *c* (Figure3.7C,E) Therefore, the PHAPI overexpression

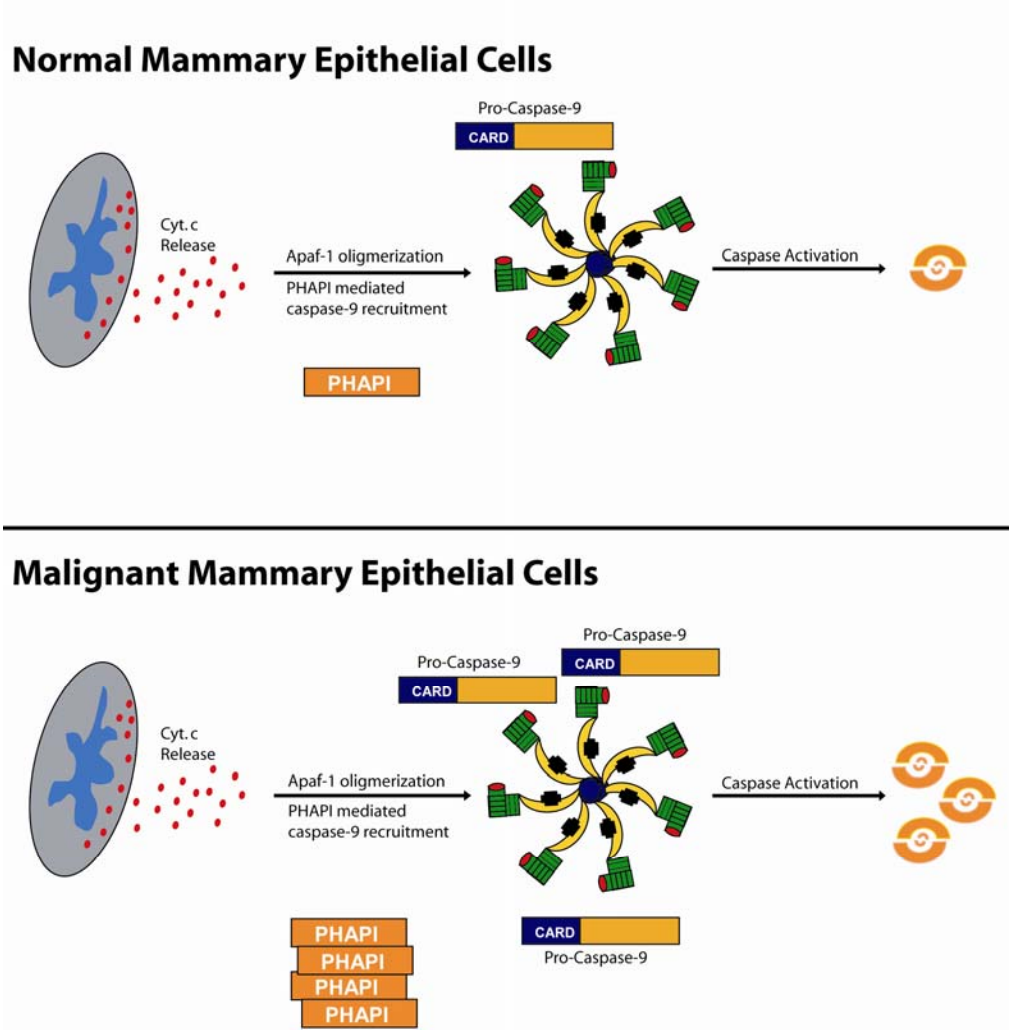

Figure 3.11: Model for Cytochrome *c* Hypersensitivity in Breast Cancer.

Figure 3.11: Normal mammary epithelial cells are less sensitive to cytochrome *c*-induced apoptosis than breast cancer cells due to the high levels of PHAPI protein in the tumor cells. Through its role as a member of the Apaf-1 nucleotide exchange complex, PHAPI enhances apoptosome formation and caspase-9 recuritment to Apaf-1. Reproduced from Schafer and Kornbluth (2006), with permission from Elsevier.

detected in malignant mammary epithelial cell lines and in human tumor tissues is likely of importance. Elevated levels of PHAPI are only observed in breast cancer cells and not in other tumor cell types examined (Figure 3.7F-H). Interestingly, it appears that the differential PHAPI expression might actually be occurring in the normal cells, as normal mammary epithelial cells express less PHAPI than normal prostate or bronchial epithelial cells, which indicates that the baseline for which PHAPI can significantly dictate sensitivity to cytochrome *c* is lower in mammary epithelial cells than the other cell types.

At the time of our work, it was unclear how PHAPI regulated the apoptosome, specifically the enhanced caspase-9 recruitment to Apaf-1. However, more recent studies from the lab of Xiaodong Wang have shown that PHAPI is one of three proteins functioning as the nucleotide exchange complex for Apaf-1 (Kim et al., 2008). In concert with hsp70 and CAS, PHAPI exchanges dADP/ADP for a fresh dATP/ATP after cytochrome *c* binding to Apaf-1. This exchange appears to be critical for proper formation of the apoptosome backbone, as Apaf-1 that remains bound to dADP/ADP forms inactive aggregates that appear larger than the apoptosome itself (Kim et al., 2005). These findings certainly help explain the enhanced interaction between caspase-9 and Apaf-1 that was detected in the breast cancer cells (Figure 3.6). In the presence of increased levels of PHAPI, the hydrolyzed nucleotide on Apaf-1 should be exchanged for a fresh dATP/ATP more quickly. Therefore, cells with higher levels of PHAPI should have faster and/or increased Apaf-1 oligomerization, which would indeed allow for augmented caspase-9 recruitment and enhanced caspase activity.

It has been reported however that PHAPI does not interact with the apoptosome itself; studies from our work support this finding (Hill et al., 2004). Given the more recent relationship established between PHAPI and Apaf-1, it would be of interest to characterize how the nucleotide exchange complex works (i.e. how does it interact with Apaf-1? What role does each individual protein play in the nucleotide exchange process?). In addition to its relationship with Apaf-1, PHAPI has been shown to promote apoptosis through other mechanisms. The RNA-binding protein HuR affects the cellular response to certain apoptotic triggers by regulating messenger RNAs (mRNA) that encode for various stress response proteins. PHAPI interacts with HuR, which appears to help stabilize it for caspase cleavage. This cleavage event makes HuR more pro-apoptotic, thus enhancing the cell's apoptotic response (Mazroui et al., 2008).

Our preliminary findings regarding the potential mechanisms for PHAPI upregulation in breast cancer indicate that its transcription and/or stability could be altered in breast cancer. A more recent study of apoptosome activity in non-small cell lung carcinoma (NSCLC) demonstrated that PHAPI was important for the cellular response to chemotherapeutics (Hoffarth et al., 2008). In cell lines with more stable PHAPI, chemotherapeutic treatments such as taxol were increasingly effective at triggering apoptosis. However, in the cell lines where the half-life of PHAPI was shorter, the cells were more refractory to these treatments. Furthermore, an examination of PHAPI status in 24 actual NSCLC patients demonstrated that PHAPI negative tumors correlated with a worse overall survival. Given the findings demonstrated here and the precedent for altered stability of PHAPI in NSCLC, it would be of interest to pursue our

preliminary findings regarding the regulation of PHAPI protein levels, especially now that the specific relationship between PHAPI and the apoptosome has been delineated.

3.3.2 The Apoptotic Sensitivity of Cancer

As discussed in Chapter 1, apoptotic evasion is a well-characterized hallmark of cancer. Thus, it initially seemed counterintuitive that breast cancer cells would be more sensitive than their normal counterparts to a direct apoptotic stimulus such as cytochrome *c*. However, using various chemotherapeutic agents, we observed that the cytochrome *c*-hypersensitive breast cancer cells were actually quite resistant to releasing mitochondrial cytochrome *c* (Figure 3.2). Therefore, the breast cancer cells appear refractory to apoptotic activation, but this apoptotic evasion results from inhibition at a different locus of control (mitochondrial cytochrome *c* release), which is dominant to (and upstream of) the apoptotic sensitivity surrounding cytochrome *c*-induced caspase activation.

In parallel with our findings, enhanced apoptosis has been previously observed in a variety of tumors. This observation makes sense, especially when considering the early tumorigenic processes that might enhance environmental and cellular stresses. As was mentioned in Chapter 1, the c-Myc protein is one example of an oncogene having pro-apoptotic functions although it is primarily known for its role as a potent inducer of cellular proliferation (Evan and Littlewood, 1998; Pelengaris et al., 2002). Thus, c-Myc-mediated apoptotic signaling serves as a balance for its ability to drive proliferation. Perhaps this is one evolutionary mechanism protecting a cell from oncogenic transformation? In cases where there are subsequent disruptions to the apoptotic pathway, c-Myc can become completely oncogenic. Although no direct relationship between c-

Myc and the apoptosome has been reported, it seems plausible that oncogenes activated in certain types of breast cancer could play this role as well; apoptosis downstream of mitochondrial cytochrome *c* release is hyperactivated, but subsequent tumorigenesis selects for acquired anti-apoptotic mechanisms upstream of the mitochondria.

In addition to c-Myc, another common oncogene, Ras, has been shown to induce pro-apoptotic pathways during tumorigenesis, including MAPK signaling through JNK (Davis, 2000; Dhillon et al., 2007). As discussed in Chapter 1, JNK may function as a tumor suppressor due to its ability to promote apoptosis. NF-κB signaling has been shown to play an opposing role to this process through inhibiting JNK-induced apoptosis during tumorigenesis (Bubici et al., 2004). More broadly, NF-κB can prevent oncogene-induced apoptosis (Kennedy et al., 2003a; Orlowski and Baldwin, 2002). In aggregate, these examples suggest that oncogene-driven tumorigenesis is a process that does not necessarily follow the most direct route to apoptotic inhibition. Expression of an oncogenic protein might first initiate a pro-apoptotic mechanism (such as PHAPI overexprssion), which is later overcome by other alterations, including potential mutations inhibiting the release of mitochondrial cytochrome *c*.

3.3.3 Activating the Apoptosome as a Cancer Treatment

As stated previously, the ultimate goal for cancer therapy is to induce the selective and specific cell death of the tumor cells (Johnstone et al., 2002). These data presented here suggest that this therapeutic strategy might be possible for breast cancer cells due to their marked sensitivity to cytochrome *c*, compared to normal mammary epithelial cells. Although there are many commonly used chemotherapeutics that trigger apoptosis

through cell cycle checkpoint-dependent release of cytochrome *c*, many recent attempts have been made to design more directed therapies, which could enhance caspase activation and thus bypass some of the potential regulatory points being altered in cancer (Lowe and Lin, 2000). For example, Smac peptides or mimetics have been developed to target and inhibit XIAP in cancers where this protein has been shown to play a crucial role in apoptotic evasion (Arnt et al., 2002; Fulda et al., 2002; Guo et al., 2002; Oost et al., 2004; Yang et al., 2003). In addition, the use of small molecules to selectively activate/enhance the apoptosome has shown some promise for targeting of cancer cells (Jiang et al., 2003; Ledgerwood and Morison, 2009; Nguyen and Wells, 2003). Therefore, exploiting the increased cytochrome *c* responsiveness of breast cancers (and brain tumors as they share the same differential sensitivity between normal and tumor cells) through a novel chemotherapeutic is appealing. The design of peptides or small molecules that mimic cytochrome *c*-mediated activation of Apaf-1 could be of great utility in the treatment of these cancers as our results demonstrate that only malignant cells would be induced to undergo apoptosis.

Other work in our laboratory has focused on small molecule, peptide, and gene therapeutic approaches to discover a cytochrome *c* mimetic. Unfortunately, at this time, we have yet to develop any successful methods. However, studies are ongoing, including some work involved in better characterizing the interaction between cytochrome *c* and Apaf-1, as this information might support the design of a small molecule or peptide that could specifically activate Apaf-1 in a manner similar to cytochrome *c*. It is possible that a novel apoptosome activator would not have to interact with Apaf-1 in exactly the same

manner as cytochrome *c*; it would only have to cause apoptosome formation and activation to be effective.

4. MAPK-mediated Suppression of Cytochrome *c*-Induced Apoptosis through Rsk Phosphorylation of Apaf-1

(A modified version of this chapter was submitted for publication and is currently being revised for resubmission.)

4.1 Introduction

As discussed in Chapter 1, cytochrome *c*-induced caspase activation is regulated by post-translational modifications and apoptosome-associated proteins, both inhibitory and activating (Tables 1.1 and 1.2) (Kurokawa and Kornbluth, 2009; Schafer and Kornbluth, 2006). The most intensively-studied post-translational modifications occur on caspase-9 where phosphorylation is known to reduce its activation and/or cleavage. Phosphorylation of threonine 125 on caspase-9, which was first identified as an Erk modification, decreases caspase-9 activation and processing (Allan et al., 2003). More recently, the cyclin dependent kinase cdk1, DYRK1A, and p38α have been shown to phosphorylate caspase-9 at this site, reducing its activity and the downstream activation of caspase-3 (Allan and Clarke, 2007; Laguna et al., 2008; Seifert et al., 2008; Seifert and Clarke, 2009).Phosphorylation at threonine 125 can be reversed by protein phosphatase 1α (PP1α)-mediated caspase-9 dephosphorylation, to relieve this inhibition (Alvarado-Kristensson and Andersson, 2005; Dessauge et al., 2006). Phosphorylation of cytochrome *c*, another core apoptosome component, has been reported to occur at tyrosines 48 and 97, though the apoptotic consequences of these modifications remain unclear (Lee et al., 2006; Yu et al., 2008).

The mitogen-activated protein kinase (MAPK) pathway promotes cell survival in response to various stimuli, including growth factors, serum, and phorbol esters (Anjum and Blenis, 2008). Activation of the MAPKKs, MEK1/2, leads to activation of the MAP kinases Erk1/2, which ultimately results in direct phosphorylation and activation of Rsk, the p90 kDa ribosomal S6 kinase. Rsk was first identified as a kinase that phosphorylated rpS6 in unfertilized *Xenopus* laevis eggs, and the MAPK/Rsk pathway is highly active during *Xenopus* oocyte maturation and mitosis (Erikson and Maller, 1985, 1989). Two Rsk isoforms have been characterized in *Xenopus* eggs, while there are four known human isoforms. Both Erk and Rsk have direct substrates that are involved in the regulation of cell survival; Rsk1 can phosphorylate the BH3-only protein, Bad at serine 112, inhibiting Bad-mediated apoptosis upstream of mitochondria, while Rsk1 and Rsk2 have both been shown to suppress the pro-apoptotic activity of DAPK through phosphorylation at serine 289 (Anjum et al., 2005; Shimamura et al., 2000).

Here we demonstrate a novel post-translational modification of Apaf-1 and its effect on apoptosome formation. While investigating apoptotic regulation in mitotic *Xenopus* egg extracts, we observed a MAPK-mediated reduction in the interaction between cytochrome *c* and Apaf-1, which inhibited apoptosome formation in a manner distinct from the previously reported Erk-mediated phosphorylation of caspase-9. Elevated MAPK signaling in mitotic egg extracts activated Rsk, which promoted direct Apaf-1 phosphorylation. This modification led to defective Apaf-1 oligomerization and diminished caspase activity, thus providing protection from cytochrome *c*-induced apoptosis. Furthermore, the phosphatase PP1 antagonized the effect of Rsk by

dephosphorylating Apaf-1. A variety of mammalian cell models with activated Rsk also contained phosphorylated endogenous Apaf-1 and exhibited a reduced sensitivity to cytochrome *c*, a finding of potential importance in tumor chemoresistance, given the elevation of Rsk activity in some cancers (Bignone et al., 2007; Clark et al., 2005; Smith et al., 2005; Thakur et al., 2007). Collectively, these data suggest a novel mode of apoptosome inhibition exerted by Rsk-mediated phosphorylation of Apaf-1, leading to post-cytochrome *c* protection from apoptosis.

4.2 Results

4.2.1 Apoptosome Formation is Defective in *Xenopus* Mitotic Extract

In this study, we again utilized *in vitro* reconstitution of the apoptosome to examine the sensitivity of cytosolic interphase or mitotic *Xenopus* egg extracts (prepared by converting interphase into mitosis with the addition of exogenous cyclin B protein) to cytochrome *c*. Given the conserved nature of the apoptotic pathway, the *Xenopus* system serves as a powerful tool for probing these questions because cytosolic extract is quite easily obtained without mitochondrial disruption. For our studies, exogenous cytochrome *c* was added to cytosolic interphase or mitotic extract, and caspase activity was assessed using the colorimetric caspase-3 substrate, Ac-DEVD-pNA. Under these conditions, we observed significantly less cytochrome *c*-induced caspase activation in mitotic *Xenopus* egg extracts than in interphase extracts (Figure 4.1A). To elucidate the mechanism for this differential sensitivity to cytochrome *c*, we utilized the cyclin dependent kinase (cdk) inhibitor, roscovitine (ROS), and a MEK1/2 inhibitor, U0126. Both of these kinase pathways are highly active during *Xenopus* mitosis, making them likely candidates for

affecting mitotic-specific signaling events. After pre-incubating extracts with inhibitor and adding exogenous cytochrome *c*, we tested the ability of these extracts to activate caspases by measuring DEVDase activity. As shown in Figure 4.1B, ROS and U0126 relieved the mitotic inhibition of caspase activation, indicating that perhaps both kinases (or, a kinase downstream of Cdc2 and MEK1/2) are involved in suppressing the responsiveness of mitotic extract to cytochrome *c*. These results were reminiscent of our previously reported results showing that meiotic extracts (also known as cytostatic factor-arrested extracts) are refractory to cytochrome *c*. In that work, we traced the inhibition to the MEK-MAPK pathway, though the mechanism of apoptosome inhibition was unknown (Tashker et al., 2002).

Since our caspase assays indicated that mitotic extract is relatively resistant to cytochrome *c*, we analyzed apoptosome formation for a potential mechanistic explanation, starting with the initial step in apoptosome formation, the binding of cytochrome *c* to Apaf-1. It has been previously reported that caspase-9 is phosphorylated at threonine 125 by cdk1 during mitosis (Allan and Clarke, 2007; Allan et al., 2003; Laguna et al., 2008; Seifert et al., 2008). Phosphorylation at this site inhibits caspase-9 processing, which serves as a marker for its activation. However, in probing earlier steps of apoptosome formation, we found that the binding of cytochrome *c* to Apaf-1, a step occurring prior to caspase-9 recruitment, is also diminished in mitotic *Xenopus* egg extract. After incubating agarose-bound cytochrome *c* in either interphase or mitotic extract, we observed that significantly less Apaf-1 was affinity precipitated from the mitotic extract compared to interphase extract (Figure 4.1C). One potential explanation

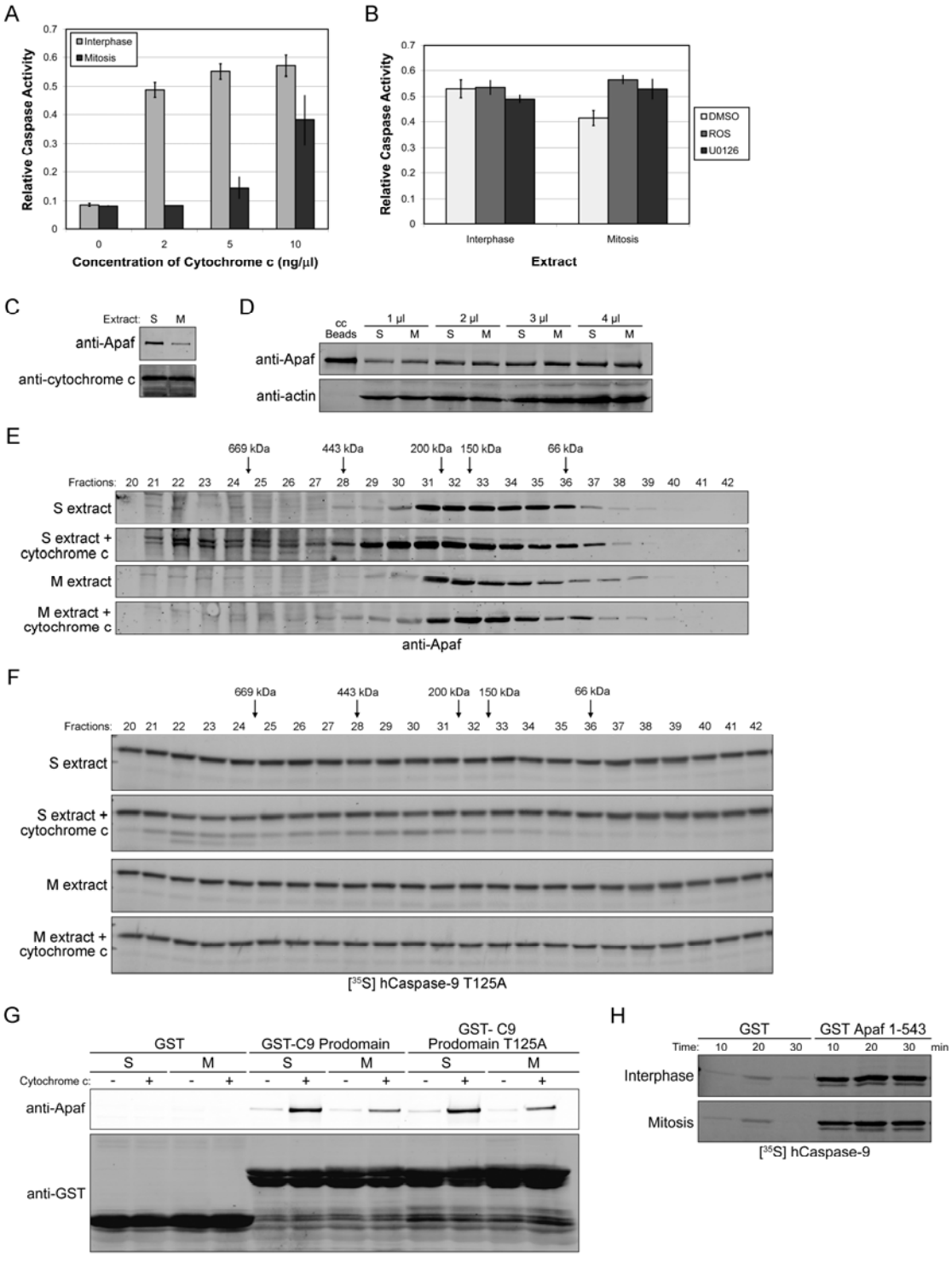

Figure 4.1: Delayed Apoptosome Formation in Mitotic *Xenopus* Extract.

Figure 4.1: A. Cytosolic interphase or mitotic extract was made from *Xenopus* eggs, and cytochrome *c* was added for 20 minutes at the indicated doses. The colorimetric substrate Ac-DEVD-pNA was used to assay caspase activity. Data shown are mean +/- SEM of three independent experiments. When comparing S/M at 2ng/μL, p-value<0.01 and at 5ng/μL, p-value<0.001. **B.** The inhibitors roscovitine (ROS) and U0126 were used to treat cytosolic extract at 1.2 mM and 200 μM, respectively. Cytochrome *c* was added at 2 ng/μL, and after 60 minutes, caspase activation was monitored with the colorimetric substrate Ac-DEVD-pNA. Data shown are mean +/- SEM of three independent experiments. For S, M+ROS, or M+U0126 compared to M+DMSO, p-value<0.05, <0.01, and <0.05, respectively. **C.** Agarose-bound cytochrome *c* was incubated in interphase (S) or mitotic (M) extract for 20 minutes. Beads were then washed in ELB+500 mM NaCl and run on SDS-PAGE to immunoblot for Apaf-1 and cytochrome *c*. **D.** The indicated volumes of interphase (S) or mitotic (M) *Xenopus* egg extract were subjected to SDS-PAGE and immunoblotted with anti-Apaf-1 or anti-actin antibodies. **E.** Cytosolic interphase (S) or mitotic (M) extract was made from *Xenopus* eggs, and 2 ng/μL of purified cytochrome *c* was added for 45 minutes at 25°C. Gel filtration chromatography was then performed, and one-tenth of each fraction was run on SDS-PAGE to immunoblot for Apaf-1. **F.** ^{35}S-labeled *in vitro* translated caspase-9 T125A was added to 50 μL of each fraction and incubated at 30°C for 1 hour. Samples were then run on SDS-PAGE, and caspase-9 activation was assessed by autoradiography by the appearance of lower-molecular-mass cleaved fragment(s). **G.** Glutathione-sepharose bound GST-caspase-9 prodomain (wildtype or mutant T125A) was incubated in interphase (S) or mitotic (M) extract for 30 minutes with or without 2 ng/μL cytochrome *c*. After washing, the samples were immunoblotted with an anti-GST or anti-Apaf-1 antibody. **H.** Glutathione-sepharose bound GST-Apaf-1 1-543 was incubated with interphase or mitotic extract at 25°C for the indicated time. Beads were then washed and assayed for binding to ^{35}S-labeled *in vitro* translated caspase-9 via autoradiography.

for this differential recruitment is that mitotic extract contains less Apaf-1 protein. However, immunoblotting analysis revealed that interphase and mitotic extracts contain comparable amounts of Apaf-1 (Figure 4.1D), suggesting that cytochrome *c* cannot bind Apaf-1 as effectively in mitotic extract.

If the interaction between cytochrome *c* and Apaf-1 is diminished in mitotic egg extract, we would also expect to observe reduced apoptosome formation (e.g. Apaf-1 oligomerization) under these conditions. Therefore, we examined Apaf-1 oligomerization by performing gel filtration chromatography on cytosolic interphase or mitotic extract. In the absence of cytochrome *c*, both interphase and mitotic extracts contained Apaf-1 in lower-molecular-mass fractions where it exists as a monomer (Figure 4.1E). However, upon addition of cytochrome *c* to the interphase extract, a proportion of the Apaf-1 shifted into higher-molecular-mass fractions (22-24), indicating the formation of Apaf-1 oligomers. This recruitment of Apaf-1 into apoptosomal fractions was not detected in the mitotic extract, suggesting that Apaf-1 fails to efficiently oligomerize during mitosis in the presence of cytosolic cytochrome *c*. When ^{35}S-labeled *in vitro* translated procaspase-9 T125A was added to each fraction following gel filtration, cleavage products of *in vitro* translated procaspase-9 were only detectable in the interphase extract supplemented with cytochrome *c* (Figure 4.1F). These results suggest that Apaf-1 oligomerization is defective in mitotic *Xenopus* egg extract, due to a decreased responsiveness to cytochrome *c*.

In order to extend our analysis of apoptosome formation, we investigated the recruitment of caspase-9 to Apaf-1. Using glutathione-sepharose bound GST-human

caspase-9 prodomain, we performed an affinity precipitation for full-length, endogenous Apaf-1. As shown in Figure 4.1G, the caspase-9 prodomain recruited less Apaf-1 from mitotic *Xenopus* egg extract, compared to interphase extract, and this interaction only occurred in the presence of cytochrome *c*, as expected. Furthermore, this decreased interaction during mitosis occurred with both the wildtype and mutant (T125A) caspase-9 prodomains. One explanation for this observation is that the interaction between caspase-9 and Apaf-1 is also reduced in mitosis. However, it is possible that our initial observation, the altered binding between cytochrome *c* and Apaf-1 during mitosis, may explain this result, as Apaf-1 would not be available to bind either the wildtype or mutant caspase-9 prodomain in the mitotic extract.

To help differentiate between the two possibilities, we examined the ability of the GST-Apaf-1 1-543 to recruit *in vitro* translated caspase-9 added to the egg extracts. Under normal conditions, cytochrome *c* binds to Apaf-1, making its caspase recruitment domain (CARD) accessible for caspase-9 binding. However, we can circumvent the requirement for cytochrome *c* by using glutathione-sepharose bound GST-Apaf-1 1-543, which lacks the COOH-terminal regulatory region. We took advantage of this Apaf-1 mutant to examine its interaction with caspase-9. After incubating ^{35}S-labeled *in vitro* translated caspase-9 in interphase or mitotic egg extract, we added GST-Apaf-1 1-543 and performed autoradiography to assess the recruitment of caspase-9 to Apaf-1. As shown in Figure 4.1H, there was no change in the binding of caspase-9 to the Apaf-1 1-543, suggesting that inhibition of apoptosome formation in the *Xenopus* mitotic egg

extract results from suppressed interactions between Apaf-1 and cytochrome *c*, rather than from defective caspase-9 recruitment.

4.2.2 The p90-kDa Ribosomal S6 Kinase Phosphorylates Apaf-1

The inhibitors ROS and U0126 can both restore the sensitivity of mitotic *Xenopus* egg extract to cytochrome *c* (Figure 4.1B). Thus, we hypothesized that one of these kinases, or a downstream signaling effector, was likely to be responsible for the observed changes in apoptosome formation during mitosis. Since we detected a decreased interaction between Apaf-1 and cytochrome *c* during mitosis (Figure 4.1C), we further analyzed this relationship in the presence of these two kinase inhibitors. As shown in Figure 4.2A, in comparison to mitotic extract alone, treatment with ROS or U0126 enhanced the amount of Apaf-1 affinity precipitated by agarose-bound cytochrome *c*. These data support the notion that these kinase signaling pathways influence the interaction between cytochrome *c* and Apaf-1.

Since these results implicate phosphorylation in controlling apoptosome formation, we examined the phosphorylation status of Apaf-1 protein in interphase and mitotic *Xenopus* egg extract. Nickel-agarose bound His-Apaf-1 incubated in egg extracts with ^{32}P-ATP was well-phosphorylated in mitotic, but not interphase, extract (Figure 4.2B). Our data indicated that the Cdc2 and MAPK pathways could play a role in post-cytochrome *c* protection by affecting apoptosome formation. Since Erk and Rsk are downstream of both Cdc2 and MEK1/2 in *Xenopus* mitotic signaling, we next investigated whether Apaf-1 could be directly phosphorylated by one of these kinases (Yue and Ferrell, 2004). As shown in Figure 4.2C, Rsk, but not its activator, Erk, was

able to robustly phosphorylate Apaf-1 directly. Interestingly, the opposite observations were made for caspase-9; Erk can phosphorylate recombinant caspase-9 *in vitro*, while Rsk cannot (data not shown).

Presumably, if Rsk is the sole/predominant kinase phosphorylating Apaf-1 in *Xenopus* mitotic extract, Rsk inhibitors should also be able to restore recruitment of Apaf-1 to the agarose-bound cytochrome *c*. After treating mitotic extract with U0126 or the Rsk inhibitors SL0101/BI-D1870, agarose-bound cytochrome *c* precipitated more Apaf-1 from the mitotic extract (Figure 4.2D, upper panel). In the lower panel, Rsk activation was examined through detection of a gel mobility shift on SDS-PAGE. Since Rsk is known to auto-phosphorylate when active, changes in its gel mobility serve as one method for identifying its activity. A comparison of Rsk2 between interphase and mitotic extracts demonstrates that Rsk is significantly phosphorylated (active) in mitosis (Figure 4.2D, lower panel). However, in the presence of U0126, SL0101, and BI-D1870, Rsk2 is less up-shifted, indicating its reduced activity.

To confirm that Apaf-1 is a substrate of Rsk in mitotic *Xenopus* egg extract, we obtained a phospho-antibody for the Rsk consensus phosphorylation motif (RXRXXS*/T*). This antibody has been utilized previously to characterize novel Rsk substrates (Anjum et al., 2005; Carriere et al., 2008). After incubating nickel-agarose bound His-Apaf-1 in interphase or mitotic extract, immunoblotting revealed that only Apaf-1 incubated in mitotic extract was easily recognizable by the phospho-antibody (Figure 4.2E, lanes 1 and 3), further implicating Rsk as an Apaf-1-directed kinase. To eliminate any direct involvement from a phosphatase toward Apaf-1, we titrated the

phosphatase inhibitor, okadaic acid (OA), into either interphase or mitotic *Xenopus* egg extract (Figure 4.2E, lanes 2 and 4). The addition of OA to interphase extract was sufficient to enhance Apaf-1 phosphorylation. It is well-recognized that the MAPK pathway is activated by OA, and this is also true in *Xenopus* extract (data not shown) (Mumby and Walter, 1993). Therefore, these results suggest that the addition of OA to interphase *Xenopus* egg extract yields Rsk activation and consequent Apaf-1 phosphorylation.

Since there are many highly active kinases in *Xenopus* mitotic extract, we wanted to confirm the specificity of the antibody used in Figure 4.2E for Rsk. After treating mitotic extract with U0126, SL0101, or BI-D1870, we added nickel-agarose bound His-Apaf-1. Immunoblotting clearly demonstrates that Apaf-1 failed to be phosphorylated in mitotic extract when a MAPK pathway/Rsk inhibitor was present (Figure 4.2F). A similar experiment was performed to validate the specificity of the Apaf-1 phosphorylation detected in interphase extract supplemented with OA. Immunoblotting of nickel-agarose bound His-Apaf-1 incubated in interphase extracts treated with OA and U0126, SL0101, or BI-D1870 revealed that Apaf-1 phosphorylation was almost completely eliminated in the presence of all three inhibitors (Figure 4.2G).

Given that the Rsk consensus site (RXRXXS*/T*) is shared by other members of the AGC kinase family, we sought to bolster the results from Figures 4.2F,G by ruling out other AGC kinases. As seen in Figure 4.2D, the addition of other inhibitors, for PKA (PKI) and Akt (LY-294002), to mitotic *Xenopus* extract failed to restore binding of Apaf-

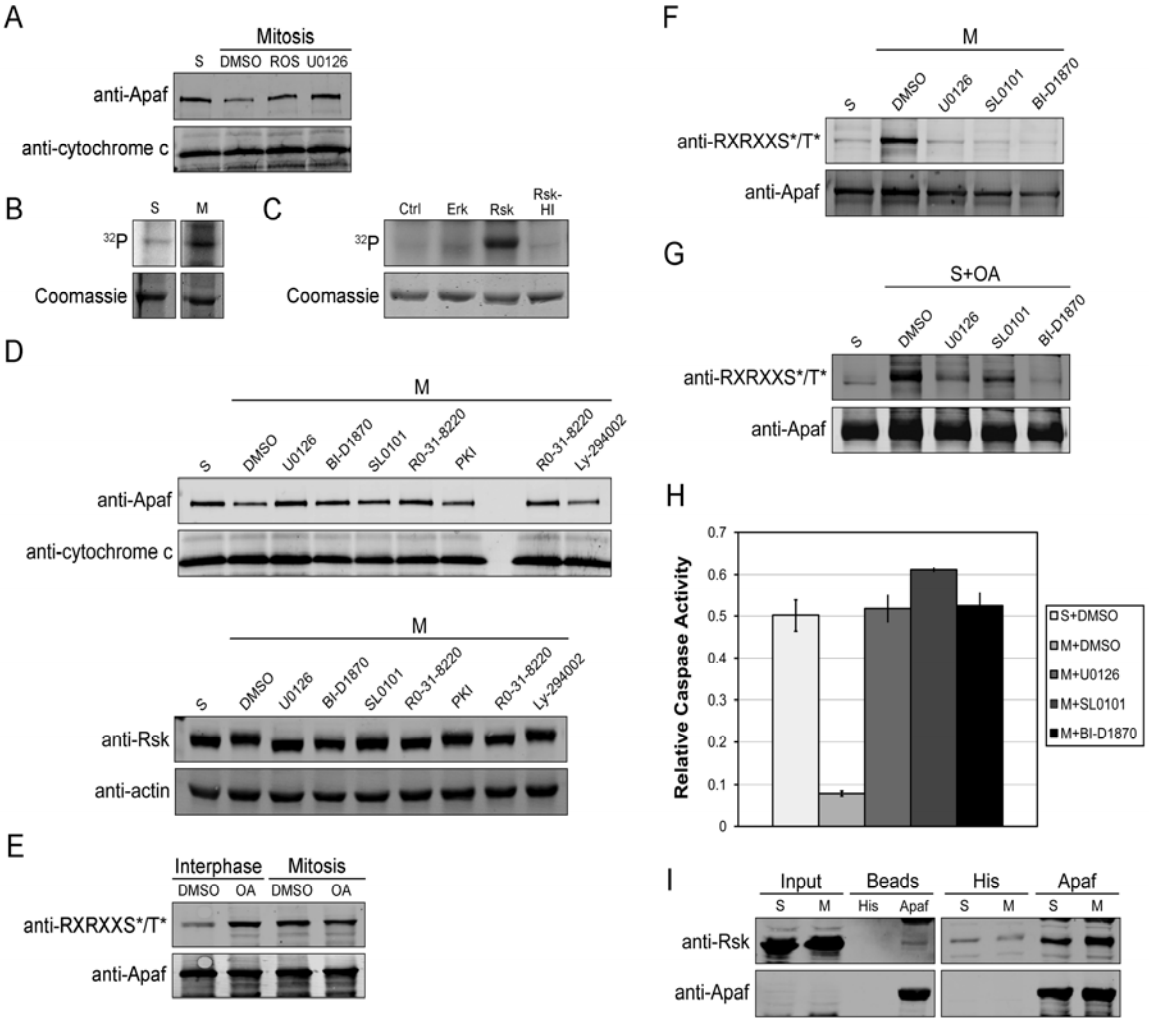

Figure 4.2: Mitotic Phosphorylation of Apaf-1 by Rsk.

Figure 4.2: A. Agarose-bound cytochrome *c* was used to affinity precipitate Apaf-1 from interphase (S) or mitotic extract pre-treated with DMSO, 1.2 mM roscovitine (ROS), or 200 μM U0126. Beads were washed and immunoblotted with anti-Apaf-1 and anti-cytochrome *c* antibodies. **B.** Nickel-agarose bound His-Apaf-1 was incubated in interphase (S) or mitotic (M) extract with γ-^{32}P-ATP. Beads were washed with buffer C and run on SDS-PAGE. Incorporation of ^{32}P was assessed by autoradiography. **C.** Nickel-agarose bound His-Apaf-1 was subjected to an *in vitro* kinase assay with active Erk, Rsk2, or heat-inactivated Rsk2 (Rsk-HI). Proteins were incubated with γ-^{32}P-ATP for 30 minutes at 30^{o}C, and incorporation of ^{32}P was assessed by autoradiography. **D.** Agarose-bound cytochrome *c* was utilized for an Apaf-1 affinity precipitation as in A except that mitotic extract was pre-treated with DMSO, 200 μM U0126, 100 μM BI-D1870, 4 mM SL0101, 4 μM/40 μM RO-31-8220, 200 μM H89/PKI, or 40 μM LY-294002. Beads were washed and subjected to immunoblotting with anti-Apaf-1 and anti-cytochrome *c* antibodies. In the lower panel, 1μL of extract from each treatment group was analyzed via immunblotting for Rsk2 and actin. **E.** Nickel-agarose bound His-Apaf-1 was incubated in the indicated extracts for 1 hour at 30^{o}C. Okadaic acid (OA) at 10μM or DMSO was added to the extract 30 minutes prior to the Apaf-1 protein. Phosphorylation of Apaf-1 was examined via immunoblotting using an antibody for Apaf-1, along with an antibody specific for residues phosphorylated at the Rsk consensus motif (anti-RXRXXS*/T*). **F.** Nickel-agarose bound His-Apaf-1 was incubated in interphase or mitotic extract as in E, except that the mitotic extracts were pre-treated with 200 μM U0126, 4 mM Sl0101, or 100 μM BI-D1870. Immunoblotting was performed as in E. **G.** Nickel-agarose bound His-Apaf-1 was incubated in interphase extract with or without OA and various inhibitors (added simultaneously). Concentrations of inhibitors and immunoblot analysis were the same as in F. **H.** The inhibitors U0126, SL0101, and BI-D1870 were used to treated cytosolic mitotic extract at 200 μM, 4 mM, and 100 μM, respectively. Cytochrome *c* was added at 5 ng/μL, and after 60 minutes, caspase activation was monitored by cleavage of the colormetric substrate, Ac-DEVD-pNA. Data shown are mean +/-SEM for three independent experiments. For S, M+U0126, M+SL0101, or M+BI-D1870 compared to M+DMSO, p-value <0.001. **I.** Empty nickel-agarose (His) or nickel-agarose bound His-Apaf-1 (Apaf) was incubated in interphase (S) or mitotic (M) extract for 30 minutes at 25^{o}C. The beads were washed and immunoblotted for Rsk2 and Apaf-1.

1 to the agarose-bound cytochrome *c*. Additionally, Rsk was still phosphorylated in these extracts, as demonstrated by the mobility shift on SDS-PAGE. The pan-PKC inhibitor (RO-31-8220) appeared to affect the recruitment of Apaf-1 to the cytochrome *c* resin, suggesting that perhaps PKC could also modulate Apaf-1 (Figure 4.2D). However, this inhibitor can in fact inhibit Rsk at lower/similar concentrations to those used for PKC. Thus, it is not specific for the PKC family (Alessi, 1997). Its effect on Rsk is supported by our immunoblot for Rsk phosphorylaion, which shows no mobility shift, suggesting reduced autophosphorylation and kinase activity (Figure 4.2D, lower panel). Given the ability of RO-31-8220 to target Rsk and the clear inhibition of Apaf-1 phosphorylation in Figures 4.2F,G, we assert that Rsk is the predominant Apaf-1-directed kinase in *Xenopus* mitotic extract. This hypothesis is further supported by agarose-bound cytochrome *c* affinity precipitations and Apaf-1 kinase assays following addition of the Rsk-activating MAPKKK, Mos, into interphase extract (data not shown). Caspase assays using the Rsk inhibitors, SL0101 and BI-D1870, also demonstrate the importance of Rsk in this apoptosome inhibition; treatment of mitotic *Xenopus* cytosol with these inhibitors restored cytochrome *c*-induced caspase activation to levels comparable with interphase extract (Figure 4.2H).

Finally, although not all kinase/substrate interactions are readily detectable, we examined this interaction by affinity precipitating Rsk from egg extract using nickel-agarose bound His-Apaf-1 (Figure 4.2I). In fact, we found that Rsk could bind to Apaf-1. Interestingly, the binding was the same in interphase and mitotic extracts. However, because Rsk is only catalytically active in the mitotic extract, Apaf-1 is not

phosphorylated in interphase. Taken together, these results suggested that Rsk can modify Apaf-1 directly *in vitro* and in mitotic *Xenopus* egg extract.

4.2.3 Rsk Modification of Apaf-1 Impairs Apoptosome Formation

Although the findings described above demonstrated that Apaf-1 is directly phosphorylated by Rsk, it remained unclear whether this Rsk-mediated modification was responsible for the altered apoptosome formation observed in mitotic *Xenopus* egg extract. To examine the ability of Rsk to phosphorylate Apaf-1 and to alter the interaction between cytochrome *c* and Apaf-1 in egg extract, we analyzed this interaction following Rsk immunodepletion. Since the concentration of Rsk2 is fifteen times that of Rsk1 in the egg extract, we started by immunodepleting Rsk2 (Bhatt and Ferrell, 1999). After complete Rsk2 depletion (Figure 4.3A), the ability of agarose-bound cytochrome *c* to affinity precipitate Apaf-1 was restored to levels comparable to interphase extract (Figure 4.3B). Importantly, removing Rsk from the extract also lessened phosphorylation of nickel-agarose bound His-Apaf-1, as detected by immunoblotting with the phospho-antibody (Figure 4.3B). In accordance with these results, addition of recombinant, active Rsk to the Rsk-depleted mitotic extract diminished the interaction between Apaf-1 and cytochrome *c* (Figure 4.3C).

Presumably, if Rsk can facilitate post-cytochrome *c* protection through phosphorylation of Apaf-1, direct modification of Apaf-1 *in vitro* should also result in decreased apoptosome activity in response to cytochrome *c*. To test this, we reconstituted the apoptosome *in vitro* using purified Apaf-1, caspase-9, and cytochrome *c*, with cleavage of ^{35}S-labeled *in vitro* translated caspase-3 serving as a marker of apoptosomal

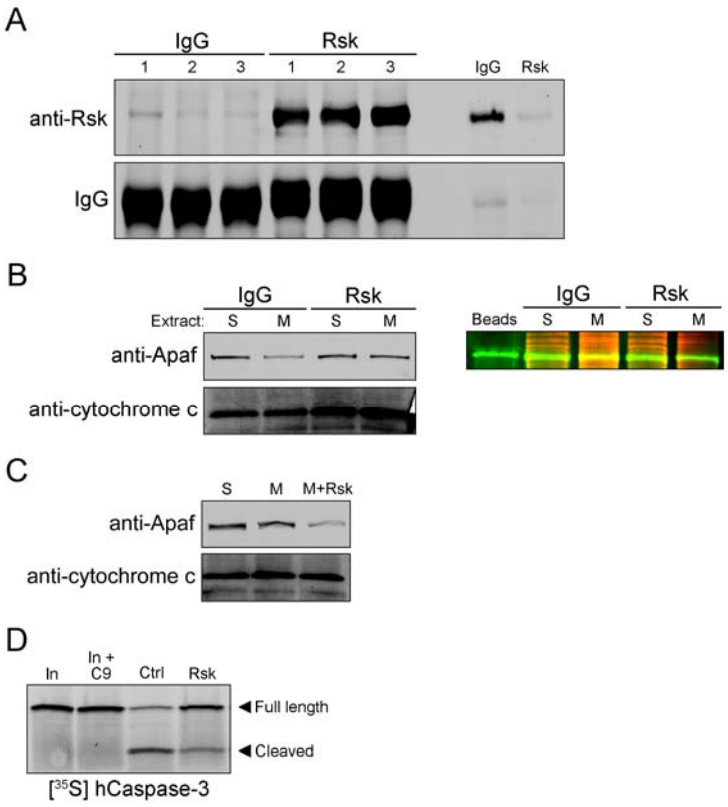

Figure 4.3: Reducing Rsk Activity Affects the Sensitivity of Apaf-1 to Cytochrome *c*.

Figure 4.3: A. Immunodepletion of Rsk2 was performed in an interphase extract. The antibody-bound beads from each round of depletion and the final depleted extract were immunoblotted for Rsk2. **B.** After Rsk immunodepletion, the extract was treated with non-degradable Cyclin B1 as indicated. Agarose-bound cytochrome *c* was incubated in interphase (S) or mitotic (M) extract for 20 minutes. Beads were washed and immunoblotted for Apaf-1 and cytochrome *c*. In the right panel, nickel-agarose bound His-Apaf-1 was incubated in interphase (S) or mitotic (M) extract for 30 minutes at 30°C. Anti-Apaf-1 (green) and anti-RXRXXS*/T* (red) antibodies were utilized for immunoblotting. Yellow indicates recognition by both antibodies. **C.** Rsk immunodepletion was performed as in B, except that in one sample, 50μM of recombinant, active Rsk was added back to the mitotic, Rsk-depleted extract. Agarose-bound cytochrome *c* was then used to precipitate Apaf-1 from the extract, and samples were immunoblotted for Apaf-1 and cytochrome *c*. **D.** Recombinant proteins were utilized to reconstitute the apoptosome *in vitro*. Apaf-1 was pre-treated with Rsk, as indicated. Caspase-9, cytochrome *c*, and ^{35}S-labeled *in vitro* translated caspase-3 were then added to the reaction. After 30 minutes, samples were run on SDS-PAGE and examined by autoradiography. In: Caspase-3 alone, In+C9: Caspase-3 and active caspase-9 without Apaf-1 or cytochrome *c*, Ctrl: Apaf-1 pre-treated with Rsk buffer alone, and Rsk: Apaf-1 pre-treated with active Rsk.

activity. As shown in Figure 4.3D, while addition of caspase-9 alone did not induce processing of caspase-3, the addition of recombinant Apaf-1, cytochrome *c*, and dATP was sufficient to promote cleavage. However, when Apaf-1 was pre-phosphorylated by Rsk, the cleavage of caspase-3 was markedly reduced, with a greater proportion remaining as full length protein. Together, these data suggest that phosphorylation of Apaf-1 by Rsk decreases cytochrome *c*-induced apoptosome formation and subsequent caspase activity.

4.2.4 Protein Phosphatase-1 Binds to and Dephosphorylates Apaf-1

As shown previously in Figure 4.2E, the addition of OA to interphase *Xenopus* egg extract induced phosphorylation of Apaf-1 as recognized by the anti-RXRXXS*/T* antibody. Accordingly, there was a decrease in the amount of Apaf-1 affinity precipitated by agarose-bound cytochrome *c* from interphase egg extract pre-treated with OA (data not shown). These results are consistent with the fact that OA can activate the MAPK pathway, and therefore Rsk, in egg extract. However, OA might also have effects on the interaction of Apaf-1 and cytochrome *c* by controlling a phosphatase acting in opposition to Rsk, to dephosphorylate Apaf-1. To test this possibility, we pre-phosphorylated nickel-agarose bound His-Apaf-1 with Rsk *in vitro* and incubated the pre-phosphorylated Apaf-1 in interphase or mitotic *Xenopus* egg extract to examine dephosphorylation over time. As seen in Figure 4.4A, Apaf-1 was dephosphorylated more rapidly in interphase than mitotic extract. Additionally, there was a noticeable downward gel mobility shift of Apaf-1 upon incubation in interphase extract. These results suggest that the Apaf-1-directed

phosphatase has reduced activity in mitosis or cannot interact with Apaf-1 as efficiently in mitosis.

Our laboratory and others have shown that the OA-inhibitable phosphatase PP1 is active in interphase and inactive in mitosis (by phosphorylation at threonine 320-T320). Given our previous results, we pursued the possibility that PP1 is a relevant Apaf-1-directed phosphatase (Dohadwala et al., 1994; Kwon et al., 1997; Wu et al., 2009). In addition to the fact that PP1 is inactive during mitosis, titrations of OA in the agarose-bound cytochrome *c* affinity precipitation assay suggested that PP1 was the relevant phosphatase (PP1 requires higher doses of OA for inhibition than the other predominant OA-inhibitable phosphatase in egg extracts, PP2A, data not shown). Therefore, we characterized the interaction between Apaf-1 and PP1 using nickel-agarose bound His-Apaf-1 to affinity precipitate *Xenopus* PP1. The Apaf-1 containing agarose recruited more PP1 than His agarose alone (Figure 4.4B). Interestingly, binding between Apaf-1 and PP1 was reduced in mitotic extract, which, along with the relative inactivity of PP1 in mitosis, could contribute to preferential phosphorylation of Apaf-1 in mitotic extract.

To bolster these results, we used a specific PP1 inhibitor, protein inhibitor-2, to suppress PP1 activity in interphase egg extract and examined dephosphorylation of Apaf-1. After adding GST-tagged inhibitor 2 (GST-I2) to interphase extract, we incubated pre-phosphorylated nickel-agarose bound His-Apaf-1 in the extract. As shown in Figure 4.4C, the dephosphorylation of Apaf-1 in interphase egg extract containing GST-I2 is reduced relative to the interphase extract alone. The downward gel mobility shift of Apaf-1 observed in interphase extract is also inhibited in the presence of GST-I2, supporting a

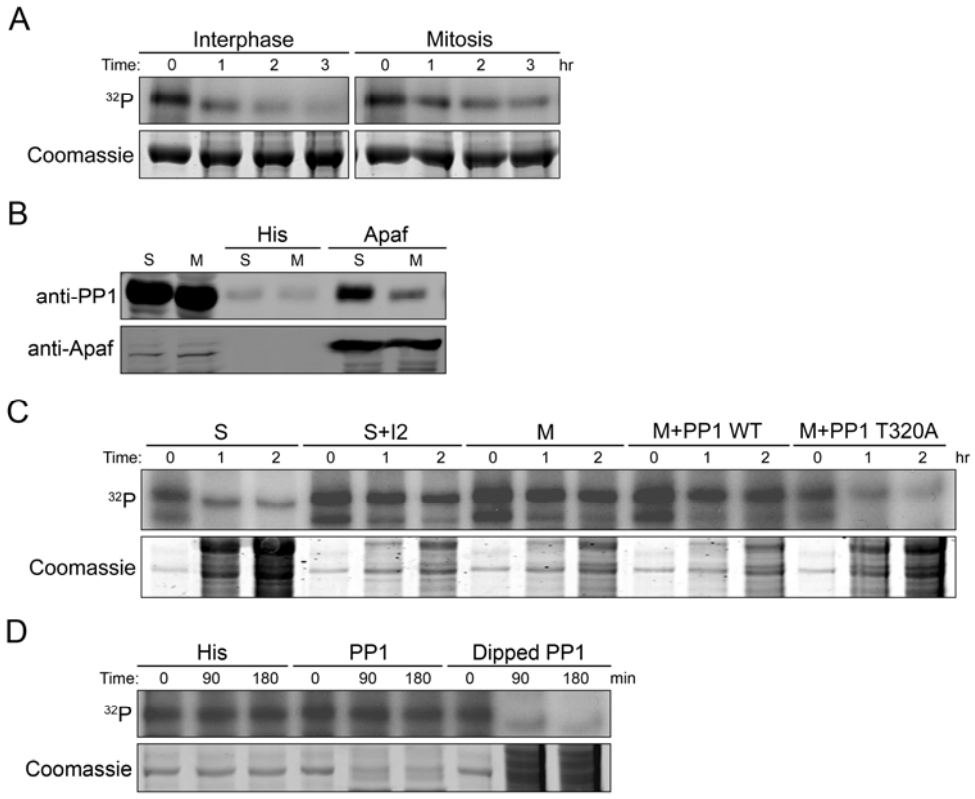

Figure 4.4: Protein Phosphatase 1 Antagonizes Rsk Phosphorylation of Apaf-1.

Figure 4.4: A. Nickel-agarose bound His-Apaf-1 was pre-phosphorylated *in vitro* with γ-^{32}P-ATP and active Rsk2. The beads were then incubated in extract, as indicated. Beads were washed, and phosphorylation of Apaf-1 was examined via autoradiography. **B.** Empty nickel-agarose (His) or nickel-agarose bound His-Apaf-1 (Apaf) was incubated in interphase (S) or mitotic (M) extract for 1 hour at 25^{o}C. Beads were then washed and immunoblotted with anti-Apaf-1 and anti-xPP1 antibodies. **C.** Nickel-agarose bound His-Apaf-1 was pre-phosphorylated as in A. The beads were then incubated in interphase (S) extract, S with GST-I2 (S+I2), mitotic extract (M), M with WT PP1 (M+WT PP1), or M with PP1 T320A (M+PP1 T320A) for the indicated times. Phosphorylation of Apaf-1 was examined via autoradiography. **D.** Nickel-agarose bound His-Apaf-1 was pre-phosphorylated as in A. The beads were retrieved, washed, and incubated *in vitro* with nickel-agarose bound His-PP1 that had been pre-incubated in interphase extract for 1 hour. Phosphorylation of Apaf-1 was examined via autoradiography.

role for PP1 in dephosphorylating Apaf-1. Furthermore, addition of a mutant PP1 (T320A) that is unable to be suppressed by phosphorylation during mitosis augmented the dephosphorylation of Apaf-1 in mitotic egg extract. However, supplementing the extract with additional wildtype PP1, which should have reduced activity due to phosphorylation at threonine 320, failed to facilitate Apaf-1 dephosphorylation in mitotic extract (Figure 4.4C).

Even though Apaf-1 interacted with PP1 in *Xenopus* egg extract, it was unclear whether PP1 could dephosphorylate Apaf-1 through a direct interaction in the absence of a targeting subunit. Therefore, we performed a dephosphorylation assay on Apaf-1 using nickel-agarose bound PP1 that had been pre-dipped in interphase extract. As shown in Figure 4.4D, Apaf-1 was sensitive to dephosphorylation by PP1 pre-incubated in extract, but not nickel-agarose bound His-PP1 alone, suggesting the requirement for a targeting subunit for complete Apaf-1 dephosphorylation. Taken together, these data suggest that Apaf-1 is not only phosphorylated by Rsk but also dephosphorylated by PP1.

4.2.5 Rsk Phosphorylates Apaf-1 in Mammalian Cells, Altering Cytochrome *c* Responsiveness

Rsk activity is high during *Xenopus* maturation and mitosis, and similarly, many types of tumors exhibit increased activation of the MAPK pathway. We wished to extrapolate from our *Xenopus* work to assess how Rsk phosphorylation of Apaf-1 might contribute to post-cytochrome *c* protection in mammalian cells with upregulated MAPK signaling. First, after overexpressing wildtype, kinase dead, or constitutively active myrostylated-Rsk1 (myr-Rsk), 293T cells were serum-starved to minimize activation of

the endogenous MAPK pathway. Immunoprecipitation of endogenous Apaf-1 from these transfected cells revealed phosphorylation recognizable by the anti-RXRXXS*/T* antibody only in the cells with myr-Rsk (Figure 4.5A). Expression of the myr-Rsk following serum starvation, was confirmed by immunoblotting for phosphorylation of the direct Rsk target, S6 (Figure 4.5A, lower panel). Additionally, cytosolic lysates from 293T cells transfected with vector or myr-Rsk were utilized for a kinase assay with nickel-agarose bound His-Apaf-1 as a substrate. Recombinant Apaf-1 was phosphorylated more robustly in the lysate from the cells transfected with constitutively active myr-Rsk (Figure 4.5B). Caspase-9 phosphorylation was not detected under these conditions (data not shown). Caspase activity was also assessed in response to cytochrome *c* using cytosolic lysates from these transfected cells. As shown in Figure 4.5C, constitutive Rsk activity decreased the responsiveness of the lysates to cytochrome *c*.

Phorbol 12-myristate 13-acetate (PMA) is known to activate the MAPK pathway, including the effectors Erk and Rsk. Therefore, we utilized PMA-treated 293T cells as an additional system to probe the relationship between Rsk and Apaf-1 in mammalian cells. Endogenous Apaf-1 immunoprecipitated from PMA-treated cells was detected by the anti-RXRXXS*/T* antibody, while control cells did not contain high levels of phosphorylated Apaf-1 (Figure 4.5D). Caspase activity of cytosolic lysates from these cells demonstrated that PMA treatment reduced the responsiveness of the lysates to cytochrome *c* (Figure 4.5E). Furthermore, as shown in Figure 4.5F, agarose-bound cytochrome *c* affinity precipitated less Apaf-1 from the PMA-treated lysates. These data

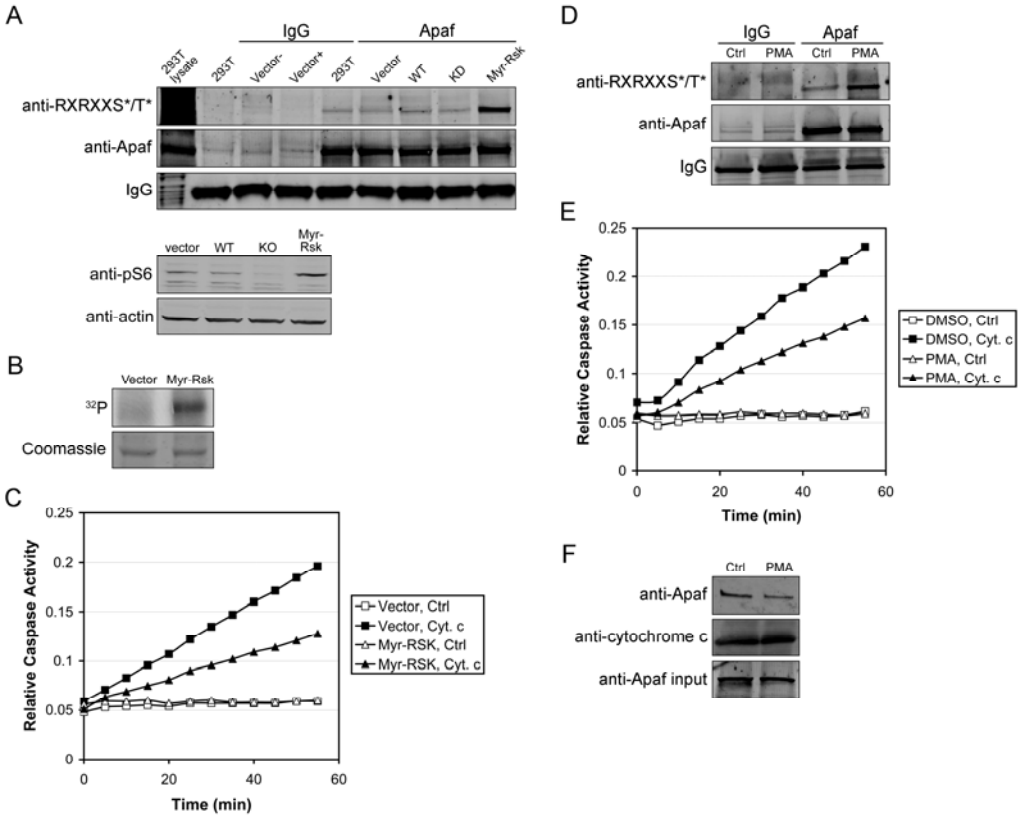

Figure 4.5: Rsk Phosphorylates Apaf-1 in 293T Cells and Reduces Sensitivity to Cytochrome *c*.

Figure 4.5: A. 293T cells were transfected with plasmids expressing the indicated forms of the Rsk kinase (293T=untransfected). Cells were incubated in complete media for 24 hours and then serum-starved with .5% FBS for an additional 24 hours. The cells were harvested, and whole cell lysates were used for immunoprecipitation with an immunoglobulin (IgG) control or with an Apaf-1 antibody. Immunoblotting was used to examine the immunoprecipitation (with an anti-Apaf-1 antibody) and phosphorylation status of Apaf-1 (with an anti-RXRXXS*/T* antibody). In the lower panels, immunoblotting was performed for phospho-S6 to indicate Rsk activity. **B.** Nickel-agarose bound His-Apaf-1 was incubated with γ-^{32}P-ATP in cytosolic lysates from 293T cells transfected with vector or myr-Rsk. Beads were then washed with buffer C and resolved by SDS-PAGE. Incorporation of ^{32}P was assessed by autoradiography. **C.** After transfecting the indicated plasmids, cells were serum-starved, and cytosolic lysates were prepared. Cytochrome *c* at 10 ng/μL and 1mM dATP were added for 30 minutes at 37°C, at which point, the colorimetric caspase substrate, Ac-DEVD-pNA, was used to examine caspase activity. **D.** 293T cells were treated with PMA for 30 minutes at 37°C after being serum-starved for 24 hours. Cells were then harvested, and whole cell lysates were used for an immunoprecipitation of Apaf-1. Analysis was performed as in A. **E.** After PMA treatment, as in D above, cytosolic lysates were made and treated with 10 ng/μL cytochrome *c* and 1 mM dATP for 30 minutes at 37°C. The colorimetric substrate, Ac-DEVD-pNA, was used to assess caspase activation. **F.** Agarose-bound cytochrome *c* was added to control or PMA-treated lysates. Beads were retrieved and washed in lysis buffer containing 500mM NaCl. Immunoblotting was performed with anti-Apaf-1 and cytochrome *c* antibodies.

are consistent with the possibility that Apaf-1 is phosphorylated by Rsk in mammalian cells, thus altering their responsiveness to cytochrome *c*. Preliminary studies using siRNA to knockdown Rsk1 and 2 demonstrate that the PMA-mediated effects on Apaf-1 are predominantly related to Rsk kinase activity; we observed decreased Apaf-1 phosphorylation and increased caspase activity/ recruitment of Apaf-1 to cytochrome *c* resin following Rsk knockdown (data not shown). To assess these findings more directly, we turned to a model where Rsk was activated endogenously.

4.2.6 Phosphorylation of Apaf-1 in Cells Expressing Oncogenic Ras12V and in PC3 Prostate Cancer Cells

The MAPK pathway is elevated in many cancers as a result of constitutively active Ras, and therefore, we examined the phosphorylation status of Apaf-1 in cells stably expressing oncogenic Ras12V. As shown in Figure 4.6A, after immunoprecipitating endogenous Apaf-1, we detected more Apaf-1 phosphorylation in the cells expressing Ras12V. Importantly, treating Ras12V cells with the MEK1/2 inhibitor, U0126, or the Rsk inhibitor, SL0101, reduced the phosphorylation of Apaf-1 (Figure 4.6B).

It has been reported that Rsk protein levels are elevated in some prostate cancers, where it can play a role in proliferation and PSA expression (Clark et al., 2005). Additionally, increased MAPK signaling has been correlated with prostate cancer progression to a more advanced disease state (Gioeli et al., 1999). To characterize the relationship between Rsk and Apaf-1 phosphorylation under conditions of high endogenous Rsk activity, we immunoprecipitated Apaf-1 from the prostate cancer cell

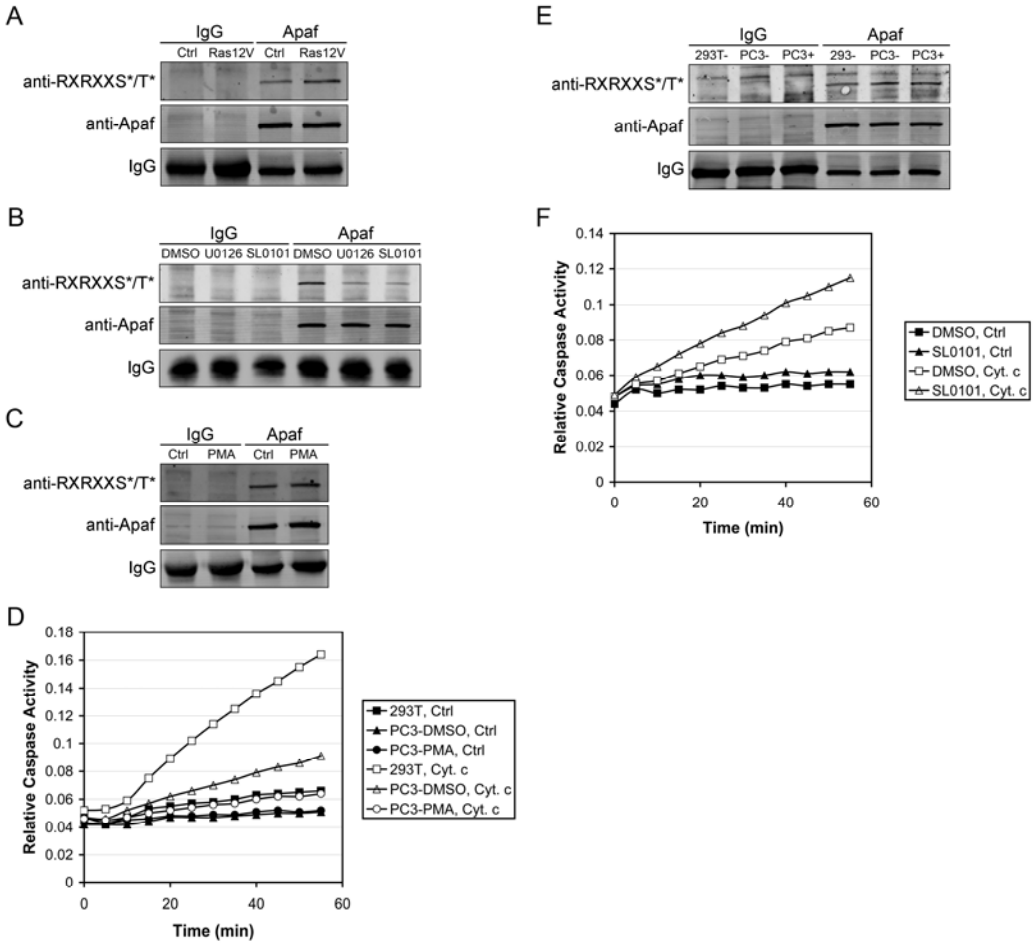

Figure 4.6: Apaf-1 Phosphorylation in Cells Expressing Ras12V and in Prostate Cancer PC3 Cells.

Figure 4.6: A. HEK-HT cells alone or stably expressing Ras12V were harvested after being serum-starved for 48 hours. Whole cell lysates were utilized for an immunoprecipitation, and immunoblot analysis was performed with anti-Apaf-1 and anti-RXRXXS*/T* antibodies. **B.** Ras12V cells were serum-starved for 48 hours and then treated with 50 μM U0126 or 100 μM SL0101 for 30 minutes or 3 hours, respectively. Whole cell lysates were used for an immunoprecipitation, as above. **C.** PC3 cells were treated with PMA for 30 minutes at 37°C after being serum-starved for 24 hours. Cells were then harvested, and whole cell lysates were used for an immunoprecipitation of Apaf-1. Analysis was performed as in A. **D.** Cells were serum-starved, and cytosolic lysates were prepared. Cytochrome *c* at 10 ng/μL and 1 mM dATP were added for 20 minutes at 37°C. The colorimetric caspase substrate, Ac-DEVD-pNA, was used to examine caspase activity. **E.** 293T and PC3 cells were serum-starved for 24 hours. PC3 cells were then treated with PMA as in C. Whole cell lysates were used for an immunoprecipitation of Apaf-1, and immunoblot analysis was performed as in A. **F.** PC3 cells were incubated with DMSO or 100 μM of the Rsk inhibitor, SL0101, for 3 hours. Cytosolic lysates were made, and 10 ng/μL cytochrome *c* and 1 mM dATP were added for 30 minutes at 37°C. The colorimetric caspase substrate, Ac-DEVD-pNA, was used to examine caspase activity.

line, PC3. Phosphorylation of Apaf-1 was detected in serum-starved PC3 cells using the anti-RXRXXS*/T* antibody (Figure 4.6C). When endogenous Apaf-1 was immunoprecipitated from PMA-treated PC3 cells, the levels of detectable phosphorylation were similar to the serum-starved cells alone (Figure 4.6C). Since serum-starved 293T cells are sensitive to cytochrome *c* and have low levels of detectable phospho-Apaf-1 (Figure 4.5D,E), we utilized 293T cells as a comparison for the cytochrome *c* sensitivity of PC3 cells. As shown in Figure 4.6D, 293T cells robustly activated caspases in response to cytochrome *c*, while PC3 cells exhibited less sensitivity to the same stimulus. Immunoblot analyses of both cytosolic and whole cell lysates from 293T and PC3 cells demonstrated that this difference in cytochrome *c* responsiveness was not due to Apaf-1 protein levels, as these cells expressed comparable amounts of Apaf-1 per total protein (data not shown). However, immunoprecipitation of equivalent levels of endogenous Apaf-1 from 293T and PC3 cells demonstrated that the PC3 cells have higher levels of phosphorylated Apaf-1, correlating with the observed differences in cytochrome *c* sensitivity (Figure 4.6E). To demonstrate the importance of Rsk kinase activity in the post-cytochrome *c* protection of PC3 cells, we treated cells with the Rsk inhibitor, SL0101. Compared to a DMSO control, cells treated with SL0101 had enhanced sensitivity to cytochrome *c*, allowing for more robust caspase activation (Figure 4.6F). The addition of SL0101 did not render the PC3 cells as sensitive to cytochrome *c* as the 293T cells, indicating that perhaps, in addition to Rsk, other signaling pathways play a role in protecting these prostate cancer cells against cytochrome *c*-induced

apoptosis. Taken together, these data suggest a role for Rsk in promoting resistance to cytochrome *c*-induced apoptosis, at least in part, through phosphorylation of Apaf-1.

4.2.7 Apaf-1 is Phosphorylated at Serine 357 and Serine 760 by Rsk

Although Apaf-1 is a large protein and has multiple putative Rsk phosphorylation sites, we sought to utilize mass spectrometry analysis to identify which site(s) was modified by Rsk. Our initial approach, using nickel-agarose bound His-Apaf-1 dipped into extract, was unsuccessful, mostly because we were unable to recover enough protein for mass spectrometry. Therefore, we decided to significantly increase the amount of recombinant Apaf-1 that we were using by submitting *in vitro* phosphorylated human Apaf-1 for analysis. As shown in Figure 4.7A, two phoshorylated peptides were identified. The first corresponded to amino acids 355 to 376. Given the mass of the peptide, it was clear that only one site was phosphorylated. However, the product ions left us unable to assign the phosphorylation to a specific residue (see the highlighted yellow box in the upper panel of Figure 4.7A). The second peptide (amino acids 757 to 768) also contained one phosphorylation modification, which was unambiguously localized to serine 760 (Figure 4.7A, lower panel). An alignment of the Apaf-1 sequence from these peptides demonstrates that the first phosphorylated peptide contains a canonical, well-conserved Rsk consensus site, serine 357 (Figure 4.7B, blue box). However, the second residue, serine 760, does not occur within a Rsk consensus site (Figure 4.7B, second red serine). Therefore, we began to speculate that perhaps this second modification represented an artifact of the *in vitro* kinase reaction and was not physiological. Attempts to mutate these residues in full length Apaf-1 are still underway.

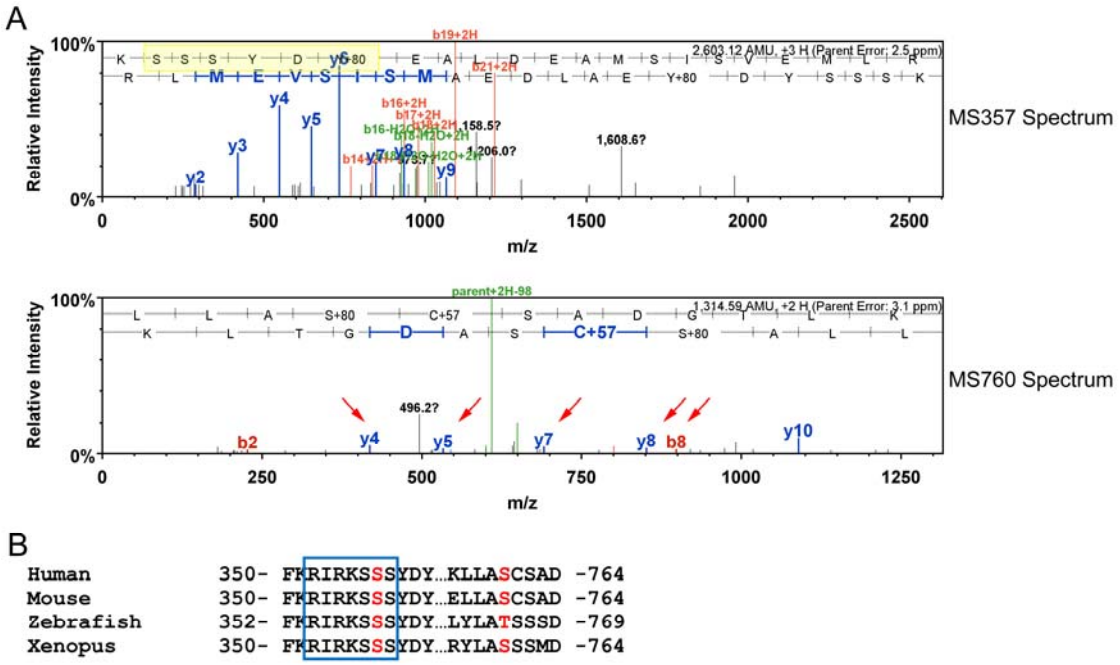

Figure 4.7: Identification of Rsk-Mediated Apaf-1 Phosphorylation Sites.

Figure 4.7: A. An *in vitro* kinase assay was performed on human His-Apaf-1 with or without Rsk, and samples were analyzed by mass spectrometry. Product ion spectra are shown for the two phosphorylated peptides identified. The yellow box in the upper panel highlights potential phosphorylated residues for peptide 355-376. The red arrows in the bottom panel indicate product ions localizing the phosphorylation site to serine 760 in the 757-768 peptide. **B.** Sequence alignment of Apaf-1 from different species. Letters in red indicate the relevant phosphorylation sites. The blue box designates the Rsk consensus motif surrounding serine 357.

Unfortunately, we have been hampered by the highly recombinogenic nature of the 13 WD40 repeats.

4.2.8 Rsk Affects Caspase-9 Activation Following Cytochrome *c*-Independent Apaf-1 Oligomerization

The first phosphorylate site, serine 357, is located within the NOD of Apaf-1. Although it is possible that phosphorylation of Apaf-1 in the NOD could affect its interaction with cytochrome *c* indirectly (through changes in protein conformation, for example), we began to speculate that Rsk phosphorylation directly affected Apaf-1 oligomerization/self-association. To test this hypothesis, we utilized mammalian cell models where we could transiently express N-terminal (amino acids 1-559) or COOH-terminal (amino acids 468-1194) Apaf-1 domains. Upon co-expressing flag-tagged Apaf-1 1-559 with myr-Rsk in 293T cells, we performed an immunoprecipitation using flag antibody. Immunoblotting clearly revealed that this portion of Apaf-1 can be phosphorylated by Rsk (Figure 4.8A, left panel). Similar studies using the HA-tagged Apaf-1 468-1194 yielded no detectable phosphorylation (Figure 4.8A, right panel). These data suggest that indeed Rsk can phosphorylate Apaf-1 between amino acids 1-559 (where serine 357 is located) but cannot phosphorylate Apaf-1 from 468-1194 (where serine 760 is located).

It has been demonstrated that expression of the Apaf-1 1-559 mutant in mammalian cells is sufficient to cause cleavage of ^{35}S-labeled *in vitro* translated caspase-9 supplemented into cytosolic lysate (Hu et al., 1998). Upon expressing this flag-tagged Apaf-1 1-559 in 293T cells, we performed immunoblotting of whole cell lysates to

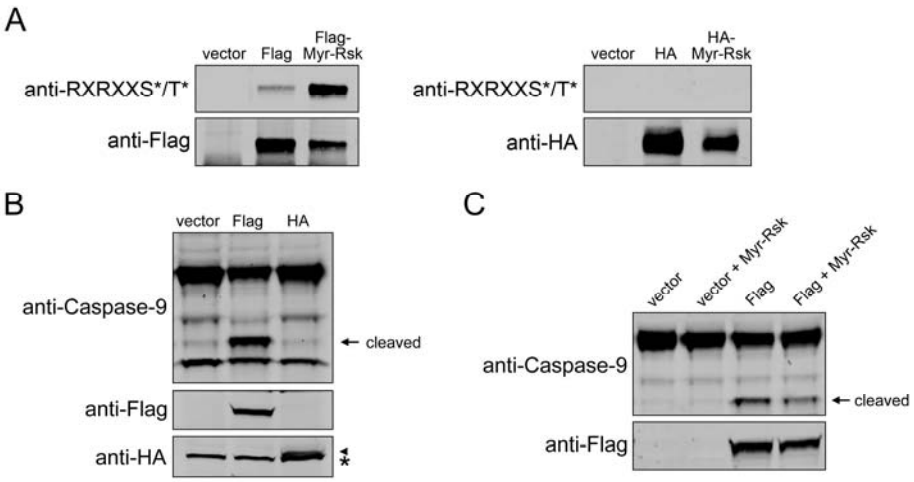

Figure 4.8: Rsk Phosphorylation Affects Caspase-9 Activation Following Apaf-1 Oligomerization Independent of Cytochrome *c*.

Figure 4.8: A. 293T cells were transfected with flag-tagged Apaf-1 1-559 or HA-tagged Apaf-1 468-1194 with and without myr-Rsk. Whole cell lysates were used for an immunoprecipitation of flag or HA, and immunoblotting was performed for transfection with the anti-flag/anti-HA antibody and for phosphorylation with the anti-RXRXXS*/T* antibody. **B.** 293T cells were transfected as in A. Whole cell lysates were prepared, and immunoblotting was performed with anti-caspase-9, anti-flag, and anti-HA antibodies. **C.** 293T cells were transfected as in A. Following preparation of whole cell lysates, immunoblot analysis with anti-flag and anti-caspase-9 antibodies was performed.

determine if we could detect cleavage of endogenous caspase-9. As shown in Figure 4.8B, expression of flag-tagged Apaf-1 1-559 caused a caspase-9 cleavage product, while the HA-tagged Apaf-1 468-1194 did not. Presumably, if Rsk phosphorylation of Apaf-1 was affecting its oligomerization, co-transfection of myr-Rsk with the flag-tagged Apaf-1 1-559 should reduce cleavage of caspase-9. Indeed, expression of constitutively active Rsk (myr-Rsk) in these cells reduced the cleavage of caspase-9 (Figure 4.8C). Preliminary studies characterizing the serine 357 mutant (alanine) using this model are progressing. We have been able to validate the mass spectrometry results using recombinant GST-tagged Apaf-1 1-543 containing a serine to alanine mutation at amino acid 357. This mutant is less phosphorylated than the wildtype protein following an *in vitro* kinase assay with Rsk (data not shown). Initial results demonstrate that mutating all three serines (356, 357, and 358) completely abolishes Rsk-mediated phosphorylation of N-terminal Apaf-1 fragments (*in vitro* and in cells). Most interestingly, when we examine caspase-9 cleavage following overexpression of this triple mutant, we fail to see any caspase-9 activation, even in the absence of Rsk phosphorylation (data not shown). This result suggests that perhaps these residues are critical for Apaf-1 self-association, and thus, mutating them, even in the absence of Rsk kinase activity, is sufficient to disrupt oligomerization. Studies to clarify this mechanism and the role of serine 357 phosphorylation are ongoing.

4.3 Discussion

The interplay between cell survival pathways and pro-apoptotic signaling maintains a critical equilibrium in the cell, and the MAPK pathway is connected, directly

or indirectly, to many of these processes. Mutations and uncontrolled alterations in this and other regulatory signals facilitate aberrant cell proliferation and aid in the progression of diseases such as cancer. Indeed, resistance to apoptotic stimuli has become well-known as a hallmark of cancer (Hanahan and Weinberg, 2000). While examining apoptosis using interphase and mitotic *Xenopus* egg extract, we identified a novel mode of apoptosome regulation involving the phosphorylation of Apaf-1 by Rsk. Apaf-1 phosphorylation suppresses the ability of cytochrome *c* to nucleate apoptosome formation, thus decreasing caspase activity. Moreover, we have demonstrated that PP1 serves as an Apaf-1-directed phosphatase, antagonizing Rsk phosphorylation of Apaf-1. Finally, mammalian cell models with high Rsk kinase activity exhibit Apaf-1 phosphorylation and resistance to cytochrome *c*, consistent with the ability of Rsk to promote cell survival through phosphorylation of Apaf-1.

4.3.1 The Cytochrome *c*/Apaf-1 Interaction

Previous studies have demonstrated that various cytochrome *c* interactors can affect its binding to Apaf-1. Bruey *et al.* revealed that the chaperone hsp27 interacts with cytochrome *c*, inhibiting its ability to activate the apoptosome (Bruey et al., 2000). Additionally, physiological levels of nucleotides, such as ATP and dATP, can directly bind to cytochrome *c*, inhibiting its interaction with Apaf-1 (Chandra et al., 2006). Other studies have shown that ions, such as calcium and potassium, can regulate the function of Apaf-1 (Bao et al., 2007; Cain et al., 2001). These data presented here demonstrate the first Apaf-1 post-translational modification that affects the ability of cytochrome *c* to nucleate apoptosome formation. Reconstitution of the apoptosome *in vitro* (Figure 4.3D),

Rsk immunodepletion (Figure 4.3A-C), and apoptosome formation assays in *Xenopus* egg extract (Figure 4.1E-H) support the notion that Rsk phosphorylation of Apaf-1 reduces the ability of cytochrome *c* to drive Apaf-1 oligomerization. Moreover, precipitation studies using agarose-bound cytochrome *c* (Figures 4.1C, 4.2A, 4.2D, 4.3B, 4.5F) suggest that the binding between cytochrome *c* and Apaf-1 is reduced when Apaf-1 is phosphorylated by Rsk. Additional studies using a cytochrome *c*-independent Apaf-1 indicate that Apaf-1 oligomerization may be defective in the presence of Rsk (Figure 4.8C). It is possible that Rsk is able to affect multiple Apaf-1 functions through its phosphorylation. However, it is equally likely that the agarose-bound cytochrome *c* we utilized to assess the interaction between Apaf-1 and cytochrome *c* was somehow able to indirectly detect Apaf-1 oligomerization. It has been reported that the interaction between Apaf-1 and cytochrome *c* is transient, which could allow for some Apaf-1 to be opened/activated by the beads, at which point it comes off, only to be recruited back to the resin indirectly through its interaction with another Apaf-1 monomer (Hill et al., 2004).

It is currently unclear exactly how cytochrome *c* interacts with Apaf-1 to initiate apoptosome formation. Thus, in the absence of a full-length Apaf-1 mutant, it is difficult to completely rule out a Rsk-mediated effect on the binding between these two proteins (see below). Structural analysis of the apoptosome using electron cyromicroscopy indicates that one cytochrome *c* molecule interacts with Apaf-1 between two β propellers formed by the 13 WD40 repeats (Yu et al., 2005a). Thus, the auto-inhibitory COOH-terminal region of Apaf-1 is necessary for its interaction with cytochrome *c*. This analysis

is consistent with data showing that Apaf-1 lacking the WD40 repeats is constitutively active in binding and activating caspase-9 (Srinivasula et al., 1998). Numerous lysine residues on cytochrome *c* are known to play crucial roles in allowing cytochrome *c* to bind Apaf-1, with K72 perhaps being the most important (Chandra et al., 2006; Purring-Koch and McLendon, 2000; Yu et al., 2001). While conserved in many species, this lysine residue on cytochrome *c* is tri-methylated in yeast, making it unable to bind Apaf-1 and activate caspases (Kluck et al., 1997; Yu et al., 2001).

Further studies on the specific structure of monomeric Apaf-1 and on the exact residues required for the cytochrome *c* and Apaf-1 interaction are necessary to determine how/if Rsk phosphorylation of Apaf-1 affects its binding to cytochrome *c*. It is possible that Apaf-1 phosphorylation sterically prevents interaction of cytochrome *c* with Apaf-1 or induces a conformational change in Apaf-1 that renders the relevant binding sites inaccessible to cytochrome *c*. Through mass spectrometric analyses (Figure 4.7A), we have identified serines 357 and 760 as potential sites of Rsk phosphorylation on Apaf-1. Although it would have been ideal to mutate these residues and restore cytochrome *c* binding and sensitivity in the face of Rsk activity, we were hampered in this approach by the extremely recombinogenic nature of the Apaf-1 gene, particularly within the WD40 repeats. All attempts to express and mutagenize Apaf-1 promoted clone rearrangements, even in recombination-defective bacterial strains. Other techniques, including yeast protein expression, BAC (bacterial artificial chromosome) cloning, and/or zinc finger nucleases could be helpful for future attempts to mutate and express full length Apaf-1.

Despite the difficulty in mutating full-length Apaf-1, data in Figure 4.3D do demonstrate that pre-phosphorylation of Apaf-1 by Rsk is sufficient to inhibit apoptosome function in an *in vitro* reaction involving purified apoptosome components. Additionally, data from Figure 4.8 indicate that perhaps Rsk phosphorylation affects Apaf-1 oligomerization. Taken together with the observations that elevating Rsk can promote protection from cytochrome *c*-induced caspase activity and that Rsk appears to affect the cytochrome *c*-induced caspase activation, even if Apaf-1 is not the sole target of Rsk, it is very likely to be an important contributor to Rsk-mediated cytochrome *c* resistance. It has been previously reported that threonine 125 of caspase-9 is a target of Erk kinase, contributing to apoptosome inhibition by the MAPK pathway (Allan et al., 2003). Our data show that the apoptosome is also inhibitable by the MAPK pathway prior to caspase-9 recruitment, and it may be that both of these modifications contribute to full inhibition of cytochrome *c*-induced apoptosis by MAPK signaling.

4.3.2 Dual Regulation of Apaf-1 Phosphorylation

It is not yet clear how the actions of Rsk and PP1 are balanced to affect the phosphorylation status of Apaf-1 and subsequent apoptosome formation. We have shown that Rsk interacts with Apaf-1, and at least in interphase and mitotic *Xenopus* egg extracts, this binding per se appears to not be regulated (Figure 4.2I). Thus, the ability of Rsk to phosphorylate Apaf-1 presumably depends on the activation state of the kinase. However, the interaction of Apaf-1 with PP1 is diminished in mitotic *Xenopus* egg extract (Figure 4.4B). Additionally, in mitotic *Xenopus* egg extract and during mammalian mitosis, PP1 is inactivated by cdc2-mediated phosphorylation at threonine

320. Therefore, it is likely that the phosphorylation status of Apaf-1 is controlled both through its interaction with the phosphatase and by the regulated activity of the kinase and phosphatase. Specifically, mitotic *Xenopus* egg extract is characterized by high levels of Rsk kinase activity and low levels of PP1 phosphatase activity, which taken together, allow for Apaf-1 to be highly phosphorylated and less sensitive to cytochrome *c*.

The exact regions of Apaf-1 responsible for its interaction with Rsk or PP1 are unknown. PP1 is reported to interact with its substrates and targeting subunits through a VxF motif (Cohen, 2002; Egloff et al., 1997; Wakula et al., 2003). There are five such motifs in human Apaf-1, and it would be of interest to specifically determine which of these docking sites facilitates the binding between Apaf-1 and PP1. It has been previously reported, using an array to identify novel PP1 interactors, that Apaf-1 was a PP1-interacting protein (Flores-Delgado et al., 2007). Immunoprecipitations by this group confirmed that Apaf-1 interacted with PP1α in murine FLECs and human A549 cells. A more stringent analysis of the Apaf-1 sequence using more specific motifs, RVxF or FxxKxK, yielded two potential PP1 docking sites in Apaf-1 (Flores-Delgado et al., 2007). Elucidating the specifics of the interactions between Apaf-1 and Rsk/PP1 would allow for more careful studies examining how phosphorylation affects the conformation of Apaf-1 and its ability to oligomerize in response to cytochrome *c*.

4.3.3 The MAPK Pathway and Cancer

Rsk is a well-known effector of Ras-MAPK signaling, and this pathway is one of the most important for promoting cell survival in response to extracellular stimuli; oncogenic Ras mutations occur in about one-third of all cancers (Bos, 1989). Additional

roles for many Ras effectors, including Rsk, have been reported in cancer. For example, Rsk1 and Rsk2 are overexpressed in breast and prostate cancers, along with head and neck squamous cell carcinoma (Clark et al., 2005; Kang et al., 2010; Smith et al., 2005). Rsk3 has been shown as a possible tumor suppressor in ovarian cancer (Bignone et al., 2007). Rsk4 is abnormally expressed in breast cancer, and it has been implicated in p53-dependent cell growth arrest (Berns et al., 2004; Thakur et al., 2007). Our findings demonstrate an additional layer of apoptotic regulation provided by the Ras-MAPK-Rsk pathway. Under conditions with constitutively active Rsk, Apaf-1 is phosphorylated, and the cells are less responsive to cytochrome *c*-induced cell death (Figure 4.5A-C). Additionally, in cells stably expressing Ras12V, we observed enhanced Rsk-mediated Apaf-1 phosphorylation (Figure 4.6A,B). It would be of interest to more completely examine the phosphorylation status of Apaf-1 in tumors with activated Rsk, along with their responsiveness to cytochrome *c*. While Apaf-1 phosphorylation is certainly not the only mode of apoptotic suppression in these tumors with an active Ras-MAPK pathway, the post-translational modification of this crucial apoptosome component appears to represent another layer of apoptotic resistance, which could potentially be targeted to develop more successful cancer treatments.

5. Conclusions and Perspectives

With the discovery that the respiration chain component cytochrome *c* was necessary for mitochondrial-mediated apoptosis came an entirely new field of study surrounding apoptosome formation and caspase activation. Although initial analyses suggested that cytochrome *c*, Apaf-1, caspase-9, and dATP were necessary and sufficient for full apoptosome activity, more recent reports indicate that other proteins, including a nucleotide exchange complex for Apaf-1, are involved in facilitating proper apoptosome activation in cells (Kim et al., 2008). Furthermore, numerous apoptosomal-associated proteins and post-translational modifications have been shown to alter apoptosome assembly and/or activity, which can ultimately impact caspase activation and cellular demise. Work from this dissertation contributes to a better understanding of the early steps of apoptosome formation, specifically those related to Apaf-1, and it advances our comprehension of how this process is regulated under both normal and pathological conditions.

5.1 PHAPI-mediated Cytochrome *c* Sensitivity in Breast Cancer Cells

In Chapter 3 of this dissertation, we examined the cytochrome *c* responsiveness of normal and malignant mammary epithelial cells. Surprisingly, we discovered that breast cancer cells were hypersensitive to cytochrome *c*, activating caspases more robustly than their normal counterparts. This enhanced caspase activation is mediated by the protein PHAPI, which is expressed at higher levels in the breast cancer cells. Preliminary data suggest that levels of PHAPI mRNA are also elevated in breast cancer cells.

Additionally, there may be changes in PHAPI protein stability between the normal and malignant mammary epithelial cells. Interestingly, PHAPI has been characterized as a component of the nucleotide exchange complex for Apaf-1.

In analyzing the expression of PHAPI in other cancers, we noticed that both lung and prostate cancer cell lines contained levels of PHAPI similar to the breast cancer cells. However, their respective normal counterparts appeared to have comparable amounts of PHAPI. Therefore, at least in the subset of cell lines that we analyzed, it is not the breast cancer cells that appear to be the anomaly, but the normal mammary epithelial cells, which seem to have less PHAPI expression than the other cell lines tested. Nevertheless, the differential PHAPI expression between normal and malignant mammary epithelial cells facilitates the cytochrome *c* hypersensitivity observed in the breast cancer cells. However, it would be of interest to identify the mechanism(s) for differential PHAPI expression in the mammary epithelial cell model. There is already a precedent for PHAPI protein stability playing a role in the cellular response of NSCLC to apoptotic stimuli and to cytochrome *c* (Hoffarth et al., 2008).

The recent characterization of PHAPI as part of the Apaf-1-directed nucleotide exchange complex was an important step forward in understanding its role as an apoptosome regulator. It is now more clear why PHAPI enhances caspase-9 binding to Apaf-1 in our model system and in the initial studies characterizing PHAPI as an apoptosome regulator (Jiang et al., 2003; Schafer et al., 2006). Given the current model of apoptosome formation, Apaf-1 only oligomerizes into the proper conformation following nucleotide hydrolysis and subsequent exchange. With hsp70 and CAS, PHAPI

facilitates nucleotide exchange on Apaf-1, which allows it to appropriately self-associate, forming the proper heptameric backbone of the apoptosome. This conformational change and self-association positions Apaf-1 to readily accept caspase-9 on its CARD. In the absence of nucleotide exchange, Apaf-1 oligomerizes into inactive aggregates. Thus, one way that proper nucleotide exchange could be readout downstream would be by probing the interaction between caspase-9 and Apaf-1.

5.1.1 Breast Cancer-Targeted Therapeutic

In addition to demonstrating that lysates made from breast cancer cells were more sensitive to addition of cytochrome *c*, we were able to perform cytochrome *c* microinjection directly into the cytosol of these cells. This microinjection of cytochrome *c* kills the malignant mammary epithelial cells more quickly than the normal cells. Given the finding that PHAPI is overexpressed in all of the human breast tumors we examined, these microinjection results suggest that a novel breast cancer therapeutic could be developed to specifically mimic the role of cytochrome *c* in activating the apoptosome. One possibility would be a small molecule that could function like cytochrome *c* to cause a conformational change in Apaf-1 leading to apoptosome formation. Studies by another graduate student in the Kornbluth lab were initially unsuccessful in identifying such an Apaf-1-specific compound, but we are working to get access to a larger small molecule library for analysis. Another potential option tested in our lab was the use of cytochrome *c*-based peptide fragments, which might mimic holocytochrome *c* sufficiently to bind Apaf-1 and induce the appropriate conformational change. Unfortunately, these peptides were unable to interact with Apaf-1, which supports the important three-dimensional

structure of holocytochrome *c* for its interaction with Apaf-1. Finally, if more was known about the interacting residues between cytochrome *c* and Apaf-1, one might be able to use an intelligent design strategy to generate a molecule or compound that could mimic the role of cytochrome *c* in activating Apaf-1.

While it seems contradictory that breast cancer cells would actually overexpress a protein that could increase sensitivity to cytochrome *c*-induced apoptosis, we assert that they are not actually that vulnerable to apoptotic stimuli. The most likely explanation is that they are actually refractory to cytochrome *c* release through protection upstream of the mitochondria. Indeed, our data support this hypothesis. While it would have been ideal to directly examine this paradigm in human mammary tumors, we were unsuccessful with experiments to test their cytochrome *c* sensitivity. Attempts to make cytosolic lysates from human tissues resulted in red blood cell contamination and low concentrated lysates. More recent studies in our lab have been increasingly successful at making functional cytosolic lysates. These studies could be resumed if a possible therapeutic treatment was identified *in vitro*.

5.2 Suppression of Apoptosome Formation Through Rsk Phosphorylation of Apaf-1

The breast cancer studies described above focused indirectly on Apaf-1 through its regulator, PHAPI. Chapter 4 of this dissertation discusses another aspect of our research on the apoptosome, which investigated Apaf-1 directly through the identification of a novel post-translational modification affecting apoptosome formation. Although we have thus far been unable to mutate these sites in full length Apaf-1, these studies are

ongoing. Our current preliminary data indicate that Apaf-1 is indeed phosphorylated at serine 357 by Rsk (and perhaps not phosphorylated at 760 in cells). Given the conserved nature of the 357 site and the fact that it falls within a Rsk consensus motif, we focused on this one site (of the two) identified by mass spectrometry. Preliminary *in vitro* kinase assays using recombinant Rsk and truncated GST-tagged Apaf-1 1-543 mutated with an alanine for serine 357 show less Apaf-1 phosphorylation of the mutant protein. The more important functional studies are ongoing. Ideally, experiments using a full length Apaf-1 mutated at the serine 357 would provide the final evidence needed to confirm the mechanistic consequences of Rsk-mediated Apaf-1 phosphorylation. Unfortunately, obtaining plasmid with wildtype, full length Apaf-1 has been a challenge due to the recombinogenic nature of the 13 WD40 repeats.

Although initial studies using agarose-bound cytochrome *c* in *Xenopus* extracts and in mammalian lysates suggested that the binding between cytochrome *c* and Apaf-1 was defective in the presence of Rsk, subsequent studies in mammalian cells indicated that the oligomerization of Apaf-1 may be altered by Rsk phosphorylation. Interestingly, the mammalian cell models proved more useful for these oligomerization experiments, allowing us to easily express truncated Apaf-1 protein (1-559), which can self-associate in the absence of cytochrome *c*. Attempts at making recombinant truncated Apaf-1 1-543 for use in *Xenopus* extract experiments yielded Apaf-1 protein that was already oligomerized after elution (making it unsuitable for our studies where we wanted it to oligomerize in the extract). However, given our findings in both *Xenopus* egg extract and mammalian cells, the important question is whether these two mechanistic observations

are mutually exclusive. We believe no. One possibility is that all of our experimental evidence can actually be explained by the latter hypothesis, that Apaf-1 oligomerization is affected by Rsk phosphorylation. We did see altered Apaf-1 oligomerization in the mitotic *Xenopus* extract via gel filtration, although we initially attributed this to the altered binding between Apaf-1 and cytochrome *c*. Additionally, it is possible that the agarose-bound cytochrome *c* affinity precipitations are indirectly detecting Apaf-1 oligomerization (if some Apaf-1 binds to the cytochrome *c* transiently and is then released to associate with other Apaf-1 protein "activated" by the agarose-bound cytochrome *c*). Finally, given that the putative phospho-site (serine 357) is located in the region responsible for oligomerization, this mechanism seems plausible. Studies with Apaf-1 1-559 mutated at serine 357 are critical to validating this hypothesis, and the mutagenesis is more easily performed in the absence of the WD40 repeats. These experiments are currently underway, and preliminary data indeed suggest that Rsk phosphorylation at serine 357 may affect Apaf-1 self-association.

The other likely mechanistic explanation is that Rsk phosphorylation of Apaf-1 actually alters both cytochrome *c* binding to Apaf-1 and its self-association. Further studies on the specific structure of monomeric Apaf-1 and on the exact residues required for the cytochrome *c* and Apaf-1 interaction are necessary to determine if Rsk phosphorylation of Apaf-1 affects its binding to cytochrome *c* separately from its self-association. Additionally, full length Apaf-1 protein would be required for these experiments since loss of the COOH-terminal region of the protein makes cytochrome *c* unnecessary for the caspase activating function of Apaf-1. Regardless of the outcome of

these experiments, these findings are interesting and novel. No post-translational modifications for Apaf-1 have been reported, and regulation of these earlier steps in apoptosome formation has been less well-studied.

Our loss of function studies in the mammalian cell models were more unclear than in the *Xenopus* egg extract. Removing Rsk activity or expression (using pharmacological inhibitors or siRNA) did not always yield a completely "black and white" change in Apaf-1 phosphorylation and/or caspase activity. The Rsk consensus site (RXRXXS*/T*) is indeed shared by many other kinases in the AGC family, including PKA, Akt, PKC, and S6 kinase to name a few. It is important to continue analyzing the mammalian cell models to determine if one/some of these other kinases contribute to Apaf-1 phosphorylation when Rsk is inhibited (or, under different stimulus conditions). Given the range of kinases that share this consensus site, it might also be of interest to obtain some cancer cell lines where these kinases are hyperactive in order to assess the phosphorylation status of Apaf-1.

5.2.1 Dual Regulation of Apaf-1 Phosphorylation

A second important finding from this work was that the actions of Rsk and PP1 appear to balance each other, affecting the phosphorylation status of Apaf-1 and subsequent apoptosome formation. This type of paradigm has already been reported for caspase-9 where phosphorylation of threonine 125 (by a number of kinases) is counterbalanced by PP1α (Dessauge et al., 2006). While the exact regions of Apaf-1 responsible for its interaction with Rsk or PP1 are unknown, identifying these sites remains critical to fully elucidating the mechanisms with which these two proteins

regulate Apaf-1 and the apoptosome. Can both kinase and phosphatase be bound at the same time, actively antagonizing each other? Where are their binding sites on Apaf-1 located relative to the phosphorylation site? Are other proteins/adaptors required for the binding of Rsk and/or PP1? Answers to these questions should allow for the design of more careful studies examining how phosphorylation affects the conformation of Apaf-1 and its ability to oligomerize in response to cytochrome *c*. As phosphatase regulation of the apoptosome is also a relatively new area of study, these questions are critical for establishing how apoptosome formation and activity are modulated when a cell survival signal is terminated or when a certain kinase is turned off.

5.2.2 Apaf-1 Phosphorylation and Cancer

A normal, healthy cell retains the ability to undergo apoptosis in response to various cell stressors. In triggering cell death, many of these stimuli proceed through the mitochondrial-mediated pathway whereby the respiratory chain component, cytochrome *c*, translocates from the intermembrane space to the cytosol. This step is highly regulated, specifically by members of the bcl-2 family, which inhibit permeabilization of the outer mitochondrial membrane and subsequent cytochrome *c* release. While cytochrome *c* release is tightly regulated, these points of control can be altered in cancer; as discussed previously, the apoptosome also serves at a locus for altered apoptotic responsiveness (usually diminished) in cancer.

The characterization of Apaf-1 phosphorylation by Rsk demonstrated an additional layer of apoptotic regulation provided in certain types of cancer, including prostate cancer and those with a hyperactive active Ras-MAPK-Rsk pathway. Under

conditions with constitutively active Rsk, Apaf-1 is phosphorylated, and the cells are less responsive to cytochrome *c*-induced cell death. In cells expressing oncogenic Ras12V, we observed enhanced Rsk-mediated Apaf-1 phosphorylation. Given the frequency of Ras mutations in cancer, it would be of interest to better characterize the phosphorylation status of Apaf-1 in tumors with activated Ras and Rsk, along with their sensitivity to cytochrome *c*. While Apaf-1 phosphorylation is certainly not the only mode of apoptotic suppression in these tumors with an active Ras-MAPK pathway, phosphorylation of this crucial apoptosome component represents another layer of apoptotic resistance.

5.3 Importance of the Apoptosome and its Regulation

Following many types of apoptotic stimuli, the mitochondrial arm of the pathway is necessary for a complete cellular response. Despite the wide body of literature examining regulation of apoptosis downstream of mitochondrial cytochrome *c* release, some groups still believe that this work is for naught due to compromised mitochondria following cytochrome *c* release. While there is likely to be some significant cell type- and stimulus-specificity to the importance of apoptosome regulation, it seems unlikely that various cancer cells and certain signaling pathways would have evolved mechanisms for inhibiting the apoptosome if they conferred no significant survival advantage. While a thorough examination of this related literature is out of the scope of this dissertation, apoptosome-related knockout mouse models and current data on mitochondrial cytochrome *c* release provide some insights into mitochondrial physiology following cytochrome *c* translocation to the cytosol.

Knockout mice have already been made for the major apoptosome components, and their phenotypes have helped forward our understanding of the mitochondrial-mediated pathway in cell death. Apaf-1 and caspase-9 knockout mice are embryonic lethal and similar in phenotype; the mice displayed brain hyperplasia and craniofacial malformations suggesting that appropriate cell death in neurons and/or neuronal precursors failed to occur (Cecconi et al., 1998; Hakem et al., 1998; Kuida et al., 1998). Interestingly, a variety of cell types (embryonic stem cells (ES), embryonic fibroblasts (MEF), and thymocytes) derived from these mice displayed unusual resistance to apoptotic stimuli. Although each cell type had a somewhat unique response to an individual stressor, cytosolic cytochrome *c* was still detected in caspase-$9^{-/-}$ ES cells and MEFs following UV radiation, even though the cells did not undergo death or caspase activation (Hakem et al., 1998). While the cytochrome *c* knockout mice were also embryonic lethal (most likely due to defects in respiration), characterization of the MEFs demonstrated continued survival in the presence of staurosporine, UV radiation, and serum withdrawal (Li et al., 2000). Using a knock-in technique, one group created a cytochrome *c* mutant mouse defective only for the apoptotic functions of cytochrome *c* (due to a lysine to alanine mutation at amino acid 72) (Hao et al., 2005). Displaying similar brain defects to the Apaf-$1^{-/-}$, caspase-$9^{-/-}$, and caspase-$3^{-/-}$ mice, these knock-in mice also have certain cell types that survive in the face of apoptotic stimuli, again suggesting that even in the presence of cytochrome *c* release, cell survival can occur (Hao et al., 2005).

In order to understand how apoptosome regulation might promote cell survival, one must also consider the mechanism for cytochrome *c* release and subsequent effects on mitochondrial physiology. Although some reports suggest that mitochondrial cytochrome *c* release is an "all or nothing" phenomenon, more recent data indicate that (at least in some cell types) feedback on the mitochondria plays an important role in "complete" cytochrome *c* release and changes in mitochondrial outer membrane potential (MOMP) (Goldstein et al., 2005; Goldstein et al., 2000; Ow et al., 2008). Interestingly, release of Ca^{++} from the endoplasmic reticulum has shown to function in a positive feedback loop with mitochondrial cytochrome *c* release due to binding of cytochrome *c* to the IP_3R (Boehning et al., 2003; Kroemer et al., 2007). If mitochondrial cytochrome *c* release does indeed occur in "waves" or steps (especially in response to caspase activation), it appears that blocking apoptosome activation could affect this later wave of cytochrome *c* release (and thus cell death) prior to amplification of the apoptotic signal. MEFs from the capsase-3 and caspase-7 double knockout mice ($C3/C7^{-/-}$) provide evidence that perhaps active effector caspases are critical for a full mitochondrial response to some apoptotic stimuli (including complete loss of mitochondrial membrane potential and cytochrome *c* release). Following treatment with UV radiation, the $C3/C7^{-/-}$ cells exhibited delayed release of cytochrome *c* and Bax translocation, suggesting that caspase activation may help to amplify an initial death signal by stimulating further cytochrome *c* release (Lakhani et al., 2006).

Some studies on mitochondrial morphology during apoptosis also suggest that there might be two pools of cytochrome *c*, which correlates with the idea that feedback

loops facilitate complete release of cytochrome *c*. One of these models suggests that one pool of cytochrome *c* is easily released following an initial apoptotic stimulus, while the majority of the cytochrome *c* is actually buried in the cristae, to be released following changes in mitochondrial morphology (Scorrano et al., 2002; Suen et al., 2008). In this model, the fission and fusion machinery play a role in apoptotic progression by facilitating mitochondrial fragmentation and cristae remodeling, which helps "free" cytochrome *c* for translocation into the cytosol (Parone et al., 2006; Pellegrini and Scorrano, 2007).

While some apoptotic researchers consider MOMP and cytochrome *c* release to be the "point of no return" for the cell, some models have demonstrated long-term survival if caspase activation is inhibited following an apoptotic stimulus. Work from Doug Green and colleagues demonstrated that active caspase-3 plays a role in affecting mitochondrial membrane potential (and, thus potentially the cell's ultimate fate) through cleavage of complex I (Ricci et al., 2004). More recent work this group has demonstrated that glyeraldehyde-3-phosphate dehydrogenase (GAPDH) and autophagy help protect cells from the non-apoptotic cell death that sometimes occurs following MOMP and caspase inhibition, again indicating that under certain circumstances, cells can survive cytochrome *c* release in the absence of caspase activation (Colell et al., 2009).

Post-mitotic, sympathetic neurons that are deprived of neurotrophic growth factors also fail to activate caspases due to low levels of Apaf-1 and high levels of XIAP (Wright et al., 2004). Most interestingly though, these cells can recover if mitochondrial membrane potential persists, in part due to fresh protein synthesis, including cytochrome

c (Deshmukh and Johnson, 1998; Martinou et al., 1999). A similar paradigm was observed in cadiomyocytes (Potts et al., 2005). Additional work from Doug Green showed that mitochondrial function, including maintenance of the transmembrane potential and generation of ATP, can actually be preserved in cells following cytochrome *c* release (through use of cytosolic cytochrome *c*) (Waterhouse et al., 2001). Perhaps overall mitochondrial physiology (and maintenance of the membrane potential) after an apoptotic stimulus is more predictive of cell survival than cytochrome *c* release itself. Although there is clearly some important cell type- and stimulus-specific variability with regard to long-term survival, regulation of the apoptosome downstream of mitochondrial cytochrome *c* release has been shown important in a variety of circumstances. Ultimately, the paramount issue regarding apoptosome regulation is not the degree to which apoptosome formation/caspase activation is altered but is instead the influence any mechanistic regulation would have on apoptotic cell death.

5.4 Concluding Remarks

The data presented in this dissertation have furthered our understanding of the apoptosome and its regulation. Through studies in mammary epithelial cells, we determined that breast cancer cells are remarkably hypersensitive to cytochrome *c*, compared to normal mammary epithelial cells. While unexpected, this result opens new possibilities for a specific, targeted therapeutic that could robustly activate caspases in the cancer cells, while sparing localized normal tissue. Mechanistically, the breast cancer cells are hypersensitive to cytochrome *c* due to overexpression of the protein PHAPI, which serves as part of the nucleotide exchange complex for Apaf-1. Further studies on

Apaf-1 from this dissertation also characterize its first post-translational modification, mediated by Rsk. Examination of apoptosome formation in conditions of high MAPK activity demonstrate that Rsk phosphorylation of Apaf-1 reduces the ability of cytochrome *c* to nucleate apoptosome formation. Phosphorylation of Apaf-1 thus inhibits Apaf-1 oligomerization and subsequent caspase activation. Antagonizing Rsk-mediated phosphorylation of Apaf-1, PP1 dephosphorylates Apaf-1. Identifying and characterizing the mechanisms of apoptosome regulation not only contribute to a better understanding of apoptotic cell death as a whole but also advance our knowledge regarding mechanisms of apoptotic evasion in diseases such as cancer.

References

Acehan, D., Jiang, X., Morgan, D.G., Heuser, J.E., Wang, X., and Akey, C.W. (2002). Three-dimensional structure of the apoptosome: implications for assembly, procaspase-9 binding, and activation. Mol Cell *9*, 423-432.

Alessi, D.R. (1997). The protein kinase C inhibitors Ro 318220 and GF 109203X are equally potent inhibitors of MAPKAP kinase-1beta (Rsk-2) and p70 S6 kinase. FEBS Lett *402*, 121-123.

Allan, L.A., and Clarke, P.R. (2007). Phosphorylation of caspase-9 by CDK1/cyclin B1 protects mitotic cells against apoptosis. Mol Cell *26*, 301-310.

Allan, L.A., and Clarke, P.R. (2009). Apoptosis and autophagy: Regulation of caspase-9 by phosphorylation. FEBS J *276*, 6063-6073.

Allan, L.A., Morrice, N., Brady, S., Magee, G., Pathak, S., and Clarke, P.R. (2003). Inhibition of caspase-9 through phosphorylation at Thr 125 by ERK MAPK. Nat Cell Biol *5*, 647-654.

Allen, J.D., Zhang, X.D., Scott, C.L., Boyle, G.M., Hersey, P., and Strasser, A. (2005). Is Apaf-1 expression frequently abrogated in melanoma? Cell Death Differ *12*, 680-681.

Alnemri, E.S., Livingston, D.J., Nicholson, D.W., Salvesen, G., Thornberry, N.A., Wong, W.W., and Yuan, J. (1996). Human ICE/CED-3 protease nomenclature. Cell *87*, 171.

Alvarado-Kristensson, M., and Andersson, T. (2005). Protein phosphatase 2A regulates apoptosis in neutrophils by dephosphorylating both p38 MAPK and its substrate caspase 3. J Biol Chem *280*, 6238-6244.

Alvarado-Kristensson, M., Melander, F., Leandersson, K., Ronnstrand, L., Wernstedt, C., and Andersson, T. (2004). p38-MAPK signals survival by phosphorylation of caspase-8 and caspase-3 in human neutrophils. J Exp Med *199*, 449-458.

Andersen, M.H., Svane, I.M., Becker, J.C., and Straten, P.T. (2007). The universal character of the tumor-associated antigen survivin. Clin Cancer Res *13*, 5991-5994.

Anjum, R., and Blenis, J. (2008). The RSK family of kinases: emerging roles in cellular signalling. Nat Rev Mol Cell Biol *9*, 747-758.

Anjum, R., Roux, P.P., Ballif, B.A., Gygi, S.P., and Blenis, J. (2005). The tumor suppressor DAP kinase is a target of RSK-mediated survival signaling. Curr Biol *15*, 1762-1767.

Arnt, C.R., Chiorean, M.V., Heldebrant, M.P., Gores, G.J., and Kaufmann, S.H. (2002). Synthetic Smac/DIABLO peptides enhance the effects of chemotherapeutic agents by binding XIAP and cIAP1 in situ. J Biol Chem *277*, 44236-44243.

Bai, J., Brody, J.R., Kadkol, S.S., and Pasternack, G.R. (2001). Tumor suppression and potentiation by manipulation of pp32 expression. Oncogene *20*, 2153-2160.

Baldi, A., Santini, D., Russo, P., Catricala, C., Amantea, A., Picardo, M., Tatangelo, F., Botti, G., Dragonetti, E., Murace, R., *et al.* (2004). Analysis of APAF-1 expression in human cutaneous melanoma progression. Exp Dermatol *13*, 93-97.

Bandyopadhyay, A., Tsuji, K., Cox, K., Harfe, B.D., Rosen, V., and Tabin, C.J. (2006). Genetic analysis of the roles of BMP2, BMP4, and BMP7 in limb patterning and skeletogenesis. PLoS Genet *2*, e216.

Bao, Q., Lu, W., Rabinowitz, J.D., and Shi, Y. (2007). Calcium blocks formation of apoptosome by preventing nucleotide exchange in Apaf-1. Mol Cell *25*, 181-192.

Barila, D., Rufini, A., Condo, I., Ventura, N., Dorey, K., Superti-Furga, G., and Testi, R. (2003). Caspase-dependent cleavage of c-Abl contributes to apoptosis. Mol Cell Biol *23*, 2790-2799.

Beere, H.M., Wolf, B.B., Cain, K., Mosser, D.D., Mahboubi, A., Kuwana, T., Tailor, P., Morimoto, R.I., Cohen, G.M., and Green, D.R. (2000). Heat-shock protein 70 inhibits apoptosis by preventing recruitment of procaspase-9 to the Apaf-1 apoptosome. Nat Cell Biol *2*, 469-475.

Berns, K., Hijmans, E.M., Mullenders, J., Brummelkamp, T.R., Velds, A., Heimerikx, M., Kerkhoven, R.M., Madiredjo, M., Nijkamp, W., Weigelt, B., *et al.* (2004). A large-scale RNAi screen in human cells identifies new components of the p53 pathway. Nature *428*, 431-437.

Bhatt, R.R., and Ferrell, J.E., Jr. (1999). The protein kinase p90 rsk as an essential mediator of cytostatic factor activity. Science *286*, 1362-1365.

Bignone, P.A., Lee, K.Y., Liu, Y., Emilion, G., Finch, J., Soosay, A.E., Charnock, F.M., Beck, S., Dunham, I., Mungall, A.J., *et al.* (2007). RPS6KA2, a putative tumour suppressor gene at 6q27 in sporadic epithelial ovarian cancer. Oncogene *26*, 683-700.

Blow, J.J., and Laskey, R.A. (1986). Initiation of DNA replication in nuclei and purified DNA by a cell-free extract of Xenopus eggs. Cell *47*, 577-587.

Boatright, K.M., Renatus, M., Scott, F.L., Sperandio, S., Shin, H., Pedersen, I.M., Ricci, J.E., Edris, W.A., Sutherlin, D.P., Green, D.R., *et al.* (2003). A unified model for apical caspase activation. Mol Cell *11*, 529-541.

Boehning, D., Patterson, R.L., Sedaghat, L., Glebova, N.O., Kurosaki, T., and Snyder, S.H. (2003). Cytochrome c binds to inositol (1,4,5) trisphosphate receptors, amplifying calcium-dependent apoptosis. Nat Cell Biol *5*, 1051-1061.

Bos, J.L. (1989). ras oncogenes in human cancer: a review. Cancer Res *49*, 4682-4689.

Brady, S.C., Allan, L.A., and Clarke, P.R. (2005). Regulation of caspase 9 through phosphorylation by protein kinase C zeta in response to hyperosmotic stress. Mol Cell Biol *25*, 10543-10555.

Brody, J.R., Kadkol, S.S., Mahmoud, M.A., Rebel, J.M., and Pasternack, G.R. (1999). Identification of sequences required for inhibition of oncogene-mediated transformation by pp32. J Biol Chem *274*, 20053-20055.

Brown, G.C., and Borutaite, V. (2008). Regulation of apoptosis by the redox state of cytochrome c. Biochim Biophys Acta *1777*, 877-881.

Bruey, J.M., Ducasse, C., Bonniaud, P., Ravagnan, L., Susin, S.A., Diaz-Latoud, C., Gurbuxani, S., Arrigo, A.P., Kroemer, G., Solary, E., *et al.* (2000). Hsp27 negatively regulates cell death by interacting with cytochrome c. Nat Cell Biol *2*, 645-652.

Bubici, C., Papa, S., Pham, C.G., Zazzeroni, F., and Franzoso, G. (2004). NF-kappaB and JNK: an intricate affair. Cell Cycle *3*, 1524-1529.

Cain, K., Brown, D.G., Langlais, C., and Cohen, G.M. (1999). Caspase activation involves the formation of the aposome, a large (approximately 700 kDa) caspase-activating complex. J Biol Chem *274*, 22686-22692.

Cain, K., Langlais, C., Sun, X.M., Brown, D.G., and Cohen, G.M. (2001). Physiological concentrations of K+ inhibit cytochrome c-dependent formation of the apoptosome. J Biol Chem *276*, 41985-41990.

Campbell, R.A., Bhat-Nakshatri, P., Patel, N.M., Constantinidou, D., Ali, S., and Nakshatri, H. (2001). Phosphatidylinositol 3-kinase/AKT-mediated activation of estrogen receptor alpha: a new model for anti-estrogen resistance. J Biol Chem *276*, 9817-9824.

Cardone, M.H., Roy, N., Stennicke, H.R., Salvesen, G.S., Franke, T.F., Stanbridge, E., Frisch, S., and Reed, J.C. (1998). Regulation of cell death protease caspase-9 by phosphorylation. Science *282*, 1318-1321.

Carriere, A., Cargnello, M., Julien, L.A., Gao, H., Bonneil, E., Thibault, P., and Roux, P.P. (2008). Oncogenic MAPK signaling stimulates mTORC1 activity by promoting RSK-mediated raptor phosphorylation. Curr Biol *18*, 1269-1277.

Cecconi, F., Alvarez-Bolado, G., Meyer, B.I., Roth, K.A., and Gruss, P. (1998). Apaf1 (CED-4 homolog) regulates programmed cell death in mammalian development. Cell *94*, 727-737.

Cerretti, D.P., Kozlosky, C.J., Mosley, B., Nelson, N., Van Ness, K., Greenstreet, T.A., March, C.J., Kronheim, S.R., Druck, T., Cannizzaro, L.A., *et al.* (1992). Molecular cloning of the interleukin-1 beta converting enzyme. Science *256*, 97-100.

Chandra, D., Bratton, S.B., Person, M.D., Tian, Y., Martin, A.G., Ayres, M., Fearnhead, H.O., Gandhi, V., and Tang, D.G. (2006). Intracellular nucleotides act as critical prosurvival factors by binding to cytochrome C and inhibiting apoptosome. Cell *125*, 1333-1346.

Chang, G.C., Hsu, S.L., Tsai, J.R., Liang, F.P., Lin, S.Y., Sheu, G.T., and Chen, C.Y. (2004). Molecular mechanisms of ZD1839-induced G1-cell cycle arrest and apoptosis in human lung adenocarcinoma A549 cells. Biochem Pharmacol *68*, 1453-1464.

Chao, Y., Shiozaki, E.N., Srinivasula, S.M., Rigotti, D.J., Fairman, R., and Shi, Y. (2005). Engineering a dimeric caspase-9: a re-evaluation of the induced proximity model for caspase activation. PLoS Biol *3*, e183.

Chau, B.N., Cheng, E.H., Kerr, D.A., and Hardwick, J.M. (2000). Aven, a novel inhibitor of caspase activation, binds Bcl-xL and Apaf-1. Mol Cell *6*, 31-40.

Chen, F.L., Xia, W., and Spector, N.L. (2008). Acquired resistance to small molecule ErbB2 tyrosine kinase inhibitors. Clin Cancer Res *14*, 6730-6734.

Cho, D.H., Hong, Y.M., Lee, H.J., Woo, H.N., Pyo, J.O., Mak, T.W., and Jung, Y.K. (2004). Induced inhibition of ischemic/hypoxic injury by APIP, a novel Apaf-1-interacting protein. J Biol Chem *279*, 39942-39950.

Chu, Z.L., Pio, F., Xie, Z., Welsh, K., Krajewska, M., Krajewski, S., Godzik, A., and Reed, J.C. (2001). A novel enhancer of the Apaf1 apoptosome involved in cytochrome c-dependent caspase activation and apoptosis. J Biol Chem *276*, 9239-9245.

Clark, D.E., Errington, T.M., Smith, J.A., Frierson, H.F., Jr., Weber, M.J., and Lannigan, D.A. (2005). The serine/threonine protein kinase, p90 ribosomal S6 kinase, is an important regulator of prostate cancer cell proliferation. Cancer Res *65*, 3108-3116.

Cohen, P.T. (2002). Protein phosphatase 1--targeted in many directions. J Cell Sci *115*, 241-256.

Colell, A., Green, D.R., and Ricci, J.E. (2009). Novel roles for GAPDH in cell death and carcinogenesis. Cell Death Differ *16*, 1573-1581.

Coleman, M.L., Sahai, E.A., Yeo, M., Bosch, M., Dewar, A., and Olson, M.F. (2001). Membrane blebbing during apoptosis results from caspase-mediated activation of ROCK I. Nat Cell Biol *3*, 339-345.

Corvaro, M., Fuoco, C., Wagner, M., and Cecconi, F. (2007). Analysis of apoptosome dysregulation in pancreatic cancer and of its role in chemoresistance. Cancer Biol Ther *6*, 209-217.

Dai, D.L., Martinka, M., Bush, J.A., and Li, G. (2004). Reduced Apaf-1 expression in human cutaneous melanomas. Br J Cancer *91*, 1089-1095.

Dan, S., Naito, M., and Tsuruo, T. (1998). Selective induction of apoptosis in Philadelphia chromosome-positive chronic myelogenous leukemia cells by an inhibitor of BCR - ABL tyrosine kinase, CGP 57148. Cell Death Differ *5*, 710-715.

Danial, N.N., and Korsmeyer, S.J. (2004). Cell death: critical control points. Cell *116*, 205-219.

Das, M., Jiang, F., Sluss, H.K., Zhang, C., Shokat, K.M., Flavell, R.A., and Davis, R.J. (2007). Suppression of p53-dependent senescence by the JNK signal transduction pathway. Proc Natl Acad Sci U S A *104*, 15759-15764.

Davies, H., Bignell, G.R., Cox, C., Stephens, P., Edkins, S., Clegg, S., Teague, J., Woffendin, H., Garnett, M.J., Bottomley, W., *et al.* (2002). Mutations of the BRAF gene in human cancer. Nature *417*, 949-954.

Davis, R.J. (2000). Signal transduction by the JNK group of MAP kinases. Cell *103*, 239-252.

Deming, P.B., Schafer, Z.T., Tashker, J.S., Potts, M.B., Deshmukh, M., and Kornbluth, S. (2004). Bcr-Abl-mediated protection from apoptosis downstream of mitochondrial cytochrome c release. Mol Cell Biol *24*, 10289-10299.

Deshmukh, M., and Johnson, E.M., Jr. (1998). Evidence of a novel event during neuronal death: development of competence-to-die in response to cytoplasmic cytochrome c. Neuron *21*, 695-705.

Dessauge, F., Cayla, X., Albar, J.P., Fleischer, A., Ghadiri, A., Duhamel, M., and Rebollo, A. (2006). Identification of PP1alpha as a caspase-9 regulator in IL-2 deprivation-induced apoptosis. J Immunol *177*, 2441-2451.

Devarajan, E., Sahin, A.A., Chen, J.S., Krishnamurthy, R.R., Aggarwal, N., Brun, A.M., Sapino, A., Zhang, F., Sharma, D., Yang, X.H., *et al.* (2002). Down-regulation of caspase 3 in breast cancer: a possible mechanism for chemoresistance. Oncogene *21*, 8843-8851.

Deveraux, Q.L., Takahashi, R., Salvesen, G.S., and Reed, J.C. (1997). X-linked IAP is a direct inhibitor of cell-death proteases. Nature *388*, 300-304.

DeVries, T.A., Neville, M.C., and Reyland, M.E. (2002). Nuclear import of PKCdelta is required for apoptosis: identification of a novel nuclear import sequence. EMBO J *21*, 6050-6060.

Dhillon, A.S., Hagan, S., Rath, O., and Kolch, W. (2007). MAP kinase signalling pathways in cancer. Oncogene *26*, 3279-3290.

Diekert, K., de Kroon, A.I., Ahting, U., Niggemeyer, B., Neupert, W., de Kruijff, B., and Lill, R. (2001). Apocytochrome c requires the TOM complex for translocation across the mitochondrial outer membrane. EMBO J *20*, 5626-5635.

Dix, M.M., Simon, G.M., and Cravatt, B.F. (2008). Global mapping of the topography and magnitude of proteolytic events in apoptosis. Cell *134*, 679-691.

Dohadwala, M., da Cruz e Silva, E.F., Hall, F.L., Williams, R.T., Carbonaro-Hall, D.A., Nairn, A.C., Greengard, P., and Berndt, N. (1994). Phosphorylation and inactivation of protein phosphatase 1 by cyclin-dependent kinases. Proc Natl Acad Sci U S A *91*, 6408-6412.

Downward, J. (2003). Targeting RAS signalling pathways in cancer therapy. Nat Rev Cancer *3*, 11-22.

Edinger, A.L., and Thompson, C.B. (2004). Death by design: apoptosis, necrosis and autophagy. Curr Opin Cell Biol *16*, 663-669.

Egloff, M.P., Johnson, D.F., Moorhead, G., Cohen, P.T., Cohen, P., and Barford, D. (1997). Structural basis for the recognition of regulatory subunits by the catalytic subunit of protein phosphatase 1. EMBO J *16*, 1876-1887.

Elenitoba-Johnson, K.S., Jenson, S.D., Abbott, R.T., Palais, R.A., Bohling, S.D., Lin, Z., Tripp, S., Shami, P.J., Wang, L.Y., Coupland, R.W., *et al.* (2003). Involvement of multiple signaling pathways in follicular lymphoma transformation: p38-mitogen-activated protein kinase as a target for therapy. Proc Natl Acad Sci U S A *100*, 7259-7264.

Erikson, E., and Maller, J.L. (1985). A protein kinase from Xenopus eggs specific for ribosomal protein S6. Proc Natl Acad Sci U S A *82*, 742-746.

Erikson, E., and Maller, J.L. (1989). In vivo phosphorylation and activation of ribosomal protein S6 kinases during Xenopus oocyte maturation. J Biol Chem *264*, 13711-13717.

Esteva, F.J., Sahin, A.A., Smith, T.L., Yang, Y., Pusztai, L., Nahta, R., Buchholz, T.A., Buzdar, A.U., Hortobagyi, G.N., and Bacus, S.S. (2004). Prognostic significance of phosphorylated P38 mitogen-activated protein kinase and HER-2 expression in lymph node-positive breast carcinoma. Cancer *100*, 499-506.

Evan, G., and Littlewood, T. (1998). A matter of life and cell death. Science *281*, 1317-1322.

Evans, E.K., Lu, W., Strum, S.L., Mayer, B.J., and Kornbluth, S. (1997). Crk is required for apoptosis in Xenopus egg extracts. Embo J *16*, 230-241.

Fadok, V.A., Bratton, D.L., Rose, D.M., Pearson, A., Ezekewitz, R.A., and Henson, P.M. (2000). A receptor for phosphatidylserine-specific clearance of apoptotic cells. Nature *405*, 85-90.

Flores-Delgado, G., Liu, C.W., Sposto, R., and Berndt, N. (2007). A limited screen for protein interactions reveals new roles for protein phosphatase 1 in cell cycle control and apoptosis. J Proteome Res *6*, 1165-1175.

Fuentes-Prior, P., and Salvesen, G.S. (2004). The protein structures that shape caspase activity, specificity, activation and inhibition. Biochem J *384*, 201-232.

Fujimoto, A., Takeuchi, H., Taback, B., Hsueh, E.C., Elashoff, D., Morton, D.L., and Hoon, D.S. (2004). Allelic imbalance of 12q22-23 associated with APAF-1 locus correlates with poor disease outcome in cutaneous melanoma. Cancer Res *64*, 2245-2250.

Fulda, S., Wick, W., Weller, M., and Debatin, K.M. (2002). Smac agonists sensitize for Apo2L/TRAIL- or anticancer drug-induced apoptosis and induce regression of malignant glioma in vivo. Nat Med *8*, 808-815.

Gerhard, M.C., Zantl, N., Weirich, G., Schliep, S., Seiffert, B., and Hacker, G. (2003). Functional evaluation of the apoptosome in renal cell carcinoma. Br J Cancer *89*, 2147-2154.

Gioeli, D., Mandell, J.W., Petroni, G.R., Frierson, H.F., Jr., and Weber, M.J. (1999). Activation of mitogen-activated protein kinase associated with prostate cancer progression. Cancer Res *59*, 279-284.

Goldstein, J.C., Munoz-Pinedo, C., Ricci, J.E., Adams, S.R., Kelekar, A., Schuler, M., Tsien, R.Y., and Green, D.R. (2005). Cytochrome c is released in a single step during apoptosis. Cell Death Differ *12*, 453-462.

Goldstein, J.C., Waterhouse, N.J., Juin, P., Evan, G.I., and Green, D.R. (2000). The coordinate release of cytochrome c during apoptosis is rapid, complete and kinetically invariant. Nat Cell Biol *2*, 156-162.

Greenberg, A.K., Basu, S., Hu, J., Yie, T.A., Tchou-Wong, K.M., Rom, W.N., and Lee, T.C. (2002). Selective p38 activation in human non-small cell lung cancer. Am J Respir Cell Mol Biol *26*, 558-564.

Guo, F., Nimmanapalli, R., Paranawithana, S., Wittman, S., Griffin, D., Bali, P., O'Bryan, E., Fumero, C., Wang, H.G., and Bhalla, K. (2002). Ectopic overexpression of second mitochondria-derived activator of caspases (Smac/DIABLO) or cotreatment with N-terminus of Smac/DIABLO peptide potentiates epothilone B derivative-(BMS 247550) and Apo-2L/TRAIL-induced apoptosis. Blood *99*, 3419-3426.

Haga, A., Funasaka, T., Niinaka, Y., Raz, A., and Nagase, H. (2003). Autocrine motility factor signaling induces tumor apoptotic resistance by regulations Apaf-1 and Caspase-9 apoptosome expression. Int J Cancer *107*, 707-714.

Hakem, R., Hakem, A., Duncan, G.S., Henderson, J.T., Woo, M., Soengas, M.S., Elia, A., de la Pompa, J.L., Kagi, D., Khoo, W., *et al.* (1998). Differential requirement for caspase 9 in apoptotic pathways in vivo. Cell *94*, 339-352.

Hanahan, D., and Weinberg, R.A. (2000). The hallmarks of cancer. Cell *100*, 57-70.

Hao, Z., Duncan, G.S., Chang, C.C., Elia, A., Fang, M., Wakeham, A., Okada, H., Calzascia, T., Jang, Y., You-Ten, A., *et al.* (2005). Specific ablation of the apoptotic functions of cytochrome C reveals a differential requirement for cytochrome C and Apaf-1 in apoptosis. Cell *121*, 579-591.

Harada, H., Quearry, B., Ruiz-Vela, A., and Korsmeyer, S.J. (2004). Survival factor-induced extracellular signal-regulated kinase phosphorylates BIM, inhibiting its association with BAX and proapoptotic activity. Proc Natl Acad Sci U S A *101*, 15313-15317.

Harris, C.C. (1996). p53 tumor suppressor gene: at the crossroads of molecular carcinogenesis, molecular epidemiology, and cancer risk assessment. Environ Health Perspect *104 Suppl 3*, 435-439.

Hill, M.M., Adrain, C., Duriez, P.J., Creagh, E.M., and Martin, S.J. (2004). Analysis of the composition, assembly kinetics and activity of native Apaf-1 apoptosomes. Embo J *23*, 2134-2145.

Hoffarth, S., Zitzer, A., Wiewrodt, R., Hahnel, P.S., Beyer, V., Kreft, A., Biesterfeld, S., and Schuler, M. (2008). pp32/PHAPI determines the apoptosis response of non-small-cell lung cancer. Cell Death Differ *15*, 161-170.

Hu, Y., Ding, L., Spencer, D.M., and Nunez, G. (1998). WD-40 repeat region regulates Apaf-1 self-association and procaspase-9 activation. J Biol Chem *273*, 33489-33494.

Inoue, S., Browne, G., Melino, G., and Cohen, G.M. (2009). Ordering of caspases in cells undergoing apoptosis by the intrinsic pathway. Cell Death Differ *16*, 1053-1061.

Itoh, N., and Nagata, S. (1993). A novel protein domain required for apoptosis. Mutational analysis of human Fas antigen. J Biol Chem *268*, 10932-10937.

Janicke, R.U., Sprengart, M.L., Wati, M.R., and Porter, A.G. (1998). Caspase-3 is required for DNA fragmentation and morphological changes associated with apoptosis. J Biol Chem *273*, 9357-9360.

Jia, L., Patwari, Y., Kelsey, S.M., Srinivasula, S.M., Agrawal, S.G., Alnemri, E.S., and Newland, A.C. (2003). Role of Smac in human leukaemic cell apoptosis and proliferation. Oncogene *22*, 1589-1599.

Jia, L., Srinivasula, S.M., Liu, F.T., Newland, A.C., Fernandes-Alnemri, T., Alnemri, E.S., and Kelsey, S.M. (2001). Apaf-1 protein deficiency confers resistance to cytochrome c-dependent apoptosis in human leukemic cells. Blood *98*, 414-421.

Jiang, X., Kim, H.E., Shu, H., Zhao, Y., Zhang, H., Kofron, J., Donnelly, J., Burns, D., Ng, S.C., Rosenberg, S.*, et al.* (2003). Distinctive roles of PHAP proteins and prothymosin-alpha in a death regulatory pathway. Science *299*, 223-226.

Johnson, C.E., Huang, Y.Y., Parrish, A.B., Smith, M.I., Vaughn, A.E., Zhang, Q., Wright, K.M., Van Dyke, T., Wechsler-Reya, R.J., Kornbluth, S.*, et al.* (2007). Differential Apaf-1 levels allow cytochrome c to induce apoptosis in brain tumors but not in normal neural tissues. Proc Natl Acad Sci U S A *104*, 20820-20825.

Johnstone, R.W., Ruefli, A.A., and Lowe, S.W. (2002). Apoptosis: a link between cancer genetics and chemotherapy. Cell *108*, 153-164.

Kang, S., Elf, S., Lythgoe, K., Hitosugi, T., Taunton, J., Zhou, W., Xiong, L., Wang, D., Muller, S., Fan, S.*, et al.* (2010). p90 ribosomal S6 kinase 2 promotes invasion and metastasis of human head and neck squamous cell carcinoma cells. J Clin Invest *120*, 1165-1177.

Karki, P., Seong, C., Kim, J.E., Hur, K., Shin, S.Y., Lee, J.S., Cho, B., and Park, I.S. (2007). Intracellular K(+) inhibits apoptosis by suppressing the Apaf-1 apoptosome formation and subsequent downstream pathways but not cytochrome c release. Cell Death Differ *14*, 2068-2075.

Katoch, B., Sebastian, S., Sahdev, S., Padh, H., Hasnain, S.E., and Begum, R. (2002). Programmed cell death and its clinical implications. Indian J Exp Biol *40*, 513-524.

Kennedy, N.J., Sluss, H.K., Jones, S.N., Bar-Sagi, D., Flavell, R.A., and Davis, R.J. (2003a). Suppression of Ras-stimulated transformation by the JNK signal transduction pathway. Genes Dev *17*, 629-637.

Kennedy, S.M., O'Driscoll, L., Purcell, R., Fitz-Simons, N., McDermott, E.W., Hill, A.D., O'Higgins, N.J., Parkinson, M., Linehan, R., and Clynes, M. (2003b). Prognostic importance of survivin in breast cancer. Br J Cancer *88*, 1077-1083.

Kerr, J.F., Wyllie, A.H., and Currie, A.R. (1972). Apoptosis: a basic biological phenomenon with wide-ranging implications in tissue kinetics. Br J Cancer *26*, 239-257.

Kim, B.J., Ryu, S.W., and Song, B.J. (2006). JNK- and p38 kinase-mediated phosphorylation of Bax leads to its activation and mitochondrial translocation and to apoptosis of human hepatoma HepG2 cells. J Biol Chem *281*, 21256-21265.

Kim, H.E., Du, F., Fang, M., and Wang, X. (2005). Formation of apoptosome is initiated by cytochrome c-induced dATP hydrolysis and subsequent nucleotide exchange on Apaf-1. Proc Natl Acad Sci U S A *102*, 17545-17550.

Kim, H.E., Jiang, X., Du, F., and Wang, X. (2008). PHAPI, CAS, and Hsp70 promote apoptosome formation by preventing Apaf-1 aggregation and enhancing nucleotide exchange on Apaf-1. Mol Cell *30*, 239-247.

Kischkel, F.C., Hellbardt, S., Behrmann, I., Germer, M., Pawlita, M., Krammer, P.H., and Peter, M.E. (1995). Cytotoxicity-dependent APO-1 (Fas/CD95)-associated proteins form a death-inducing signaling complex (DISC) with the receptor. EMBO J *14*, 5579-5588.

Kluck, R.M., Ellerby, L.M., Ellerby, H.M., Naiem, S., Yaffe, M.P., Margoliash, E., Bredesen, D., Mauk, A.G., Sherman, F., and Newmeyer, D.D. (2000). Determinants of cytochrome c pro-apoptotic activity. The role of lysine 72 trimethylation. J Biol Chem *275*, 16127-16133.

Kluck, R.M., Martin, S.J., Hoffman, B.M., Zhou, J.S., Green, D.R., and Newmeyer, D.D. (1997). Cytochrome c activation of CPP32-like proteolysis plays a critical role in a Xenopus cell-free apoptosis system. EMBO J *16*, 4639-4649.

Krepela, E., Prochazka, J., Liul, X., Fiala, P., and Kinkor, Z. (2004). Increased expression of Apaf-1 and procaspase-3 and the functionality of intrinsic apoptosis apparatus in non-small cell lung carcinoma. Biol Chem *385*, 153-168.

Kroemer, G., Galluzzi, L., and Brenner, C. (2007). Mitochondrial membrane permeabilization in cell death. Physiol Rev *87*, 99-163.

Kuida, K., Haydar, T.F., Kuan, C.Y., Gu, Y., Taya, C., Karasuyama, H., Su, M.S., Rakic, P., and Flavell, R.A. (1998). Reduced apoptosis and cytochrome c-mediated caspase activation in mice lacking caspase 9. Cell *94*, 325-337.

Kuida, K., Zheng, T.S., Na, S., Kuan, C., Yang, D., Karasuyama, H., Rakic, P., and Flavell, R.A. (1996). Decreased apoptosis in the brain and premature lethality in CPP32-deficient mice. Nature *384*, 368-372.

Kurokawa, M., and Kornbluth, S. (2009). Caspases and kinases in a death grip. Cell *138*, 838-854.

Kurokawa, M., Zhao, C., Reya, T., and Kornbluth, S. (2008). Inhibition of apoptosome formation by suppression of Hsp90beta phosphorylation in tyrosine kinase-induced leukemias. Mol Cell Biol *28*, 5494-5506.

Kwon, Y.G., Lee, S.Y., Choi, Y., Greengard, P., and Nairn, A.C. (1997). Cell cycle-dependent phosphorylation of mammalian protein phosphatase 1 by cdc2 kinase. Proc Natl Acad Sci U S A *94*, 2168-2173.

Lacroix, M., and Leclercq, G. (2004). Relevance of breast cancer cell lines as models for breast tumours: an update. Breast Cancer Res Treat *83*, 249-289.

Lademann, U., Cain, K., Gyrd-Hansen, M., Brown, D., Peters, D., and Jaattela, M. (2003). Diarylurea compounds inhibit caspase activation by preventing the formation of the active 700-kilodalton apoptosome complex. Mol Cell Biol *23*, 7829-7837.

Laguna, A., Aranda, S., Barallobre, M.J., Barhoum, R., Fernandez, E., Fotaki, V., Delabar, J.M., de la Luna, S., de la Villa, P., and Arbones, M.L. (2008). The protein kinase DYRK1A regulates caspase-9-mediated apoptosis during retina development. Dev Cell *15*, 841-853.

Lakhani, S.A., Masud, A., Kuida, K., Porter, G.A., Jr., Booth, C.J., Mehal, W.Z., Inayat, I., and Flavell, R.A. (2006). Caspases 3 and 7: key mediators of mitochondrial events of apoptosis. Science *311*, 847-851.

Ledgerwood, E.C., and Morison, I.M. (2009). Targeting the apoptosome for cancer therapy. Clin Cancer Res *15*, 420-424.

Lee, I., Salomon, A.R., Yu, K., Doan, J.W., Grossman, L.I., and Huttemann, M. (2006). New prospects for an old enzyme: mammalian cytochrome c is tyrosine-phosphorylated in vivo. Biochemistry *45*, 9121-9128.

Leo, C., Richter, C., Horn, L.C., Schutz, A., Pilch, H., and Hockel, M. (2005). Expression of Apaf-1 in cervical cancer correlates with lymph node metastasis but not with intratumoral hypoxia. Gynecol Oncol *97*, 602-606.

Levine, A.J. (1997). p53, the cellular gatekeeper for growth and division. Cell *88*, 323-331.

Levine, B., and Kroemer, G. (2009). Autophagy in aging, disease and death: the true identity of a cell death impostor. Cell Death Differ *16*, 1-2.

Li, K., Li, Y., Shelton, J.M., Richardson, J.A., Spencer, E., Chen, Z.J., Wang, X., and Williams, R.S. (2000). Cytochrome c deficiency causes embryonic lethality and attenuates stress-induced apoptosis. Cell *101*, 389-399.

Li, M., Makkinje, A., and Damuni, Z. (1996). Molecular identification of I1PP2A, a novel potent heat-stable inhibitor protein of protein phosphatase 2A. Biochemistry *35*, 6998-7002.

Li, P., Nijhawan, D., Budihardjo, I., Srinivasula, S.M., Ahmad, M., Alnemri, E.S., and Wang, X. (1997). Cytochrome c and dATP-dependent formation of Apaf-1/caspase-9 complex initiates an apoptotic protease cascade. Cell *91*, 479-489.

Liu, J.R., Opipari, A.W., Tan, L., Jiang, Y., Zhang, Y., Tang, H., and Nunez, G. (2002). Dysfunctional apoptosome activation in ovarian cancer: implications for chemoresistance. Cancer Res *62*, 924-931.

Liu, X., Kim, C.N., Yang, J., Jemmerson, R., and Wang, X. (1996). Induction of apoptotic program in cell-free extracts: requirement for dATP and cytochrome c. Cell *86*, 147-157.

Livak, K.J., and Schmittgen, T.D. (2001). Analysis of relative gene expression data using real-time quantitative PCR and the 2(-Delta Delta C(T)) Method. Methods *25*, 402-408.

Lowe, S.W., and Lin, A.W. (2000). Apoptosis in cancer. Carcinogenesis *21*, 485-495.

Luthi, A.U., and Martin, S.J. (2007). The CASBAH: a searchable database of caspase substrates. Cell Death Differ *14*, 641-650.

Mahrus, S., Trinidad, J.C., Barkan, D.T., Sali, A., Burlingame, A.L., and Wells, J.A. (2008). Global sequencing of proteolytic cleavage sites in apoptosis by specific labeling of protein N termini. Cell *134*, 866-876.

Malladi, S., Challa-Malladi, M., Fearnhead, H.O., and Bratton, S.B. (2009). The Apaf-1*procaspase-9 apoptosome complex functions as a proteolytic-based molecular timer. EMBO J *28*, 1916-1925.

Mandlekar, S., and Kong, A.N. (2001). Mechanisms of tamoxifen-induced apoptosis. Apoptosis *6*, 469-477.

Margolis, S.S., Walsh, S., Weiser, D.C., Yoshida, M., Shenolikar, S., and Kornbluth, S. (2003). PP1 control of M phase entry exerted through 14-3-3-regulated Cdc25 dephosphorylation. Embo J *22*, 5734-5745.

Martin, M.C., Allan, L.A., Lickrish, M., Sampson, C., Morrice, N., and Clarke, P.R. (2005). Protein kinase A regulates caspase-9 activation by Apaf-1 downstream of cytochrome c. J Biol Chem *280*, 15449-15455.

Martinou, I., Desagher, S., Eskes, R., Antonsson, B., Andre, E., Fakan, S., and Martinou, J.C. (1999). The release of cytochrome c from mitochondria during apoptosis of NGF-deprived sympathetic neurons is a reversible event. J Cell Biol *144*, 883-889.

Marusawa, H., Matsuzawa, S., Welsh, K., Zou, H., Armstrong, R., Tamm, I., and Reed, J.C. (2003). HBXIP functions as a cofactor of survivin in apoptosis suppression. Embo J *22*, 2729-2740.

Mashima, T., Oh-hara, T., Sato, S., Mochizuki, M., Sugimoto, Y., Yamazaki, K., Hamada, J., Tada, M., Moriuchi, T., Ishikawa, Y.*, et al.* (2005). p53-defective tumors with a functional apoptosome-mediated pathway: a new therapeutic target. J Natl Cancer Inst *97*, 765-777.

Mazroui, R., Di Marco, S., Clair, E., von Roretz, C., Tenenbaum, S.A., Keene, J.D., Saleh, M., and Gallouzi, I.E. (2008). Caspase-mediated cleavage of HuR in the cytoplasm contributes to pp32/PHAP-I regulation of apoptosis. J Cell Biol *180*, 113-127.

McDonnell, M.A., Abedin, M.J., Melendez, M., Platikanova, T.N., Ecklund, J.R., Ahmed, K., and Kelekar, A. (2008). Phosphorylation of murine caspase-9 by the protein kinase casein kinase 2 regulates its cleavage by caspase-8. J Biol Chem *283*, 20149-20158.

Mei, Y., Yong, J., Liu, H., Shi, Y., Meinkoth, J., Dreyfuss, G., and Yang, X. (2010). tRNA Binds to Cytochrome c and Inhibits Caspase Activation. Mol Cell *37*, 668-678.

Mohsin, S.K., Weiss, H.L., Gutierrez, M.C., Chamness, G.C., Schiff, R., Digiovanna, M.P., Wang, C.X., Hilsenbeck, S.G., Osborne, C.K., Allred, D.C.*, et al.* (2005). Neoadjuvant trastuzumab induces apoptosis in primary breast cancers. J Clin Oncol *23*, 2460-2468.

Morison, I.M., Cramer Borde, E.M., Cheesman, E.J., Cheong, P.L., Holyoake, A.J., Fichelson, S., Weeks, R.J., Lo, A., Davies, S.M., Wilbanks, S.M.*, et al.* (2008). A mutation of human cytochrome c enhances the intrinsic apoptotic pathway but causes only thrombocytopenia. Nat Genet *40*, 387-389.

Mumby, M.C., and Walter, G. (1993). Protein serine/threonine phosphatases: structure, regulation, and functions in cell growth. Physiol Rev *73*, 673-699.

Murray, A.W. (1991). Cell cycle extracts. Methods Cell Biol *36*, 581-605.

Murray, A.W., and Kirschner, M.W. (1989). Cyclin synthesis drives the early embryonic cell cycle. Nature *339*, 275-280.

Newmeyer, D.D., Farschon, D.M., and Reed, J.C. (1994). Cell-free apoptosis in Xenopus egg extracts: inhibition by Bcl-2 and requirement for an organelle fraction enriched in mitochondria. Cell *79*, 353-364.

Newport, J.W., and Forbes, D.J. (1987). The nucleus: structure, function, and dynamics. Annu Rev Biochem *56*, 535-565.

Nguyen, J.T., and Wells, J.A. (2003). Direct activation of the apoptosis machinery as a mechanism to target cancer cells. Proc Natl Acad Sci U S A *100*, 7533-7538.

Nicholson, D.W. (1999). Caspase structure, proteolytic substrates, and function during apoptotic cell death. Cell Death Differ *6*, 1028-1042.

Nicholson, D.W., Ali, A., Thornberry, N.A., Vaillancourt, J.P., Ding, C.K., Gallant, M., Gareau, Y., Griffin, P.R., Labelle, M., Lazebnik, Y.A.*, et al.* (1995). Identification and inhibition of the ICE/CED-3 protease necessary for mammalian apoptosis. Nature *376*, 37-43.

Nutt, L.K., Margolis, S.S., Jensen, M., Herman, C.E., Dunphy, W.G., Rathmell, J.C., and Kornbluth, S. (2005). Metabolic regulation of oocyte cell death through the CaMKII-mediated phosphorylation of caspase-2. Cell *123*, 89-103.

Oost, T.K., Sun, C., Armstrong, R.C., Al-Assaad, A.S., Betz, S.F., Deckwerth, T.L., Ding, H., Elmore, S.W., Meadows, R.P., Olejniczak, E.T.*, et al.* (2004). Discovery of potent antagonists of the antiapoptotic protein XIAP for the treatment of cancer. J Med Chem *47*, 4417-4426.

Orlowski, R.Z., and Baldwin, A.S., Jr. (2002). NF-kappaB as a therapeutic target in cancer. Trends Mol Med *8*, 385-389.

Ow, Y.P., Green, D.R., Hao, Z., and Mak, T.W. (2008). Cytochrome c: functions beyond respiration. Nat Rev Mol Cell Biol *9*, 532-542.

Pandey, P., Saleh, A., Nakazawa, A., Kumar, S., Srinivasula, S.M., Kumar, V., Weichselbaum, R., Nalin, C., Alnemri, E.S., Kufe, D.*, et al.* (2000). Negative regulation of cytochrome c-mediated oligomerization of Apaf-1 and activation of procaspase-9 by heat shock protein 90. Embo J *19*, 4310-4322.

Park, S.E., Kim, N.D., and Yoo, Y.H. (2004). Acetylcholinesterase plays a pivotal role in apoptosome formation. Cancer Res *64*, 2652-2655.

Parone, P.A., James, D.I., Da Cruz, S., Mattenberger, Y., Donze, O., Barja, F., and Martinou, J.C. (2006). Inhibiting the mitochondrial fission machinery does not prevent Bax/Bak-dependent apoptosis. Mol Cell Biol *26*, 7397-7408.

Pathan, N., Marusawa, H., Krajewska, M., Matsuzawa, S., Kim, H., Okada, K., Torii, S., Kitada, S., Krajewski, S., Welsh, K., *et al.* (2001). TUCAN, an antiapoptotic caspase-associated recruitment domain family protein overexpressed in cancer. J Biol Chem *276*, 32220-32229.

Pattingre, S., Tassa, A., Qu, X., Garuti, R., Liang, X.H., Mizushima, N., Packer, M., Schneider, M.D., and Levine, B. (2005). Bcl-2 antiapoptotic proteins inhibit Beclin 1-dependent autophagy. Cell *122*, 927-939.

Pelengaris, S., Khan, M., and Evan, G.I. (2002). Suppression of Myc-induced apoptosis in beta cells exposes multiple oncogenic properties of Myc and triggers carcinogenic progression. Cell *109*, 321-334.

Pellegrini, L., and Scorrano, L. (2007). A cut short to death: Parl and Opa1 in the regulation of mitochondrial morphology and apoptosis. Cell Death Differ *14*, 1275-1284.

Peltenburg, L.T., de Bruin, E.C., Meersma, D., Smit, N.P., Schrier, P.I., and Medema, J.P. (2005). Expression and function of the apoptosis effector Apaf-1 in melanoma. Cell Death Differ *12*, 678-679.

Perez-Paya, E., Orzaez, M., Mondragon, L., Wolan, D., Wells, J.A., Messeguer, A., and Vicent, M.J. (2010). Molecules that modulate Apaf-1 activity. Med Res Rev.

Piddubnyak, V., Rigou, P., Michel, L., Rain, J.C., Geneste, O., Wolkenstein, P., Vidaud, D., Hickman, J.A., Mauviel, A., and Poyet, J.L. (2007). Positive regulation of apoptosis by HCA66, a new Apaf-1 interacting protein, and its putative role in the physiopathology of NF1 microdeletion syndrome patients. Cell Death Differ *14*, 1222-1233.

Pomerance, M., Quillard, J., Chantoux, F., Young, J., and Blondeau, J.P. (2006). High-level expression, activation, and subcellular localization of p38-MAP kinase in thyroid neoplasms. J Pathol *209*, 298-306.

Pop, C., Timmer, J., Sperandio, S., and Salvesen, G.S. (2006). The apoptosome activates caspase-9 by dimerization. Mol Cell *22*, 269-275.

Potts, M.B., Vaughn, A.E., McDonough, H., Patterson, C., and Deshmukh, M. (2005). Reduced Apaf-1 levels in cardiomyocytes engage strict regulation of apoptosis by endogenous XIAP. J Cell Biol *171*, 925-930.

Potts, P.R., Singh, S., Knezek, M., Thompson, C.B., and Deshmukh, M. (2003). Critical function of endogenous XIAP in regulating caspase activation during sympathetic neuronal apoptosis. J Cell Biol *163*, 789-799.

Purring-Koch, C., and McLendon, G. (2000). Cytochrome c binding to Apaf-1: the effects of dATP and ionic strength. Proc Natl Acad Sci U S A *97*, 11928-11931.

Qin, H., Srinivasula, S.M., Wu, G., Fernandes-Alnemri, T., Alnemri, E.S., and Shi, Y. (1999). Structural basis of procaspase-9 recruitment by the apoptotic protease-activating factor 1. Nature *399*, 549-557.

Raina, D., Pandey, P., Ahmad, R., Bharti, A., Ren, J., Kharbanda, S., Weichselbaum, R., and Kufe, D. (2005). c-Abl tyrosine kinase regulates caspase-9 autocleavage in the apoptotic response to DNA damage. J Biol Chem *280*, 11147-11151.

Raman, M., Chen, W., and Cobb, M.H. (2007). Differential regulation and properties of MAPKs. Oncogene *26*, 3100-3112.

Rao, P.N., Gullipalli, D., and Bhuyan, A.K. (2009). Bacterially expressed recombinant WD40 domain of human Apaf-1. Protein Expr Purif *67*, 53-60.

Read, S.H., Baliga, B.C., Ekert, P.G., Vaux, D.L., and Kumar, S. (2002). A novel Apaf-1-independent putative caspase-2 activation complex. J Cell Biol *159*, 739-745.

Renatus, M., Stennicke, H.R., Scott, F.L., Liddington, R.C., and Salvesen, G.S. (2001). Dimer formation drives the activation of the cell death protease caspase 9. Proc Natl Acad Sci U S A *98*, 14250-14255.

Ricci, J.E., Munoz-Pinedo, C., Fitzgerald, P., Bailly-Maitre, B., Perkins, G.A., Yadava, N., Scheffler, I.E., Ellisman, M.H., and Green, D.R. (2004). Disruption of mitochondrial function during apoptosis is mediated by caspase cleavage of the p75 subunit of complex I of the electron transport chain. Cell *117*, 773-786.

Riedl, S.J., Li, W., Chao, Y., Schwarzenbacher, R., and Shi, Y. (2005). Structure of the apoptotic protease-activating factor 1 bound to ADP. Nature *434*, 926-933.

Riedl, S.J., and Salvesen, G.S. (2007). The apoptosome: signalling platform of cell death. Nat Rev Mol Cell Biol *8*, 405-413.

Riedl, S.J., and Shi, Y. (2004). Molecular mechanisms of caspase regulation during apoptosis. Nat Rev Mol Cell Biol *5*, 897-907.

Rotonda, J., Nicholson, D.W., Fazil, K.M., Gallant, M., Gareau, Y., Labelle, M., Peterson, E.P., Rasper, D.M., Ruel, R., Vaillancourt, J.P., *et al.* (1996). The three-

dimensional structure of apopain/CPP32, a key mediator of apoptosis. Nat Struct Biol *3*, 619-625.

Ruiz-Vela, A., and Korsmeyer, S.J. (2007). Proapoptotic histone H1.2 induces CASP-3 and -7 activation by forming a protein complex with CYT c, APAF-1 and CASP-9. FEBS Lett *581*, 3422-3428.

Sakai, T., Liu, L., Teng, X., Mukai-Sakai, R., Shimada, H., Kaji, R., Mitani, T., Matsumoto, M., Toida, K., Ishimura, K.*, et al.* (2004). Nucling recruits Apaf-1/pro-caspase-9 complex for the induction of stress-induced apoptosis. J Biol Chem *279*, 41131-41140.

Saleh, A., Srinivasula, S.M., Balkir, L., Robbins, P.D., and Alnemri, E.S. (2000). Negative regulation of the Apaf-1 apoptosome by Hsp70. Nat Cell Biol *2*, 476-483.

Sanchez-Olea, R., Ortiz, S., Barreto, O., Yang, Q., Xu, C.J., Zhu, H., and Yuan, J. (2008). Parcs is a dual regulator of cell proliferation and apaf-1 function. J Biol Chem *283*, 24400-24405.

Schafer, Z.T., and Kornbluth, S. (2006). The apoptosome: physiological, developmental, and pathological modes of regulation. Dev Cell *10*, 549-561.

Schafer, Z.T., Parrish, A.B., Wright, K.M., Margolis, S.S., Marks, J.R., Deshmukh, M., and Kornbluth, S. (2006). Enhanced sensitivity to cytochrome c-induced apoptosis mediated by PHAPI in breast cancer cells. Cancer Res *66*, 2210-2218.

Schonhoff, C.M., Gaston, B., and Mannick, J.B. (2003). Nitrosylation of cytochrome c during apoptosis. J Biol Chem *278*, 18265-18270.

Scorrano, L., Ashiya, M., Buttle, K., Weiler, S., Oakes, S.A., Mannella, C.A., and Korsmeyer, S.J. (2002). A distinct pathway remodels mitochondrial cristae and mobilizes cytochrome c during apoptosis. Dev Cell *2*, 55-67.

Seifert, A., Allan, L.A., and Clarke, P.R. (2008). DYRK1A phosphorylates caspase 9 at an inhibitory site and is potently inhibited in human cells by harmine. FEBS J *275*, 6268-6280.

Seifert, A., and Clarke, P.R. (2009). p38alpha- and DYRK1A-dependent phosphorylation of caspase-9 at an inhibitory site in response to hyperosmotic stress. Cell Signal.

Semenkova, L., Dudich, E., Dudich, I., Tokhtamisheva, N., Tatulov, E., Okruzhnov, Y., Garcia-Foncillas, J., Palop-Cubillo, J.A., and Korpela, T. (2003). Alpha-fetoprotein positively regulates cytochrome c-mediated caspase activation and apoptosome complex formation. Eur J Biochem *270*, 4388-4399.

Seo, S.B., Macfarlan, T., McNamara, P., Hong, R., Mukai, Y., Heo, S., and Chakravarti, D. (2002). Regulation of histone acetylation and transcription by nuclear protein pp32, a subunit of the INHAT complex. J Biol Chem *277*, 14005-14010.

Shimamura, A., Ballif, B.A., Richards, S.A., and Blenis, J. (2000). Rsk1 mediates a MEK-MAP kinase cell survival signal. Curr Biol *10*, 127-135.

Skulachev, V.P. (1998). Cytochrome c in the apoptotic and antioxidant cascades. FEBS Lett *423*, 275-280.

Slee, E.A., Harte, M.T., Kluck, R.M., Wolf, B.B., Casiano, C.A., Newmeyer, D.D., Wang, H.G., Reed, J.C., Nicholson, D.W., Alnemri, E.S., *et al.* (1999). Ordering the cytochrome c-initiated caspase cascade: hierarchical activation of caspases-2, -3, -6, -7, -8, and -10 in a caspase-9-dependent manner. J Cell Biol *144*, 281-292.

Smith, J.A., Poteet-Smith, C.E., Xu, Y., Errington, T.M., Hecht, S.M., and Lannigan, D.A. (2005). Identification of the first specific inhibitor of p90 ribosomal S6 kinase (RSK) reveals an unexpected role for RSK in cancer cell proliferation. Cancer Res *65*, 1027-1034.

Smythe, C., and Newport, J.W. (1991). Systems for the study of nuclear assembly, DNA replication, and nuclear breakdown in Xenopus laevis egg extracts. Methods Cell Biol *35*, 449-468.

Soengas, M.S., Capodieci, P., Polsky, D., Mora, J., Esteller, M., Opitz-Araya, X., McCombie, R., Herman, J.G., Gerald, W.L., Lazebnik, Y.A., *et al.* (2001). Inactivation of the apoptosis effector Apaf-1 in malignant melanoma. Nature *409*, 207-211.

Soengas, M.S., Gerald, W.L., Cordon-Cardo, C., Lazebnik, Y., and Lowe, S.W. (2005). Apaf-1 expression in malignant melanoma. Cell Death Differ.

Sohn, D., Essmann, F., Schulze-Osthoff, K., and Janicke, R.U. (2006). p21 blocks irradiation-induced apoptosis downstream of mitochondria by inhibition of cyclin-dependent kinase-mediated caspase-9 activation. Cancer Res *66*, 11254-11262.

Srinivasula, S.M., Ahmad, M., Fernandes-Alnemri, T., and Alnemri, E.S. (1998). Autoactivation of procaspase-9 by Apaf-1-mediated oligomerization. Mol Cell *1*, 949-957.

Srinivasula, S.M., Hegde, R., Saleh, A., Datta, P., Shiozaki, E., Chai, J., Lee, R.A., Robbins, P.D., Fernandes-Alnemri, T., Shi, Y., *et al.* (2001). A conserved XIAP-interaction motif in caspase-9 and Smac/DIABLO regulates caspase activity and apoptosis. Nature *410*, 112-116.

Suen, D.F., Norris, K.L., and Youle, R.J. (2008). Mitochondrial dynamics and apoptosis. Genes Dev *22*, 1577-1590.

Sun, Y., Orrenius, S., Pervaiz, S., and Fadeel, B. (2005). Plasma membrane sequestration of apoptotic protease-activating factor-1 in human B-lymphoma cells: a novel mechanism of chemoresistance. Blood *105*, 4070-4077.

Sunayama, J., Tsuruta, F., Masuyama, N., and Gotoh, Y. (2005). JNK antagonizes Akt-mediated survival signals by phosphorylating 14-3-3. J Cell Biol *170*, 295-304.

Suzuki, A., Tsutomi, Y., Akahane, K., Araki, T., and Miura, M. (1998). Resistance to Fas-mediated apoptosis: activation of caspase 3 is regulated by cell cycle regulator p21WAF1 and IAP gene family ILP. Oncogene *17*, 931-939.

Tanaka, K., Iwamoto, S., Gon, G., Nohara, T., Iwamoto, M., and Tanigawa, N. (2000). Expression of survivin and its relationship to loss of apoptosis in breast carcinomas. Clin Cancer Res *6*, 127-134.

Tashker, J.S., Olson, M., and Kornbluth, S. (2002). Post-cytochrome C protection from apoptosis conferred by a MAPK pathway in Xenopus egg extracts. Mol Biol Cell *13*, 393-401.

Thakur, A., Rahman, K.W., Wu, J., Bollig, A., Biliran, H., Lin, X., Nassar, H., Grignon, D.J., Sarkar, F.H., and Liao, J.D. (2007). Aberrant expression of X-linked genes RbAp46, Rsk4, and Cldn2 in breast cancer. Mol Cancer Res *5*, 171-181.

Thornberry, N.A., and Lazebnik, Y. (1998). Caspases: enemies within. Science *281*, 1312-1316.

Tran, T.H., Andreka, P., Rodrigues, C.O., Webster, K.A., and Bishopric, N.H. (2007). Jun kinase delays caspase-9 activation by interaction with the apoptosome. J Biol Chem *282*, 20340-20350.

Trauth, B.C., Klas, C., Peters, A.M., Matzku, S., Moller, P., Falk, W., Debatin, K.M., and Krammer, P.H. (1989). Monoclonal antibody-mediated tumor regression by induction of apoptosis. Science *245*, 301-305.

Tsuruta, F., Sunayama, J., Mori, Y., Hattori, S., Shimizu, S., Tsujimoto, Y., Yoshioka, K., Masuyama, N., and Gotoh, Y. (2004). JNK promotes Bax translocation to mitochondria through phosphorylation of 14-3-3 proteins. EMBO J *23*, 1889-1899.

Ulitzur, N., Humbert, M., and Pfeffer, S.R. (1997). Mapmodulin: a possible modulator of the interaction of microtubule-associated proteins with microtubules. Proc Natl Acad Sci U S A *94*, 5084-5089.

Vaughn, A.E., and Deshmukh, M. (2008). Glucose metabolism inhibits apoptosis in neurons and cancer cells by redox inactivation of cytochrome c. Nat Cell Biol *10*, 1477-1483.

Vaux, D.L., Cory, S., and Adams, J.M. (1988). Bcl-2 gene promotes haemopoietic cell survival and cooperates with c-myc to immortalize pre-B cells. Nature *335*, 440-442.

Voss, O.H., Kim, S., Wewers, M.D., and Doseff, A.I. (2005). Regulation of monocyte apoptosis by the protein kinase Cdelta-dependent phosphorylation of caspase-3. J Biol Chem *280*, 17371-17379.

Wagner, E.F., and Nebreda, A.R. (2009). Signal integration by JNK and p38 MAPK pathways in cancer development. Nat Rev Cancer *9*, 537-549.

Wakula, P., Beullens, M., Ceulemans, H., Stalmans, W., and Bollen, M. (2003). Degeneracy and function of the ubiquitous RVXF motif that mediates binding to protein phosphatase-1. J Biol Chem *278*, 18817-18823.

Watanabe, T., Hirota, Y., Arakawa, Y., Fujisawa, H., Tachibana, O., Hasegawa, M., Yamashita, J., and Hayashi, Y. (2003). Frequent LOH at chromosome 12q22-23 and Apaf-1 inactivation in glioblastoma. Brain Pathol *13*, 431-439.

Waterhouse, N.J., Goldstein, J.C., von Ahsen, O., Schuler, M., Newmeyer, D.D., and Green, D.R. (2001). Cytochrome c maintains mitochondrial transmembrane potential and ATP generation after outer mitochondrial membrane permeabilization during the apoptotic process. J Cell Biol *153*, 319-328.

Weston, C.R., and Davis, R.J. (2007). The JNK signal transduction pathway. Curr Opin Cell Biol *19*, 142-149.

Wolf, B.B., Schuler, M., Li, W., Eggers-Sedlet, B., Lee, W., Tailor, P., Fitzgerald, P., Mills, G.B., and Green, D.R. (2001). Defective cytochrome c-dependent caspase activation in ovarian cancer cell lines due to diminished or absent apoptotic protease activating factor-1 activity. J Biol Chem *276*, 34244-34251.

Wright, K.M., Linhoff, M.W., Potts, P.R., and Deshmukh, M. (2004). Decreased apoptosome activity with neuronal differentiation sets the threshold for strict IAP regulation of apoptosis. J Cell Biol *167*, 303-313.

Wu, J.Q., Guo, J.Y., Tang, W., Yang, C.S., Freel, C.D., Chen, C., Nairn, A.C., and Kornbluth, S. (2009). PP1-mediated dephosphorylation of phosphoproteins at mitotic exit is controlled by inhibitor-1 and PP1 phosphorylation. Nat Cell Biol *11*, 644-651.

Wyllie, A.H., Kerr, J.F., and Currie, A.R. (1980). Cell death: the significance of apoptosis. Int Rev Cytol *68*, 251-306.

Xia, W., Bacus, S., Hegde, P., Husain, I., Strum, J., Liu, L., Paulazzo, G., Lyass, L., Trusk, P., Hill, J., *et al.* (2006). A model of acquired autoresistance to a potent ErbB2 tyrosine kinase inhibitor and a therapeutic strategy to prevent its onset in breast cancer. Proc Natl Acad Sci U S A *103*, 7795-7800.

Yamashita, S., Masuda, Y., Kurizaki, T., Haga, Y., Murayama, T., Ikei, S., Kamei, M., Takeno, S., and Kawahara, K. (2007). Survivin expression predicts early recurrence in early-stage breast cancer. Anticancer Res *27*, 2803-2808.

Yang, L., Mashima, T., Sato, S., Mochizuki, M., Sakamoto, H., Yamori, T., Oh-Hara, T., and Tsuruo, T. (2003). Predominant suppression of apoptosome by inhibitor of apoptosis protein in non-small cell lung cancer H460 cells: therapeutic effect of a novel polyarginine-conjugated Smac peptide. Cancer Res *63*, 831-837.

Yin, Q., Park, H.H., Chung, J.Y., Lin, S.C., Lo, Y.C., da Graca, L.S., Jiang, X., and Wu, H. (2006). Caspase-9 holoenzyme is a specific and optimal procaspase-3 processing machine. Mol Cell *22*, 259-268.

Yoshida, H., Kong, Y.Y., Yoshida, R., Elia, A.J., Hakem, A., Hakem, R., Penninger, J.M., and Mak, T.W. (1998). Apaf1 is required for mitochondrial pathways of apoptosis and brain development. Cell *94*, 739-750.

Youle, R.J., and Strasser, A. (2008). The BCL-2 protein family: opposing activities that mediate cell death. Nat Rev Mol Cell Biol *9*, 47-59.

Yu, H., Lee, I., Salomon, A.R., Yu, K., and Huttemann, M. (2008). Mammalian liver cytochrome c is tyrosine-48 phosphorylated in vivo, inhibiting mitochondrial respiration. Biochim Biophys Acta *1777*, 1066-1071.

Yu, J., and Zhang, L. (2005). The transcriptional targets of p53 in apoptosis control. Biochem Biophys Res Commun *331*, 851-858.

Yu, L.G., Packman, L.C., Weldon, M., Hamlett, J., and Rhodes, J.M. (2004). Protein phosphatase 2A, a negative regulator of the ERK signaling pathway, is activated by tyrosine phosphorylation of putative HLA class II-associated protein I (PHAPI)/pp32 in response to the antiproliferative lectin, jacalin. J Biol Chem *279*, 41377-41383.

Yu, T., Wang, X., Purring-Koch, C., Wei, Y., and McLendon, G.L. (2001). A mutational epitope for cytochrome C binding to the apoptosis protease activation factor-1. J Biol Chem *276*, 13034-13038.

Yu, X., Acehan, D., Menetret, J.F., Booth, C.R., Ludtke, S.J., Riedl, S.J., Shi, Y., Wang, X., and Akey, C.W. (2005a). A structure of the human apoptosome at 12.8 A resolution provides insights into this cell death platform. Structure *13*, 1725-1735.

Yue, J., and Ferrell, J.E., Jr. (2004). Mos mediates the mitotic activation of p42 MAPK in Xenopus egg extracts. Curr Biol *14*, 1581-1586.

Zech, B., Kohl, R., von Knethen, A., and Brune, B. (2003). Nitric oxide donors inhibit formation of the Apaf-1/caspase-9 apoptosome and activation of caspases. Biochem J *371*, 1055-1064.

Zimmermann, K.C., Bonzon, C., and Green, D.R. (2001). The machinery of programmed cell death. Pharmacol Ther *92*, 57-70.

Zlobec, I., Minoo, P., Baker, K., Haegert, D., Khetani, K., Tornillo, L., Terracciano, L., Jass, J.R., and Lugli, A. (2007). Loss of APAF-1 expression is associated with tumour progression and adverse prognosis in colorectal cancer. Eur J Cancer *43*, 1101-1107.

Zong, W.X., Ditsworth, D., Bauer, D.E., Wang, Z.Q., and Thompson, C.B. (2004). Alkylating DNA damage stimulates a regulated form of necrotic cell death. Genes Dev *18*, 1272-1282.

Zou, H., Henzel, W.J., Liu, X., Lutschg, A., and Wang, X. (1997). Apaf-1, a human protein homologous to C. elegans CED-4, participates in cytochrome c-dependent activation of caspase-3. Cell *90*, 405-413.

Zou, H., Li, Y., Liu, X., and Wang, X. (1999). An APAF-1.cytochrome c multimeric complex is a functional apoptosome that activates procaspase-9. J Biol Chem *274*, 11549-11556.

Biography

Amanda Baumann Parrish

Born Amanda Kirsch Baumann to James and Marlene Baumann on February 19, 1980 in Ann Arbor, MI;

Married to Judson Lee Parrish on June 18, 2005 in Atlanta, GA;

Had her first child, Tyler Zachary Parrish on March 27, 2009 in Durham, NC.

Education

Ph.D. in Molecular Cancer Biology, Certificate in Cell and Molecular Biology
Duke University, Durham, NC, May 2010

B.S. in Biology
Emory University, Atlanta, GA, May 2002

Publications

Parrish A.B.*, Kim J.*, Kurokawa M., Freel C.D., Andersen J.L., Johnson C.E., Kornbluth S. MAPK-mediated Suppression of Cytochrome *c*-Induced Apoptosis Through Rsk Phosphorylation of Apaf-1. *EMBO Journal*. In review.

Andersen, J.L., Johnson, C.E., Freel, C.D., **Parrish A.B.**, Day, J.L., Buchakjian, M.R., Nutt, L.K., Thompson, J.W., Moseley, M.A., Kornbluth, S. Restraint of Apoptosis During Mitosis Through Interdomain Phosphorylation of Caspase-2. *EMBO Journal.* 28:20, 3216-3227 (2009).

Johnson, C.E., Huang, Y.Y., **Parrish, A.B.**, Smith, M.I., Vaughn, A.E., Wright, K.M., Zhang, Q., Van Dyke, T., Weschler-Reya, R.J., Kornbluth, S., Deshmukh, M. Differential Apaf-1 Levels Allow Cytochrome *c* to Induce Apoptosis in Brain Tumors but not in Normal Neural Tissues. *Proceedings of the National Academy of Sciences* 104: 52, 20820-20825 (2007).

Sun, Q.C., Arnold, R., Fernandez-Golarz, C., **Parrish, A.B.**, Almekinder, T., He, J., Ho, S., Svboda, P., Pohl, J., Marshall, F.F., Petros, J.A. Human Beta Defensin-1, a Potential Chromosome 8p Tumor Suppressor: Control of Transcription and Induction of Apoptosis in Renal Cell Carcinoma. *Cancer Research* 66:17, 8542-8549 (2006).

Schafer, Z.T.*, **Parrish, A.B.***, Wright, K.M., Margolis, S.S., Marks, J.R., Deshmukh, M., Kornbluth, S. Enhanced Sensitivity to Cytochrome *c*-Induced Apoptosis Mediated by PHAPI in Breast Cancer Cells. *Cancer Research* 66:4, 2210-2218 (2006).

Booker, L.M., Habermacher, G.M., Jessie, B.C, Sun, Q.C., **Baumann A.K.,** Amin, M., Lim, S.D., Fernandez-Golarz, C., Lyles, R.H., Brown, M.D., Marshall, F.F., Petros, J.A. North American Caucasian Mitochondrial Haplogroups in Prostate and Renal Cancer. *Journal of Urology* 175:2, 468-472 (2006).

Petros, J.A., **Baumann, A.K.,** Ruiz-Pesini, E., Amin, M.B., Sun, C.Q., Hall, J., Lim, S.D., Issa, M.M., Flanders, W.D., Hosseini, S.H., Marshall, F.F., Wallace, D.C. mtDNA Mutations Increase Tumorigenicity in Prostate Cancer. *Proceedings of the National Academy of Sciences* 102:3, 719-724 (2005).

Aldridge B.A., Lim S.D., **Baumann A.K.,** Hosseini S., Buck W., Almekinder T.L., Sun C.Q., Petros J.A. Automated Sequencing of Complete Mitochondrial Genomes from Laser-Capture Microdissected Samples. *BioTechniques* 35:3, 606-614 (2003).

*Co-equal first authors.

Honors and Awards

2004-2010: **Cell and Molecular Biology Training Program**

2004-2006: **Cell and Molecular Biology NIH Training Grant**